



University of Pennsylvania
ScholarlyCommons


Publicly Accessible Penn Dissertations

2020

The Development Of Multivalent Nano-Self Peptides As Antagonists For Antibody-Dependent Macrophage Phagocytosis

Abdelaziz Jalil
University of Pennsylvania

Follow this and additional works at: <https://repository.upenn.edu/edissertations>

 Part of the [Allergy and Immunology Commons](#), [Biochemistry Commons](#), [Immunology and Infectious Disease Commons](#), and the [Medical Immunology Commons](#)

Recommended Citation

Jalil, Abdelaziz, "The Development Of Multivalent Nano-Self Peptides As Antagonists For Antibody-Dependent Macrophage Phagocytosis" (2020). *Publicly Accessible Penn Dissertations*. 4069.
<https://repository.upenn.edu/edissertations/4069>

This paper is posted at ScholarlyCommons. <https://repository.upenn.edu/edissertations/4069>
For more information, please contact repository@pobox.upenn.edu.

The Development Of Multivalent Nano-Self Peptides As Antagonists For Antibody-Dependent Macrophage Phagocytosis

Abstract

Macrophages are immune cells that are capable of physically engulfing and clearing whole cells and particles. This process of phagocytosis is modulated by an important interaction between membrane protein CD47, present on all 'self' cells, and the macrophage immune-receptor SIRP α . Upon binding to CD47, SIRP α delivers "do not eat me" signals to the macrophage allowing the contact cell or particle to evade engulfment. Cancer cells, which are abnormal human cells, express, and sometimes over-express CD47, which is one mechanism used to escape immune clearance. While there has been success in targeting CD47 on cancer cells in the clinic, indiscriminate binding of anti-CD47 antibodies to CD47 on healthy blood cells is unavoidable, leading to toxic side effects such as anemia. Here, we describe the design and synthesis of short, multivalent, soluble peptide (nano-Self) antagonists engineered to block SIRP α on macrophages. We report potent activity of bivalent and tetravalent nano-Self peptides relative to the monovalent variants in enhancing macrophage engulfment of IgG-opsonized target cells. These multivalent nano-Self peptides associate with macrophages and also suppress tyrosine phosphorylation in macrophages, all consistent with inhibiting the macrophage 'self' signaling axis. These peptides potentially serve as novel biomolecular tools for macrophage immunotherapy, replacing anti-CD47 therapies currently being investigated in the clinic.

Degree Type

Dissertation

Degree Name

Doctor of Philosophy (PhD)

Graduate Group

Chemistry

First Advisor

Dennis Discher

Second Advisor

David Chenoweth

Keywords

antibodies, CD47, Immune Checkpoint, Macrophages, peptides, SIRP α

Subject Categories

Allergy and Immunology | Biochemistry | Immunology and Infectious Disease | Medical Immunology

This dissertation is available at ScholarlyCommons: <https://repository.upenn.edu/edissertations/4069>

THE DEVELOPMENT OF MULTIVALENT NANO-SELF PEPTIDES AS ANTAGONISTS
FOR ANTIBODY-DEPENDENT MACROPHAGE PHAGOCYTOSIS

AbdelAziz R. Jalil

A DISSERTATION

in

Chemistry

Presented to the Faculties of the University of Pennsylvania

in

Partial Fulfillment of the Requirements for the

Degree of Doctor of Philosophy

2020

Supervisor of Dissertation

Co-Supervisor of Dissertation

Dennis E. Discher, Ph.D.
Robert D. Bent Professor of Chemical
and Biomolecular Engineering

David M. Chenoweth, Ph.D.
Associate Professor of Chemistry

Graduate Group Chairperson

Daniel J. Mindiola, Ph.D.
Brush Family Professor of Chemistry

Dissertation Committee

E. James Petersson, Ph.D. (Committee Chairperson) Professor of Chemistry
David M. Chenoweth, Ph.D. Associate Professor of Chemistry
Tobias Baumgart, Ph.D. Professor of Chemistry

ACKNOWLEDGEMENTS

I begin by remembering the excitement of receiving my acceptance letter to join the University of Pennsylvania's Department of Chemistry graduate program. The mere thought of that moment makes my heart race as I prepare to depart a place I have called home for the past five years. I am truly grateful for my time at Penn Chemistry & Engineering, the experiences that have shaped the scientist that I have now become, the mentors and amazing people that have all contributed towards my success, and all of the people behind the scenes who supported and motivated me to achieve and succeed.

Dr. Dennis Discher, my research mentor, supervisor, and source of encouragement. You have been a tremendous source of support throughout my PhD journey, always having answers to questions I thought were unsolvable. You have taught me to always think outside of the box and to remain FULL SPEED AHEAD! I am truly fortunate to have joined a group that is at the frontier of the high impact science and is lead by an enthusiastic and passionate scientist. I thank you, Dr. Discher, for believing in me and for granting me the opportunity to harness my passion for research under your supervision.

Dr. E. James Petersson, my committee chair, and quite frankly the person I have had the most ties with throughout the entire Department of Chemistry. My first experience with you was when I rotated in your lab my first semester at Penn. Your patience and support for a newcomer with no experience in biology was something I truly appreciate to this day. After all, it was because of my rotation in your lab and learning peptide synthesis that I was accepted in the Discher group! I then took your graduate course my second semester and also was your TA for undergraduate biochemistry. You volunteered to be my committee chair even before my committee was decided and indeed you chose to be the

committee chair once it was determined. Your guidance during committee meetings have assisted me in paving the path to correctly steer my research. I am grateful for you and thank you for all that you have done to help me reach where I am today.

Dr. David Chenoweth, my research co-adviser and committee member. You are a down-to-earth individual and super cheerful. I love your personality and your style of simplifying the most complicated of subjects. You did not hesitate to have me join your lab as an adjunct student and you were very welcoming. I am fortunate to have been part of your lab sharing your resources and also benefitting from your mentorship.

Dr. Tobias Baumgart, my committee member and also the graduate chair during the first half of my PhD program. My first interaction with you was while you were graduate chair which was pleasant and allowed me to see your sincerity in seeing students succeeding. After knowing that you also know Dr. Dennis Discher pretty well, it only made sense to have your insight and guidance throughout my stay at Penn. Thank you for your thought-provoking questions during our committee meetings, which I honestly thought were always the toughest (i.e. made me learn more)!

The members of both the Discher and Chenoweth groups have been amazing people and company. I have met so many outstanding and brilliant individuals during my time in both labs that I will never forget. I love you all and appreciate all of you for your help and great times we all spent together. I would also like to thank the great people I have met in the Departments of Chemistry and Engineering; graduate, undergraduate and professionals. You all have been great friends and acquaintances. Lastly, I would like to thank everyone outside of these departments for also etching my fantastic experience here

at Penn; people whom I have met at Penn through my participation in student orgs and the Chaplain's office.

Kristen M. Simon, the best listener I have ever met! I want to thank you from the bottom of my heart for always providing the space to vent and pour out frustration upon! You have a pure heart and have been a huge source of motivation for me personally. Thank you for being awesome!

Last and not least, I owe my parents all the gratitude in the world. I will never be able to pay them back for their unconditional love and outpouring support and for raising me to be independent and fearless of pursuing the impossible. I love you, mom and dad, for everything you have done for me since the day I was born to this day where I proudly can tell you, "I made it!" With that being said, I would also like to thank my wife, Mariam. Even though you have entered my life very recently, you have been a monumental beam of support during the last stretch of my PhD career. Thank you for being there for me. I am excited to see what the future has in store for us.

ABSTRACT

THE DEVELOPMENT OF MULTIVALENT NANO-SELF PEPTIDES AS ANTAGONIST FOR ANTIBODY-DEPENDENT MACROPHAGE PHAGOCYTOSIS

AbdelAziz R. Jalil

Dennis E. Discher

Macrophages are immune cells that are capable of physically engulfing and clearing whole cells and particles. This process of phagocytosis is modulated by an important interaction between membrane protein CD47, present on all ‘self’ cells, and the macrophage immune-receptor SIRP α . Upon binding to CD47, SIRP α delivers “do not eat me” signals to the macrophage allowing the contact cell or particle to evade engulfment. Cancer cells, which are abnormal human cells, express, and sometimes over-express CD47, which is one mechanism used to escape immune clearance. While there has been success in targeting CD47 on cancer cells in the clinic, indiscriminate binding of anti-CD47 antibodies to CD47 on healthy blood cells is unavoidable, leading to toxic side effects such as anemia. Here, we describe the design and synthesis of short, multivalent, soluble peptide (nano-Self) antagonists engineered to block SIRP α on macrophages. We report potent activity of bivalent and tetravalent nano-Self peptides relative to the monovalent variants in enhancing macrophage engulfment of IgG-opsonized target cells. These multivalent nano-Self peptides associate with macrophages and also suppress tyrosine phosphorylation in macrophages, all consistent with inhibiting the macrophage ‘self’ signaling axis. These peptides potentially serve as novel biomolecular tools for macrophage immunotherapy, replacing anti-CD47 therapies currently being investigated in the clinic.

TABLE OF CONTENTS

Acknowledgements	ii
Abstract.....	v
List of Tables	vii
List of Figures.....	viii
Chapter 1: Introduction	1
1.1 Background.....	2
1.2 Motivation and thesis outline.....	4
Chapter 2: Macrophage checkpoint blockade: a perspective on results from initial clinical trials and on CD47-SIRPα structure-function	7
2.1 Abstract.....	8
2.2 Introduction.....	9
2.3 The ubiquitous ‘marker of self’ ligand, CD47	10
2.4 The macrophage immune receptor SIRP α	14
2.5 Binding of CD47-SIRP α and their other ligands	16
2.6 CD47-SIRP α as an immune checkpoint	19
2.7 Clinical targeting CD47-SIRP α in cancer.....	22
2.8 Sequence-function relationships for CD47-SIRP α	31
2.9 Structure-function relationship of the CD47-SIRP α axis	38
2.10 Conclusions.....	42
Chapter 3: Multivalent, soluble nano-Self peptides increase phagocytosis of antibody-opsionized targets by suppressing self-signaling	43
3.1 Abstract.....	44
3.2 Introduction.....	45
3.3 Experimental Methods	49
3.4 Results and Discussion	60
3.4.1 nano-Self peptide designs, synthesis, and characterization	60
3.4.2 nS peptide agonists for human macrophage engulfment of opsonized human cells ...	63
3.4.3 Multivalent nS peptides inhibit CD47-Fc binding to human macrophages.....	80
3.4.4 Tyrosine phosphorylation in macrophages is suppressed by nS peptides	85
3.4.5 Competitive binding of nS peptides to macrophages	88
3.4.6 nS peptides are mainly disordered, with binding likely to enhance β -hairpin structure	95
3.4.7 Safety of nS-FF injections in a pre-clinical trial.....	103
3.5 Conclusions.....	106
Chapter 4: Future directions	108
Works cited.....	123

LIST OF TABLES

Table 2.1:	Known affinities of CD47-SIRP α ligands	18
Table 2.2:	CD47-SIRP α immune checkpoint inhibitors used for <i>in vitro</i> phagocytosis assays against cancer cells	21
Table 2.3:	Therapeutic CD47-SIRP α antibodies currently being investigated in the clinic.....	28

LIST OF FIGURES

Figure 2.1:	Phagocytosis is maximized by inhibiting CD47 on ‘self’ cells (the target) or SIRP α on macrophages in combination with antibodies that opsonize the target	12
Figure 2.2:	Novel re-analysis of TTI-621 binding data from Ref 72	29
Figure 2.3:	Conserved contact residues across various species of CD47 and SIRP α provides potential rationale for cross-species reactivity	36
Figure 2.4:	Crystal structures of various bound CD47/SIRP α inhibitors show location of constant contact residues	40
Figure 3.1:	nano-Self peptides are designed based on the CD47 binding loop as competitive inhibitors	47
Figure 3.2:	Synthesis and purity of nano-self peptides are characterized and confirmed by analytical HPLC and MALDI-TOF mass spectrometry	61
Figure 3.3:	Multivalent nano-Self peptides enhance human macrophage phagocytosis of opsonized targets	67
Figure 3.4:	PMA differentiated THP-1 cells share identical gene profiles as primary macrophages for key, pathway-relevant factors	70
Figure 3.5:	Successful synthesis and purification of tetravalent nano-Self-F peptide (nS-F4)	72
Figure 3.6:	Treatment of human macrophages with multivalent nano-Self peptides enhances phagocytosis levels significantly relative to peptide and antibody controls.....	74
Figure 3.7:	Using optimal concentration of opsonin allows for comparison of macrophage phagocytosis	76
Figure 3.8:	CD47 expression on RBCs and K562 cancer cells	78
Figure 3.9:	CD47-Fc binding curve.....	81
Figure 3.10:	Binding of nano-Self peptides is consistent with SIRP α inhibition.....	83
Figure 3.11:	Bivalent nano-Self peptides suppress macrophage phosphotyrosine levels consistent with disruption ‘Self’ signaling in <i>cis</i>	86
Figure 3.12:	Bivalent nano-Self outcompete monovalent association with macrophages	89
Figure 3.13:	Immobilized nano-Self peptides bind to soluble SIRP α	91
Figure 3.14:	nano-Self peptides bind to membrane bound SIRP α and are also internalized by human and mouse macrophages	93
Figure 3.15:	Random coil structure with some hairpin folding suggests induced fit mechanism into SIRP α binding pocket.....	97
Figure 3.16:	nano-Self peptides conform to some β -hairpin structure but mainly random coil.....	99
Figure 3.17:	Avidity of SIRP α appears to scale with the increase of nano-Self multivalency.....	101
Figure 3.18:	Pre-clinical assessments indicate nS-FF is safe <i>in vivo</i>	104
Figure 4.1:	The sequence of the cyclic nano-Self peptide is not found in nature suggesting low immunogenicity	111
Figure 4.2:	RBC phagocytosis by human and mouse macrophages increases with the addition of nS-Cyc	115

Figure 4.3: Proposed monovalent nS-F-Cyc and bivalent nS-FF-Cyc structures for phagocytosis and binding assays117

Figure 4.4: Multiple mutant versions of CD47-GFP transduced in HEK-293 cells will be used for SIRP α -Fc binding assays120

Chapter 1: Introduction

1.1 Background

Clearance of cancer cells, or any other foreign cell, by immune cells requires a balanced response of competing inhibitory and activating signals. Ligands that signal inhibitory responses are necessary to maintain healthy cells from being cleared by immune cells. Nevertheless, cancer cells have evolved to upregulate non-immunogenic signals or deregulate immunogenic signaling proteins in order to bypass immune clearance. This prompts one to look for strategies to manipulate inhibitory receptors on immune cells or their counter-ligands on cancer cells to promote cancer elimination.

Immunotherapy has gained much interest in the past decade. This approach stimulates the body's own immune cells by targeting checkpoint proteins that are involved in inhibiting the clearance of cancer cells. The most broadly studied and characterized immune checkpoints are the cytotoxic T-lymphocyte-associated protein 4 (CTLA-4) and programmed cell death protein (PD-1), found on activated T-cell membranes, and PD-L1 (PD-1 ligand), found on the surface of cancer (and healthy) cells.^{1,2} Normally, when these T-cell receptors interact with their ligands, elimination of cancer cells is halted. Targeting these receptors has established the foundation of immune checkpoint blockade therapy, motivating the search for additional immune checkpoints.³⁻⁶

While anti-CTLA-4 and anti-PD-1/PD-L1 immunotherapies have shown unprecedented success in treating liquid tumors, solid tumors remain a challenge. Macrophages have been sought as potential immunotherapeutic candidates against solid tumors given that macrophages can infiltrate into solid tumors and are the main phagocytic population within the tumor microenvironment.^{7,8} An innate macrophage immune checkpoint is that between the signal regulatory protein- α or SIRP α on macrophages and

the ubiquitous membrane protein CD47 found on all cells, including cancer cells.⁹⁻¹³ This interaction signals “self” or “do not eat me” to the macrophage, outweighing phagocytic “eat me” antigens present on the surface of tumors or from tumor-targeting drugs, leading to the escape of the cancer cell from macrophage engulfment.

While CD47 was known to be expressed in ovarian cancer decades ago,¹⁴ its role as an immune checkpoint has only been discovered recently.^{11-13,15} CD47 blockade on tumors serves as the predominant therapeutic approach in disrupting the CD47-SIRP α axis.¹⁶ While CD47-blockade seems promising and efficacious, indiscriminate binding of anti-CD47 antibodies to CD47 on all cells (ex. red blood cells) results in toxic side effects (ex. anemia).¹⁶ SIRP α on macrophages has also been targeted with checkpoint inhibitors.¹⁷⁻¹⁹ SIRP α is less abundant than CD47, thus targeting this immune receptor, in principle, is a more plausible and safer alternative relative to CD47 blockade.¹⁹⁻²¹

1.2 Motivation and thesis outline

The motivation for this research project stemmed from mouse and human data demonstrating that SIRP α blockade with antibodies is as effective as anti-CD47 therapies. Furthermore, the first demonstration of adapting macrophages to clear solid tumors by blocking SIRP α was done in our laboratory.¹⁹ The technique of harvesting macrophages from both mouse and human bone marrow, blocking the SIRP α receptor and also priming the macrophage with a targeting IgG-antibody against human tumors was successful in diminishing human cancers while maintaining safety. This inspires the development of SIRP α inhibitors of which this dissertation will discuss in detail.

The development of our peptide checkpoint inhibitors against SIRP α is based on the discovery of the Self peptide, also work that was done by our group.²² This synthetic 21-amino acid peptide, derived from the binding region of human CD47, was shown to bind to SIRP α and also mimic the function of full length CD47 by impeding phagocytosis of particles that display it. Here, we further minimalized this peptide to nano-Self peptides that are 8-amino acids in length but comprised of the sequence that makes up more than 40% of the contact residues between the paired receptors. Our proof-of-principle work is the first that demonstrates SIRP α blockade with peptides to be used as potential agents for macrophage immunotherapy.

This dissertation will cover two aspects of the field. Chapter 2 will provide an extensive overview of the CD47-SIRP α macrophage checkpoint. It begins by discussing the discovery and relevance of both proteins in cancer. Then, current clinical trials and treatments of various malignancies targeting both CD47 and SIRP α are discussed along with controversial and challenging safety concerns attributed to anti-CD47 therapies. The

end of the chapter provides new insights to the sequence and structure dependency of the CD47-SIRP α interaction and how these fundamental, but rather understudied aspects, relate to the binding and function of these paired receptors. This will hopefully inspire the development of new, potent, and functional macrophage checkpoint antagonists.

Chapter 3 will focus on the novelty of this dissertation. The rational re-design and innovation in developing various nano-Self peptides is explained in detail. Our monomeric peptides were further engineered to bivalent and tetravalent adjuvants to increase their avidity to SIRP α dimers. We show that these peptides enhance macrophage-mediated phagocytosis of human red blood cells and human erythroleukemia K562 cells when these target cells are “opsonized,” or complimented with an “eat me signal.” Our data show potent and pharmacological activity for bivalent and tetravalent constructs ($K_{eff} \sim 5-10$ nM). A simple inhibition assay shows multivalent nano-Self peptides outcompete soluble CD47 binding which suggests peptide binding to SIRP α . We further investigated the potential mechanism of phagocytosis and whether the binding we observed was indeed to SIRP α , by measuring phosphorylation levels in macrophages. This is based on the assumption that inhibiting the CD47-SIRP α axis by the addition of the nano-Self peptides will prevent SIRP α phosphorylation. Indeed, we observe significant suppression of phosphorylation in human macrophages even with the addition of low concentrations (20 nM) of bivalent nano-Self, consistent with SIRP α blockade and inhibition of ‘self’ signaling. Lastly, we injected our most potent peptide into mice to simply understand if there were any immediate inflammatory or toxic effects. From the hematological data, no anemia or weight loss was observed in the mice indicating some level of safety.

Chapter 4 provides explanation on future experiments with more engineered peptides and how to introduce these peptides *in vivo*. This chapter begins with a brief discussion on our ongoing efforts in exploring cyclic nano-Self peptides. Sequence searches reveal the presence of some of the linear nano-Self peptide sequences in various organisms, mainly bacteria. Most importantly, the sequence of our cyclic nano-Self peptide does not occur in nature. Preliminary phagocytosis data for our monovalent cyclic peptide in both human and mouse macrophages are presented, and the implications are discussed. We then present the expression of human CD47 variants - mutated at a key residue involved in binding and which also had a crucial effect in promoting macrophage phagocytosis – on the surface of HEK293 cells. Different binding assays to be done on these cells are explained. Additionally, mutated and bivalent cyclic nano-Self peptides are proposed. We conclude with potential caveats as we begin to transition into *in vivo* studies and how we plan to address them using linear and cyclic nano-Self peptides.

Chapter 2: Macrophage checkpoint blockade: a perspective on results from initial clinical trials and on CD47-SIRP α structure-function

Text in this chapter was previously published in:

Antibody Therapeutics, 2020, 3, 80-94

Jalil, A.; Andrechak, J.; Discher, D.

I was responsible for writing the main text, generating the tables as well as making all illustrations presented in this Chapter except for:

- a. The text in Section 2.7 (done by **J. Andrechak**)
- b. Table 3 (generated by **J. Andrechak**)
- c. Figures 2.1 and 2.2 (made by **J. Andrechak**)

2.1 Abstract

The macrophage checkpoint is an anti-phagocytic interaction between SIRP α on a macrophage and CD47 on all cell types. This interaction has emerged over the last decade as a potential co-target in cancer, which also expresses CD47, with antibodies against CD47 and SIRP α currently in preclinical and clinical development for a variety of hematological and solid malignancies. Monotherapy with CD47 blockade is ineffective in human clinical trials against many tumor types tested to date, except for some cutaneous and peripheral lymphomas. In contrast, pre-clinical results show efficacy in several syngeneic mouse models of cancer, suggesting that many of these tumor models are more immunogenic or otherwise artificial than human tumors. However, combination therapies in humans of anti-CD47 with agents such as the anti-tumor antibody rituximab do show efficacy against liquid tumors (lymphoma) and are promising for the field. Here, we review such trials as well as the key structural and interaction features of CD47-SIRP α in order to inform further potential therapeutic strategies.

2.2 Introduction

Cancer immunotherapy has rapidly expanded into the clinic over the past decade with significant success for therapies that target functionally suppressed immune cells in tumor microenvironments.²³ T-cells have been the primary focus of cancer immunotherapy with immune checkpoint inhibitors developed to antagonize either CTLA-4 and PD-1 expressed on T-cell membrane proteins, or PD-1's ligand, PD-L1, which is on the surface of many cells including cancer cells.^{1,2} While this receptor-ligand interaction normally inhibits an activated T-cell, inhibiting this paired receptor interaction with blocking antibodies enables suitably activated T-cells to eliminate cancer cells. Dramatic and durable effects are seen in some patients for some malignancies, with tumors having high mutational loads being most likely to activate T-cells, but most patients do not respond to this type of immunotherapy, which presents a challenge and an opportunity.^{24,25}

Macrophages are part of the innate immune response, are often abundant in solid tumors, and have a general ability to clear foreign cells through the activated process of phagocytosis.^{26,27} Phagocytosis is modulated by a checkpoint interaction between the signal regulatory protein alpha (SIRP α) on macrophages and the surface glycoprotein CD47 found on all cells.^{10,28} This review focuses on the structure of SIRP α and CD47, the role of this checkpoint in macrophage function, and therapeutic antibody strategies that target the SIRP α -CD47 interaction in cancer clinical trials. We also examine the sequence-structure-function relationships of these paired receptors in efforts to stimulate new therapeutics.

2.3 The ubiquitous ‘marker of self’ ligand, CD47

CD47 is an integral membrane glycoprotein that is expressed in all normal and diseased tissues at the RNA and protein levels. This glycoprotein was first discovered as an overexpressed ovarian carcinoma antigen (OA3).²⁹ It was also described as associating with β -integrin proteins and thus named integrin associated protein (IAP).³⁰ The protein was found on the surface of erythrocytes (which lack integrins) through binding of two different antibodies and was then designated CD47.³¹

CD47 belongs to the immunoglobulin superfamily (IgSF) with a single N-terminal extracellular Ig-like domain, five transmembrane helices, and a C-terminal cytoplasmic tail. Four cytoplasmic tails range in length from four amino acids (Type 1) to 34 amino acids (Type 4), but the 16 amino acid tail isoform (Type 2) is the most abundant and is expressed on the majority of cells in humans and mice.³²

An X-ray crystal structure of CD47 reveals an IgV (variable) topology with α -helical as well as β -sheet secondary structures and a conserved intramolecular disulfide bridge spanning the middle of the β -sandwich.⁹ An additional disulfide bridge also forms between the extracellular domain and one of the transmembrane domains, which is unusual for IgSF proteins and some evidence suggests it orients the Ig domain for optimal receptor binding.³³ CD47 interacts primarily with three categories of extracellular receptors: integrins, thrombospondin-1 (TSP-1) protein and SIRP α . Cell adhesion, cell migration, and regulation of inflammation and phagocytosis are among the reported functions of receptor interactions with CD47.³⁴

CD47 was first termed a “marker of self” after CD47-deficient red blood cells (RBCs) from a mouse knockout (C57BL/6 strain) were found to be rapidly cleared from

the circulation of wildtype mice by splenic macrophages.³⁵ The *in vitro* evidence is compelling that the CD47 interaction with SIRP α is a “don’t eat me” anti-phagocytic signal when occurring in parallel with some types of “eat me” signal – most clearly with IgG bound to the phagocytic target (**Figure 2.1**). In principle, the expression of CD47 allows all cells, including cancer cells, to evade macrophage engulfment. Nonetheless, two mysteries continue to persist since this seminal observation: (i) CD47-knockout mice do not exhibit anemia or any evident RBC or platelet deficiencies, and (ii) the *in vivo* “eat me” signal on RBCs in CD47-knockout mice remains unclear. Some might argue that the clearance cue is the senescence signal that leads to RBC phagocytosis after circulating weeks (in mouse) or months (in human), but CD47-knockout RBCs are *all* cleared within 1-2 days in the circulation of the wildtype mouse implying that all CD47-knockout RBCs display the senescence signal.

Figure 2.1: Antagonizing either CD47 on target cancer cell or SIRPα on the macrophage results with phagocytosis and is enhanced with macrophage FcR opsonization

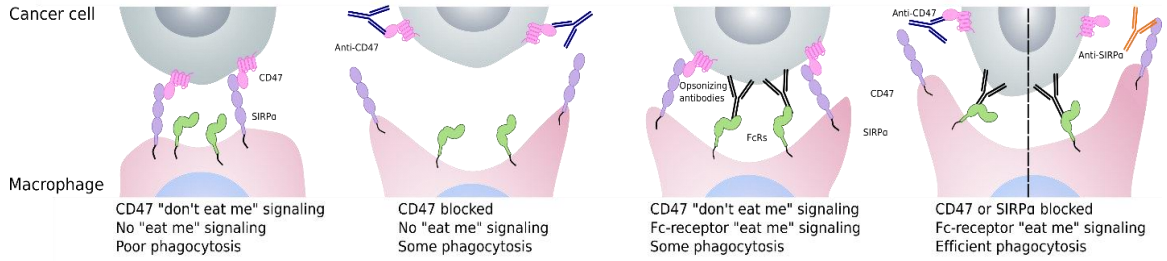


Figure 2.1: Phagocytosis is maximized by inhibiting CD47 on ‘self’ cells (the target) or SIRP α on macrophages in combination with antibodies that opsonize the target

CD47 binding to SIRP α signals “don’t eat me” to the macrophage (leftmost). Neither antibody blockade of CD47-SIRP α nor antibody opsonization of a target is sufficient to make target engulfment efficient (middle two), whereas the combination maximizes phagocytosis (rightmost).

2.4 The macrophage immune receptor, SIRP α

SIRP α is also an IgSF, integral membrane glycoprotein, and although it is expressed on many if not all cell types, its expression on hematopoietic cells is restricted to myeloid cells: macrophages, monocytes, dendritic cells, and granulocytes (and not T-cells, etc.).³⁶ SIRP α was first identified on rat fibroblasts as PTPNS1 (protein tyrosine phosphatase, non-receptor type substrate 1) in association with the cytoplasmic tyrosine phosphatase SHP-2 (Src homology region 2 domain containing phosphatase-2).³⁷ SIRP α was later found to be expressed on human myeloid cells,³⁸ although expression can vary even within subtypes of macrophages.¹⁹

SIRP α has three IgSF domains, one N-terminal V-like domain (domain-1, D1) and two C1-like domains – which is a structure shared by a larger family of SIRPs.^{39,40} One transmembrane helix connects to cytoplasmic tails of varying lengths that govern signaling in the SIRPs. SIRP α 's cytoplasmic tail has four tyrosine residues that conform to an immunoreceptor tyrosine-based inhibitory motif (ITIM) which mediates association with SHP-1 and SHP-2 for inhibitory signaling.³⁷

Two closely related SIRP members are SIRP β and SIRP γ . SIRP β has a short cytoplasmic tail (6 amino acids) and lacks phosphatase binding motifs suggesting it lacks inhibitory activity. However, SIRP β associates with DNAX activation protein 12 (DAP12) and can transmit activating signals.⁴¹ SIRP γ has an even shorter cytoplasmic region (4 amino acids) and is also unlikely to signal. Two uncharacterized members of the SIRP family are SIRP β 2 and SIRP δ .^{23,39}

The extracellular domains of the SIRP members share highly conserved sequence homology with very subtle differences.^{39,40} X-ray crystal structures of D1 for each of

SIRP α , SIRP β , SIRP β 2, and SIRP γ closely resemble each other.⁹ Additionally, SIRP α is known to be highly polymorphic.⁴² Across 10 distinct human SIRP α alleles, 18 amino acids have been identified as polymorphic residues, all located in the N-terminal IgV domain of SIRP α .

While CD47 is the main extracellular ligand for SIRP α and might also weakly bind SIRP γ ,^{9,28,39} additional extracellular ligands that interact with SIRP α include surfactant proteins A and D (Sp-A and Sp-D), found primarily in the lungs.^{43,44} Insulin secretion and muscle formation are among some of the functions that somehow involve SIRP α .⁴⁵ However, the best characterized function of SIRP α is its role in inhibiting macrophage phagocytosis upon binding CD47 on another cell.^{10,23,46}

2.5 Binding of CD47-SIRP α and their other ligands

CD47 is the main ligand for SIRP α across mouse, rat and human,⁴⁶ but the interaction is often weak with only sub-micromolar affinity^{28,47,48} – as summarized here for various CD47 and SIRP α ligands (**Table 2.1**). The single N-terminal IgV domain of CD47 interacts with the D1 of SIRP α . The interaction between these paired receptors is species-specific to an extent, with limited cross reactivity across species.⁴⁷ The X-ray crystal structure of the CD47-SIRP α complex reveals three distinct binding sites with the highest density of interactions occurring between the β -strands comprising the FG loop of CD47 and a wide binding pocket made up of SIRP α 's BC, C'D, DE and FG loops.⁹ More than 50% of the interfacial surface between the two proteins occurs at this site. Furthermore, about 45% of CD47's contact residues with SIRP α consist of the 8 amino acids that make up the loop region between strands F and G. Their binding is mediated mainly by charge complementarity (SIRP α mostly positive and CD47 mostly negative). The FG loop in CD47 is conserved across different species which may explain why human-CD47 binds to some SIRP α polymorphs from different species – such as SIRP α in non-obese diabetic (NOD) mice⁴⁸ and also porcine SIRP α .⁴⁹

Binding of CD47 to other ligands such as integrins, TSP-1 and TSP-1-derived peptides, also involves the IgV domain of CD47.³⁴ While the precise regions of interaction with integrins have not been determined, binding studies have shown that CD47 can activate integrins in *cis* independently as well as while bound to TSP-1 derived peptides or SIRP α ,⁵⁰⁻⁵² indicating that the binding site for integrins on CD47 is not occupied by either protein. Binding of CD47 to TSP-1, however, inhibits the binding of SIRP α . This finding was further demonstrated with a monoclonal anti-CD47 antibody, B6H12, that inhibited

binding of both ligands to CD47.⁵³ Although these results suggest that TSP-1 and SIRP α compete for overlapping binding sites on CD47, mutational and biochemical studies have also revealed that post-translational modifications of a critical serine residue on CD47 away from the SIRP α binding site is required for TSP-1 binding.⁵⁴

SIRP α also interacts with ligands other than CD47 such as Sp-A and Sp-D, respectively. Sp-D has been shown to bind SIRP α in D3, rather than D1.⁴⁴ CD47 binding to SIRP α in D1 is not impaired in the presence of Sp-D. Sp-A binds SIRP α ; however, the binding site is currently unknown. While the binding domain of SIRP α is highly polymorphic, there has been controversy on whether the polymorphic residues affect CD47 binding. The crystal structure reveals that the 18 polymorphic amino acids all lie outside of the CD47 interaction interface,^{9,55} although this does not preclude an allosteric effect that is common in protein-protein interactions. Indeed, CD47 affinity to the different SIRP α alleles seems to vary.²² Separate data suggest SIRP α polymorphism alters post-translational modifications which could also affect CD47 engagement.⁴²

Table 2.1: Known affinities of CD47-SIRP α ligands

Ligand	Receptor	Affinity (μ M)	Reference
SIRP α V1	CD47	0.46 / 0.74	22, 55
SIRP α V2	CD47	1.0-2.0	9,28,56
SIRP α V2	CD47	0.44 / 0.64	22, 55
SIRP α V3	CD47	0.84	22
SIRP α V4	CD47	0.91	22
SIRP α V5	CD47	2.50 / 0.78	22, 55
SIRP α V6	CD47	0.30	22
SIRP α V7	CD47	3.21 / 0.65	22, 55
SIRP α V8	CD47	0.65	22
SIRP α V9	CD47	1.14	22
SIRP α V10	CD47	0.08 / 0.67	22, 55
NOD SIRP α	CD47	0.08	48
'Self' peptide	SIRP α	0.16	22
FD6	CD47	4.1×10^{-5}	57
CV1	CD47	1.1×10^{-5}	57
PKHB1 (peptide)	CD47	'micromolar' affinity	58
CD47AP	SIRP α	1.1×10^{-2}	59
N3612 (Velcro CD47)	SIRP α V1	2.5×10^{-3}	60
	SIRP α V2	3.7×10^{-4}	
DSP-107 (SIRP α -41BBL)	CD47	1.5×10^{-3}	61

2.6 CD47-SIRP α as an immune checkpoint

Inhibitory immune signaling occurs upon CD47 binding, with phosphorylation of the ITIM motifs in SIRP α that then recruit and activate the cytoplasmic phosphatases SHP-1 and SHP-2.⁶²⁻⁶⁴ Downstream targets of dephosphorylation include paxillin and nonmuscle myosin IIA, decreasing the efficiency of phagocytosis analogous to direct inhibition of nonmuscle myosin IIA – at least for IgG-opsonized targets.⁶⁵ Integrin mediated activation also leads to the recruitment of the phosphatases and enhanced inhibitory phosphorylation signals.⁶⁶

When a target for phagocytosis is IgG opsonized, engulfment begins with the activation of Fc receptors (FcRs) on the surface of the phagocytic cell. This activation leads to the formation of a “phagocytic synapse” with rapid cytoskeletal rearrangement and accumulation of signaling proteins inside the macrophage at its point of contact with the targeted cell, microbe, or particle. The three main events that occur at the synapse are adhesion of the cell or particle with the phagocyte, pseudopod extension of the phagocyte around the target and final internalization.⁶⁷ CD47 on the target does not eliminate adhesion, but tends to impede the pseudopod formation and significantly suppresses the internalization.

The initial description of elevated CD47 levels in ovarian cancer followed by the characterization of its role in signaling “don’t eat me” to macrophages eventually inspired investigation of CD47 as a therapeutic target in cancer – particularly because CD47 tends to be modestly elevated in many hematologic and solid malignancies.^{11-13,15} Many proof-of-principle applications have been developed to target the CD47-SIRP α immune checkpoint including fully humanized anti-CD47 antibodies, anti-SIRP α antibodies,

SIRP α -fusion IgG proteins, among other protein and peptide antagonists. **Table 2.2** summarizes these antagonists and their *in vitro* applications against various types of cancer malignancies. Early preclinical studies demonstrated the efficacy of anti-CD47 treatment of various malignancies, with many of these indicating activity as a mono-therapy.^{11,15,68,69} Importantly, however, anti-CD47 is an opsonizing IgG, and so it is difficult with monotherapy to identify the results as (i) the pro-phagocytic effects of opsonizing a cancer cell – which is not novel but potentially useful, and/or (ii) blocking the anti-phagocytic effects of the “don’t eat me” signal – which is novel. Antibody-dependent phagocytosis activates the macrophage FcR, which directs the macrophage towards the target.^{70,71} Investigations with FcR-deficient mice and with Fab blocking antibodies (lacking the Fc chain) has suggested the mechanism of antibody-dependent macrophage phagocytosis differs depending on the type of malignancy.⁷² For a few cancers, it seems sufficient to interrupt the CD47-SIRP α interaction, but it is ineffective for many cancers, especially solid tumors.^{57,73}

Macrophages also express CD47, and recent evidence suggests this interacts in *cis* with SIRP α . As with the *trans* interaction, the *cis* interaction leads to relatively high phosphorylation of SIRP α 's cytoplasmic tail and to relatively low levels of phagocytosis compared to CD47-knockout macrophages.⁷⁴ The potency of an anti-CD47 therapy might thus reflect the cumulative effects of inhibiting *trans* interactions between a macrophage and a cancer cell as well as inhibiting passivating *cis* interactions on the same macrophage.

Table 2.2: CD47-SIRP α immune checkpoint inhibitors used for *in vitro* phagocytosis assays against cancer cells

Cancer Type	CD47 Antagonists	SIRP α Antagonists
Acute Lymphoblastic Leukemia	B6H12 ^{68,75} , BRIC126 ⁷⁵ , TTI-622 ⁷⁶ , ZF1 ⁷⁷	anti-mouse SIRP α (not specified) ⁷⁵
Acute Myeloid Leukemia	anti-CD47 (not specified) ⁷⁸ , B6H12 ^{13,68,79} , BRIC126 ¹³ , C47B222 ⁷⁹ , DSP-107 (CD47/4-1BB bispecific) ⁶¹ , Magrolimab ⁸⁰ , NI-1701 (CD47/CD19 bispecific) ⁸¹ , SIRP α -FC ⁸² , SRF231 ⁸³ , TTI-621 ⁸⁴ , TTI-622 ⁷⁶ , ZF1 ⁷⁷	P84 (anti-mouse SIRP α) ¹²
B Cell Lymphoma	ALX148 ⁸⁵ , B6H12 ^{68,86-88} , BRIC126 ⁸⁷ , CD20-CD47LL (CD47/CD20 bispecific) ⁸⁹ , CD20-CD47SL (CD47/CD20 bispecific) ⁸⁹ , CV1 ⁵⁷ , FD6 ⁵⁷ , DSP-107 ⁶¹ , Inhibrix ⁹⁰ , NI-1701 ⁸¹ , SRF231 ⁸³ , TG-1801 (CD47/CD20 bispecific) ⁹¹ , TTI-621 ⁸⁴ , TTI-622 ⁷⁶	040 ¹⁷ , SE12C3 ¹⁷ , ADU-1805 ⁹² , KWAR23 ¹⁸ , N3612 ⁶⁰
Bladder Cancer	anti-CD47 (not specified) ⁹³ , B6H12 ^{11,68}	None
Brain Cancer	B6H12 ^{11,68} , BRIC126 ¹¹ , Magrolimab ^{15,94,95}	None
Breast Cancer	B6H12 ^{11,96} , BRIC126 ¹¹ , CV1 ⁵⁷ , FD6 ⁵⁷ , RRx-001 ⁹⁷ , TTI-621 ⁸⁴	1.23A ⁹⁶ , 12C4 ⁹⁶ , 040 ¹⁷ , SE12C3 ¹⁷ , KWAR23 ¹⁸ , N3612 ⁶⁰
Chronic Lymphocytic Leukemia	PKHB1 ⁵⁸	None
Chronic Myeloid Leukemia	B6H12 ⁶⁸ , TTI-621 ⁸⁴	None
Colon Cancer	ALX148 ⁸⁵ , B6H12 ^{11,98} , BRIC126 ¹¹ , CV1 ⁵⁷ , FD6 ⁵⁷ , DSP-107 ⁶¹ , TTI-621 ⁸⁴	FAB 119 ⁹⁹ , FAB 136 ⁹⁹ , KWAR23 ¹⁸ , N3612 ⁶⁰
Colorectal Cancer	TTI-622 ⁷⁶	None
Endometrial Cancer	B6H12 ¹⁰⁰	None
Epidermoid Cancer	TTI-621 ⁸⁴	None
Esophageal Cancer	ALX148 ⁸⁵	FAB 119 ⁹⁹ , FAB 15 ⁹⁹ , FAB 136 ⁹⁹
Gastric Cancer	B6H12 ¹⁰¹	None
Hepatocellular Cancer	Ab400 (cross reacts human and mouse CD47) ¹⁰² , B6H12 ¹⁰²	None
Leiomyosarcoma	B6H12 ¹⁰³	None
Lung Cancer	CV1 ¹⁰⁴ , FD6 ¹⁰⁴ , DSP-107 ⁶¹ , Magrolimab ¹⁰⁴ , RRx-001 ⁹⁷ , SIRP α D1-Fc ¹⁰⁵ , TTI-621 ⁸⁴ , TTI-622 ⁷⁶	SE7C2 ¹⁹
Melanoma	A4 (anti-mouse CD47) ⁷³ , TTI-621 ⁸⁴	MY-1 (anti-mouse SIRP α) ¹⁰⁶ , P84 ¹⁰⁶
Medulloblastoma	Magrolimab ¹⁵	None
Myelodysplastic Syndrome	TTI-622 ⁷⁶	None
Myeloma	ALX148 ⁸⁵ , B6H12 ¹⁰⁷ , TTI-621 ⁸⁴	None
Osteosarcoma	Ab400 ¹⁰⁸ , B6H12 ¹⁰⁸	None
Ovarian Cancer	B6H12 ¹¹ , BRIC126 ¹¹ , DSP-107 ⁶¹ , TTI-621 ⁸⁴	None
Pancreatic Cancer	B6H12 ^{109,110} , CV1 ¹⁰⁹ , FD6 ¹⁰⁹ , Magrolimab ¹⁰⁹	None
Pharynx Cancer	DSP-107 ⁶¹	None
Renal Carcinoma	None	KWAR23 ¹⁸ , MY-1 ¹⁰⁶ , P84 ¹⁰⁶
Skin Cancer	TTI-621 ⁸⁴	None
T-Cell Lymphoma	B6H12 ¹¹¹ , SRF231 ¹¹¹ , TTI-621 ⁸⁴	None
T-Cell Leukemia	B6H12 ⁷⁹ , C47B157 ⁷⁹ , C47B161 ⁷⁹ , C47B222 ⁷⁹ , TTI-621 ⁸⁴	SE7C2 ¹⁹

2.7 Clinical targeting CD47-SIRP α in cancer

Decades ago, one anti-CD47 antibody was injected into ovarian cancer patients in order to image the tumors; the study demonstrated some targetability but provided no insight into therapeutic effects or safety issues.¹⁴ This of course pre-dates by a decade the description in mouse of CD47 as a ‘Marker of Self’.³⁵ Over the past decade, CD47 has indeed emerged as a potential therapeutic target for macrophage checkpoint blockade in clinical trials against cancer, with monoclonal antibodies being the primary antagonists.

Clinical trials up to Phase 2 have rapidly expanded in numbers, diversity of approach, and targets studied.^{16,112,113} Key strategies and current results from trial reports and conference proceedings are reviewed here (**Table 2.3**). A main conclusion is that monotherapy with anti-CD47 shows little to no efficacy across multiple cancer types when administered systemically, and while it often leads to rapid loss of a large fraction of blood cells (consistent with rapid loss of CD47-knockout mouse blood cells upon infusion in normal mice³⁵), anti-CD47 *can show efficacy* in humans in combination therapies. In reviewing the clinical trials (below) with this macrophage checkpoint blockade, it seems that some efforts with anti-CD47 are based on the hope that human tumors would possess macrophage activating activity that could be unleashed by simply preventing the inhibitory signaling from CD47-SIRP α (i.e. a monotherapy). As noted earlier, T-cell checkpoint blockade (using antagonists of PD-1’s interaction with PD-L1) succeeds primarily against human tumors with high mutational loads that tend to activate T-cells via their T-cell receptor (TCR).^{24,25}

Magrolimab, previously known as Hu5F9-G4, is the anti-human-CD47 monoclonal that is most advanced in clinical trials. Two Phase 1 dose escalation trials have been

completed in acute myeloid leukemia (AML) and solid tumors. Magrolimab is a humanized monoclonal IgG4 antibody that was engineered to not only block CD47 signaling but to also minimize engagement of FcRs and thereby limit macrophage activation.¹⁵ This is because the IgG4's Fc region has weaker affinity for FcRs compared to other IgG subtypes; Magrolimab is therefore more likely to work as an inhibitor and less as an opsonizing antibody. On the other hand, CD47 expression on all cells in the body means that there is a large sink for infused anti-CD47.

First reports of efficacy required a combination treatment of magrolimab and rituximab (anti-CD20) in relapsed/refractory (r/r) non-Hodgkin's lymphoma (NHL) patients that were refractory to rituximab alone.¹¹⁴ Phase 1b results showed 36% complete response rate (CRR) and 50% objective response rate (ORR) for a small cohort of a few dozen patients. Addition of the tumor-specific antibody to activate macrophage effector functions is a growing trend in CD47 blockade trials, reflecting the need for pro-phagocytic cues (e.g. antibody engagement of FcRs) in combination with blockade of 'don't eat me' signals to drive tumor regression. CD24 was recently proposed as another cell-surface 'don't eat me' signal and target, although in magrolimab-treated Phase 2 NHL patients, neither CD24 nor CD47 showed prognostic value.^{115,116} In another combination Phase 1b trial with the chemotherapeutic azacitidine, ongoing results reported 92% ORR in untreated higher-risk myelodysplastic syndrome (MDS) and 64% ORR in untreated AML patients.^{117,118} A tentative mechanism for this combination is that azacitidine results in surface display of pro-phagocytic calreticulin (normally intracellular), which synergizes with CD47 blockade in cancer cell phagocytosis.¹¹⁹ These latest data contributed to Forty-Seven, Inc's multi-billion dollar acquisition by the much larger firm, Gilead Sciences,

announced in March 2020.

TTI-621 and TTI-622 are SIRP α -Fc fusion proteins in trials against hematologic and solid malignancies.¹²⁰⁻¹²³ Both consist of the CD47-binding domain of human SIRP α fused to a human Fc domain: IgG1 for TTI-621 and IgG4 for TTI-622. The IgG1 domain of TTI-621 contributes to its increased potency, at least in preclinical models.⁸⁴ The TTI's were reported to have no affinity for human RBCs, but a re-analysis of TTI-621 data suggests otherwise. Magrolimab (5F9) and BRIC126 clearly cause hemagglutination by antibody-mediated cross-bridging,⁸⁴ which is not observed with TTI-621 and other select anti-CD47 agents (**Figure 2.2A**). On the other hand, addition of 'saturating concentrations' (~1 μ M based on hemagglutination results) to RBCs and then assayed for binding by flow cytometry, TTI-621 (and also TTI-622) gives a signal well above several non-specific antibodies albeit far below several anti-CD47 antibodies; the difference allows one to estimate a weak sub- μ M affinity of TTI-621 for RBCs (**Figure 2.2B**). This is only slightly weaker than TTI-621 binding (with ~10 nM to ~1 μ M affinities) to fresh white blood cells and platelets as well as to primary hematopoietic tumor samples, and to various human tumor cell lines (**Figure 2.2C**). Curiously, the effective concentrations (EC50) for phagocytosis of the tumor cell lines was ~10-100 fold stronger (~nM) than the above binding affinities, which perhaps relates to dominance of the Fc domain, and it is also curious that RBC phagocytosis results have not been reported. Indeed, tight binding of ~10 nM does not predict efficient phagocytosis (**Figure 2.2D**). Although TTI-621 showed some efficacy when administered intratumorally to patients with cutaneous T-cell lymphoma (mycosis fungoides), intravenous administration showed grade 3 thrombocytopenia in 18% of a varied cohort of leukemia, lymphoma, and other solid tumor patients (25% overall

showed some level of thrombocytopenia). It should be noted that platelet measurements are much noisier than RBC counts, and confident measurements of cytopenias/anemias also require measurements of any compensating production (e.g. reticulocytes). Despite potential safety concerns, monotherapies with TTI-621 in B- and T-cell lymphomas produce 18-29% ORR at low doses (0.5 mg/kg) with dose escalation in progress, which is unlike other anti-CD47 monotherapies under clinical study.¹²⁴ TTI-622 is being studied in combination with other tumor-specific agents, including rituximab and a PD-1 inhibitor to engage adaptive immune responses with continued claims of preferential tumor cell phagocytosis and no RBC binding.⁷⁶ For a deeper understanding of mechanism, future experiments should address RBC phagocytosis effects (i.e. EC50 *in vitro*) as well as the effect of bivalent/multivalent protein/peptide binding and blocking of SIRP α in the absence of a Fc domain.

CC-90002 is a humanized, high affinity (sub-nanomolar) monoclonal IgG4 CD47 antibody in Phase 1 trials against advanced solid and hematologic malignancies in combination with rituximab, with an earlier trial terminated due to discouraging safety profiles. In r/r NHL patients of the combined trial, 13% showed a response rate with 25% showing stable disease,¹²⁵ but 50% showed anemia (of any grade) with 33% showing thrombocytopenia.

ALX 148 is a fusion protein that consists of the CD47 binding domains of SIRP α and a fully inactive Fc domain.^{85,126} Notably, its molecular mass is 50% that of a typical antibody, which may enable lower dosing (e.g. 10 mg/kg) to saturate CD47 targets. The most recent reported data show that just 13.3% and 6.7% of patients (n = 30) show thrombocytopenia and anemia, respectively, in a combination cohort with ALX148 and

trastuzumab (anti-HER2). Another cohort receiving ALX148 and pembrolizumab (anti-PD1) reported 7.7% in both of the same measures.¹²⁷ In a cohort for r/r NHL with rituximab, the maximum tolerated dose was not reached, similar levels of anemia and thrombocytopenia were shown, and ongoing preliminary ORRs varied from 31% to 50% depending on tumor type.

Safety concerns with anti-CD47 remain due to the lack of specificity in targeting a ubiquitously expressed protein. Anemia and thrombocytopenia are widespread in patients and only partially mitigated by priming and dosing strategies.¹⁶ One fully human monoclonal antibody, SRF231, caused blood toxicities at such low doses (12 mg/kg) halting further expansion cohorts in its Phase 1 trial.⁸³ The addition of tumor-specific agents alongside anti-CD47 may increase efficacy but does not necessarily address safety issues, even in the case of bispecific or Fc-inactive antibodies.

Other current candidates in early trials have yet to report results as they monitor patient safety and dosing profiles such as AO-176, a humanized monoclonal anti-CD47 IgG2 antibody, and HX009, an anti-PD-1/CD47 bispecific antibody.¹¹⁹ IBI-188 is a CD47 IgG4 monoclonal antibody under Phase 1 trials in the US and China against advanced malignant tumors and lymphomas.¹²⁸ TJC4 (also known as TJ011133) is another CD47 monoclonal antibody that recently entered Phase 1 trials in the US for solid tumors and lymphoma in combination with pembrolizumab and rituximab.^{129,130} Many other drugs are in active preclinical development by startups and major pharmaceutical companies. The expanding field of candidates indicates an exciting but potentially challenging time in the development of CD47 therapeutics for cancer.

SIRP α is also a target for antibody blockade under preclinical and clinical study in

efforts to address the safety and efficacy concerns of early CD47 drugs, especially given CD47's ubiquitous expression.⁹⁹ Several anti-SIRP α antibodies are in active development in efforts to augment anti-tumor responses and overcome the significant off-target toxicities with anti-CD47.¹³¹ BI 765063/OSE-172 is a monoclonal SIRP α antagonist in a Phase 1 trial that dosed its first patient in June 2019 as a monotherapy and in combination with an anti-PD-1 monoclonal antibody.¹³²

Table 2.3: Therapeutic CD47-SIRP α antibodies currently being investigated in the clinic

Drug	Company	Clinical trials	Phase	Status	Targets	Combinations
Magrolimab (Hu5F9-G4)	Forty Seven, Inc.	NCT02678338	Phase 1	Completed	Acute myeloid leukemia, myelodysplastic syndrome	Monotherapy
		NCT02216409	Phase 1	Completed	Solid tumors	Monotherapy
		NCT03248479	Phase 1	Ongoing	Acute myeloid leukemia, myelodysplastic syndrome	Monotherapy, azacitidine
		NCT02953782	Phase 1/2	Ongoing	Colorectal neoplasms, solid tumors	Cetuximab
		NCT02953509	Phase 1/2	Ongoing	Lymphoma, Non-Hodgkin lymphoma, Large B-Cell, diffuse indolent lymphoma	Rituximab
TTI-621	Trillium Therapeutics, Inc.	NCT02663518	Phase 1	Ongoing	Hematologic malignancies, solid tumors	Monotherapy, rituximab, nivolumab
		NCT02890368	Phase 1	Ongoing	Solid tumors, mycosis fungoides	Monotherapy, PD-1/PD-L1 inhibitor, pegylated interferon- α 2a, T-Vec, radiation
TTI-622		NCT03530683	Phase 1	Ongoing	Lymphoma, myeloma	Monotherapy, rituximab, PD-1 inhibitor, proteasome-inhibitor regimen
CC-90002	Celgene	NCT02367196	Phase 1	Ongoing	Hematologic neoplasms	Monotherapy, rituximab
ALX 148	ALX Oncology, Inc.	NCT03013218	Phase 1	Ongoing	Solid tumors, Non-Hodgkin lymphoma	Monotherapy, pembrolizumab, trastuzumab, rituximab, ramucirumab + paclitaxel, 5-FU + cisplatin
SRF231	Surface Oncology	NCT03512340	Phase 1	Ongoing	Advanced solid cancers, hematologic cancers	Monotherapy
AO-176	Arch Oncology	NCT03834948	Phase 1	Ongoing	Solid tumors	Monotherapy
BI 765063	Boehringer Ingelheim	NCT03990233	Phase 1	Ongoing	Solid tumors	Monotherapy, PD-1 inhibitor
HX009	Waterstone Hanxbio Pty Ltd.	NCT04097769	Phase 1	Ongoing	Advanced solid tumors	Monotherapy
TJ011133 (TJC4)	I-Mab Biopharma, Co. Ltd.	NCT03934814	Phase 1	Ongoing	Solid tumors, lymphoma	Monotherapy, pembrolizumab, rituximab
IBI-188	Innovent Biologics Co. Ltd.	NCT03763149	Phase 1	Ongoing	Advanced malignancies	Monotherapy
		NCT03717103	Phase 1	Ongoing	Advanced malignancies	Monotherapy, rituximab

Figure 2.2: Novel analyses of SIRP α -Fc fusion antibody (TTI-621) interacting with blood cells and cancer cells (reported in Ref 72) elucidate aspects of molecular mechanism

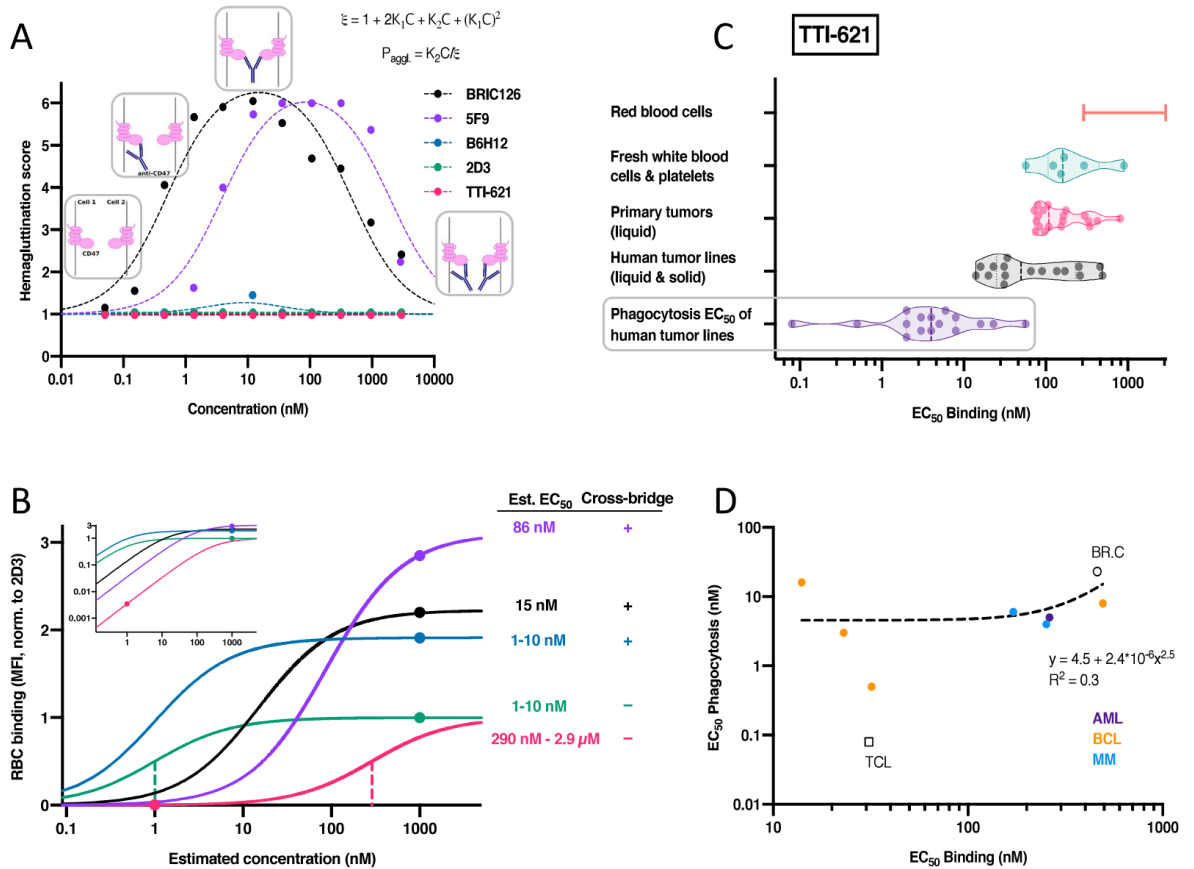


Figure 2.2: Novel re-analysis of TTI-621 binding data from Ref 72

A. Molecular partition function (ξ) fitting to the hemagglutination data. K_1 and K_2 are association constants, inversely related to dissociation constants or EC50. Schematic of possible binding states of various CD47 affinity agents is shown for two apposed RBC membranes. Magrolimab (5F9) and BRIC126 both exhibit high hemagglutination and show cross-bridging, which can be fit (5F9: $K_1 = 1.2 \times 10^{-2} \text{ nM}^{-1}$, $K_2 = 0.24 \text{ nM}^{-1}$; BRIC126: $K_1 = 6.6 \times 10^{-2} \text{ nM}^{-1}$; $K_2 = 1.9 \text{ nM}^{-1}$), whereas TTI-621, B6H12, and 2D3 do not.

B. TTI-621 shows non-zero binding to RBCs, which is weaker than anti-CD47 antibodies but consistent with past reports of sub- μM affinity between CD47 and SIRP α .¹³³ Inset: same data plotted with y-axis on log scale. Note that the plot follows the same color scheme as in panel A.

C. TTI-621 binding data show sub- μM affinity for white blood cells, primary tumor samples, and human tumor cell lines. Phagocytosis of the human tumor lines requires less binding for effective phagocytosis.

D. TTI-621 binding affinities do not predict phagocytic efficiency across various cancer cell types. BR.C: breast cancer, AML: acute myeloid leukemia, BCL: B cell lymphoma, MM: multiple myeloma, TCL: T-cell lymphoma.

2.8 Sequence-function relationships for CD47-SIRP α

Understanding the residues in CD47 and SIRP α that are key to binding and function will assist in developing new classes of checkpoint blocking proteins and peptides. Antibodies used for blocking are extremely large, glycoprotein complexes with >1,000 amino acid residues (~150 kDa). They also possess multiple disulfide bridges that require specialized eukaryotic machinery to faithfully produce the numerous post-translational modifications. For these reasons and more monoclonal antibodies with specificity for one protein such as CD47 are costly to produce in large quantities even though Good Manufacturing Practice for monoclonals is now a mainstay in biopharma.¹³⁴ Indeed, the average annual cost to a patient for a monoclonal antibody treatment is about \$100,000, which adds greatly to the rapidly rising costs of drugs and healthcare.^{135,136}

The co-crystal structure of CD47-SIRP α shows 13 residues in CD47 that contact 12 residues in SIRP α (polymorphic variants 1 and 2) through hydrogen bonding and salt bridges.^{9,55} Cross-species interactions, such as between pig CD47 and human SIRP α ⁴⁷ or between human CD47 and NOD mouse SIRP α ,⁴⁸ have a potential basis in some critical contact residues based on sequence alignments (**Figure 2.3**). Contact residues in human CD47 are all conserved in pig CD47 except for Lys-6, which is an Ile in pig. From the crystal structure, this residue is outside of the CD47 FG binding loop, and Lys is similar in size to Ile, making it likely that contact is maintained. For similar reasons, monkey CD47 that shares the same contact residues as human CD47, and dog CD47 that shares the same contact residues as pig CD47, should both bind human SIRP α . Mouse and rat CD47 have two non-conserved mutations at human residues Asp-46 and Glu-106, respectively. Mutating Asp to a bulky Tyr residue should interfere with the FG loop in SIRP α and

remove an important H-bond. Replacing the negative Glu with a positively charged Lys eliminates a critical salt bridge with Lys-53 in SIRP α 's binding pocket. Likewise, cow, sheep, and chicken all have mutations at critical H-bonding sites, which explain the lack of binding to human SIRP α .

The 12 contact residues in human SIRP α are conserved across its polymorph variants that all bind human CD47.²² NOD-SIRP α reportedly binds human CD47 65-fold more tightly than human SIRP α .⁴⁸ Sequence analysis reveals conserved mutations with SIRP α V1 except at residues Gln-52 and Lys-53 (**Figure 2.3**). From crystal structure analysis, the H-bond formed via Lys-53 is potentially maintained with a Thr mutation found in NOD-SIRP α , a possible explanation for the increased affinity may be due to the increased hydrophobicity of the Q52F mutation. Phe-52 has the propensity to engage in hydrophobic interactions with pyroGlu-1 in SIRP α which might compensate for the loss of the noncritical H-bond. Variance in mouse SIRP α shows that Lys-53 is mutated to aliphatic Ala, eliminating a critical H-bond with Glu-106 in CD47 and perhaps explaining the lack of human CD47 binding. Moreover, two residues in mouse SIRP α (Ser-102 & Glu-103) are absent in NOD-SIRP α and in human SIRP α , which suggests enhanced CD47 affinity for NOD-SIRP α relative to other mouse SIRP α 's.

Interestingly, human CD47 binding to pig SIRP α inhibits phagocytosis, which indicates that the sequence variance between pig and human SIRP α does not prevent signaling.⁴⁹ Two contact residue changes between human and pig, Q52F, which is the same mutation found in NOD mouse strains, and G97E, a nonconserved mutation that introduces a salt bridge interaction with Lys37 in CD47 (**Figure 2.3**). In NOD-SIRP α , the Q52F mutation seemingly enhanced CD47 affinity suggesting the same may be true with pig

SIRP α , especially with the addition of a favorable H-bonding interaction at Gly97. However, phagocytosis is inhibited by the interaction of NOD-SIRP α and human CD47, implying that the sequence complementarity of the remaining contact residues, namely Lys53, between the paired receptors is important for signaling regardless of species. When comparing this to the 10 polymorphs of human SIRP α , which all bind human CD47,^{22,42,55} the resultant “don’t eat me” signal is dependent on which SIRP α variant CD47 interacts with, even though both are from the same species.¹³⁷ When comparing monkey and dog SIRP α sequences, the contact residues are also conserved in the same manner as CD47 (monkey conserved with human sequence and dog conserved with pig sequence except at Gly97). This becomes significant for preclinical safety and efficacy models and modulating engraftment of human cells in other species.

Although both CD47 and SIRP α are glycosylated post-translationally, glycosylation is not a requisite of CD47-SIRP α interaction, with amino acid residues driving the binding.^{138,139} Monomeric, recombinant CD47 and SIRP α expressed in *E. coli* and lacking glycosylation indeed disrupt the CD47-SIRP α interaction *in vitro*.¹⁴⁰ Glycosylation of SIRP α and of CD47 may sometimes inhibit their binding¹⁴¹ but otherwise seem important for *cis* dimerization of SIRP α on the surface of cells.⁵⁹ An important post-translational modification, however, is the N-terminal modification of CD47 by glutaminyl-peptide cyclotransferase-like protein (QPCTL) to produce pyroglutamate.¹⁴² This modification has been demonstrated to contribute to SIRP α binding as well as signaling, although the earlier results with CD47 expressed in *E. coli* did not seem to account for this modification.¹⁴⁰ Nonetheless, inhibiting QPCTL enhanced antibody-mediated phagocytosis.¹⁴²

Major advances have been made in engineering high affinity versions of CD47 and SIRP α to function as immune checkpoint inhibitors. The most potent protein CD47 inhibitors developed are FD6 and CV1, which inhibit SIRP α binding at, remarkably, picomolar concentrations.⁵⁷ Analysis of the sequence and contact points between wildtype SIRP α and these engineered variants shows that three contact residues are mutated: K53R (conserved), E54Q (non-conserved), and L66T (non-conserved compared to SIRP α V1 but conserved compared to V2). The remaining 9 mutations in FD6 (6 mutations in CV1) appear to contribute to the stability of the engineered variants and add more hydrophobic contacts with CD47. It is important to note that these engineered variants cross-react with mouse CD47. Notably, an engineered CD47 variant, Velcro-CD47 N3612, potently antagonized SIRP α with no changes made to the binding region.⁶⁰ Rather, a three amino acid extension was added (Trp-Gln-Pro) to the N-terminus of CD47 and only a single point mutation made on Gln-1 (pyroGlu) to a Pro residue. Adding additional N-terminus contact residues between CD47 and SIRP α V1 and V2 effectively enhanced CD47 affinity to nanomolar and picomolar concentrations for the SIRP α variants, respectively. A 21-amino acid 'Self' peptide derived from the FG binding loop of CD47 was also shown to bind, antagonize SIRP α , and inhibit phagocytosis, suggesting that binding and function primarily converge to this sequence.²²

Pan-allelic anti-SIRP α antibodies that interact with more than one polymorph and/or species of SIRP α have also been engineered in order to overcome limitations that arise in targeting various polymorphs of SIRP α . One study discovered various classes of pan-allelic antibodies against SIRP α variants that antagonized human, mouse and monkey SIRP α .⁹⁹ Interestingly, some of these anti-SIRP α antibodies promote phagocytosis without

physically blocking the SIRP α binding groove and inhibiting CD47 interaction – although the mechanism remains unknown. A second study reports on ADU-1805, a humanized pan-allelic anti-SIRP α antibody that interacts with SIRP α variants 1, 2 and 8.⁹² ADU-1805 blocks CD47 binding to SIRP α and SIRP γ , and it does not bind to SIRP β . Pan-allelic agents that bind all SIRP α variants as well as pan-allelic peptides and proteins have yet to be discovered.

Figure 2.3: Sequence alignment show conserved contact residues in CD47 and SIRP α , respectively, across different species potentially explaining cross-species interactions

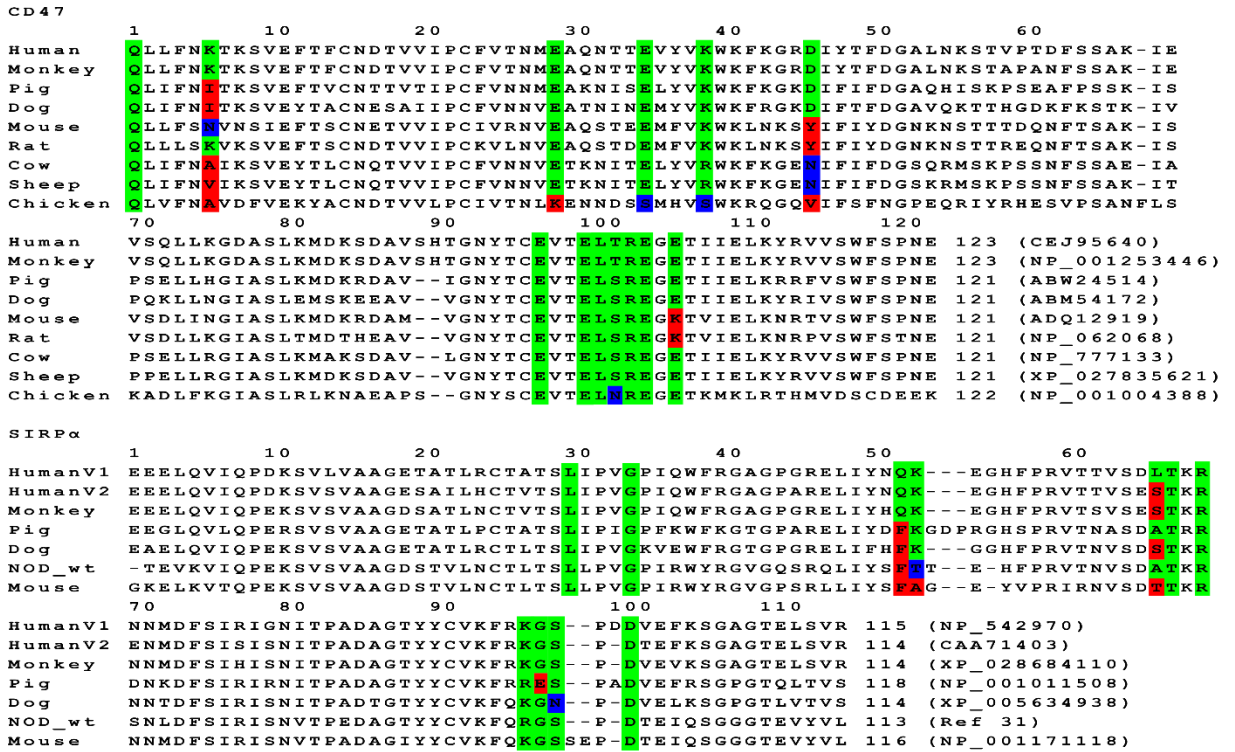


Figure 2.3: Conserved contact residues across various species of CD47 and SIRP α provides potential rationale for cross-species reactivity

Sequence overlays of CD47 and SIRP α , respectively, reveal conserved residues across different species. Green highlighted residues are conserved relative to human wildtype sequence. Blue highlighted residues are non-conserved mutations relative to human wildtype; however, maintain H-bonding. Red highlights are non-conserved mutations. Porcine CD47 binds human SIRP α and this can be seen from the conservation of most of the contact residues. Based on this, monkey CD47, which shares the same contact residues as human CD47, and dog CD47, which shares the same contact residues as pig CD47, should bind to human SIRP α . Likewise, when comparing SIRP α variants across different species, the conservation of contact residues among the sequences of NOD mice and pig SIRP α with human SIRP α provide some rationale as to why human CD47 interacts with these variants. Based on this, human CD47 should interact with monkey and dog SIRP α .

2.9 Structure-function relationship of the CD47-SIRP α axis

In addition to sequence analysis, crystal structures also assist in determining important structural factors that lead to potent antagonism (**Figure 2.4A**). For the fully humanized antibody magrolimab (Hu5F9-G4) that was made to block CD47,⁸⁰ the crystal structure reveals a magrolimab-CD47 binding complex like that of the SIRP α -CD47 complex showing magrolimab competing for the same SIRP α binding site.¹⁰⁴ Crystal structures of the older monoclonal B6H12 as well as hybridoma (C47B161) and phage (C47B222) derived monoclonal anti-CD47 antibodies also show that SIRP α is inhibited due to competitive binding to the same CD47 FG loop binding site.⁷⁹ 2D3 is a monoclonal anti-CD47 antibody that binds CD47 but reportedly does not block the interaction with SIRP α nor the inhibitory signal, indicating it interacts at a site away from the CD47 FG binding loop.¹³

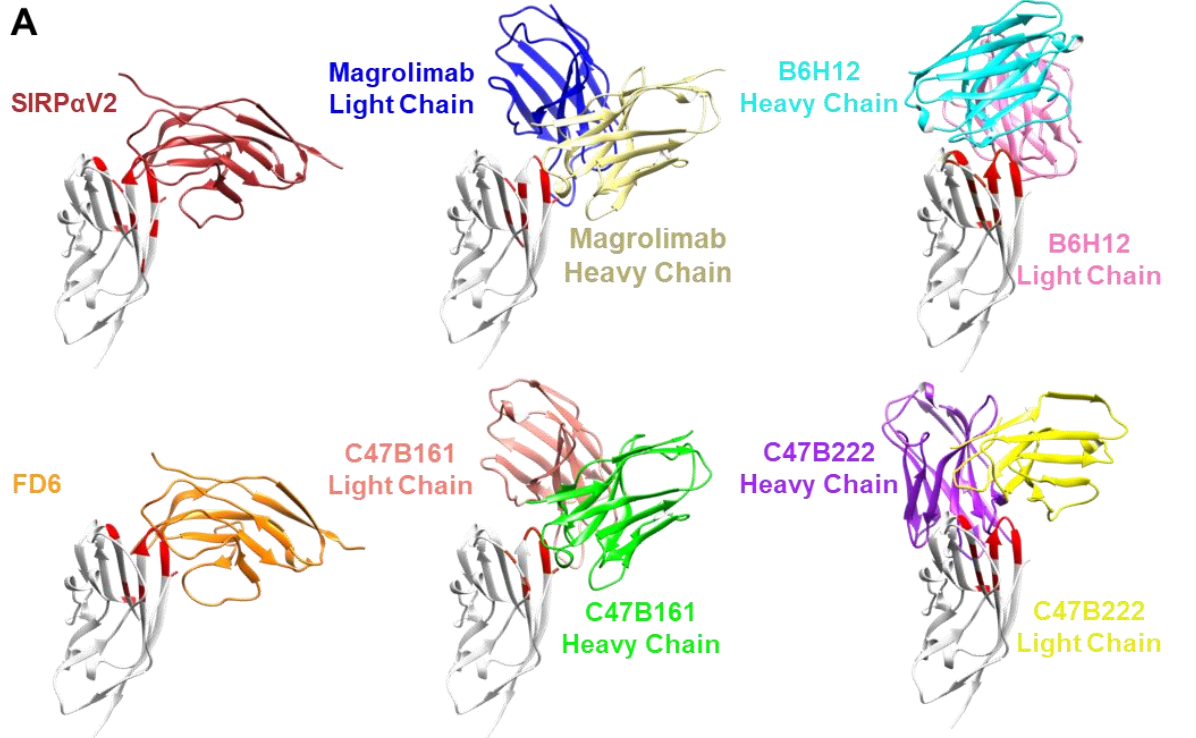
SIRP α directed antagonists likewise bind and block CD47 by competing for the ligand binding groove in SIRP α (**Figure 2.4B**). KWAR23, an anti-SIRP α blocking antibody, overlaps the same binding region as CD47, revealing a basis for competitive binding.¹⁸ Most recently, a series of blocking and non-blocking anti-SIRP α antibodies have been crystalized in complex with SIRP α .⁹⁹ The blocking antibodies all compete for the same binding site in SIRP α as CD47; however, one antibody epitope shares only a single common residue with CD47 in the SIRP α binding groove, but is enough to displace CD47 engagement. These anti-SIRP α blocking and non-blocking antibodies, were potent to different degrees in promoting phagocytosis of colon and esophageal carcinoma cells *in vitro*. These effects were also observed with monoclonal anti-mouse SIRP α , P84, which does not block CD47 binding, but rather inhibits SIRP α signaling by some other

mechanism to promote macrophage phagocytosis.¹⁰⁶

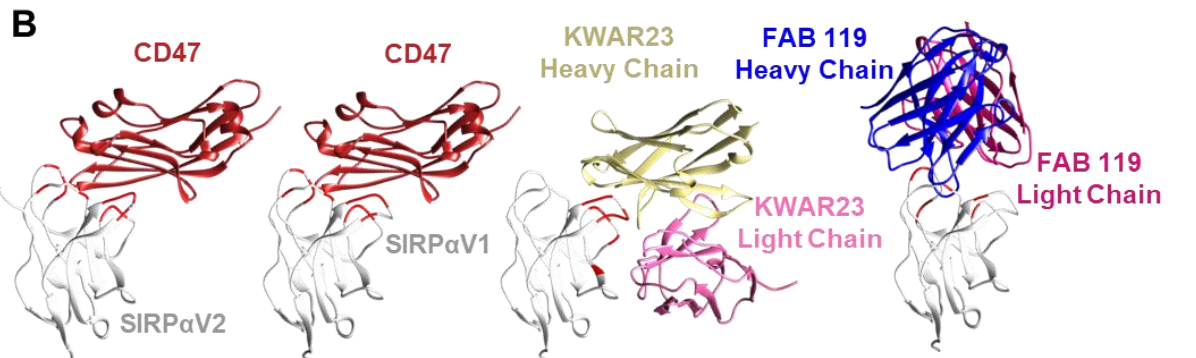
When comparing the crystal structures of bound CD47 and SIRP α , respectively, there are conserved contact residues in both proteins that interact with the bound ligand. In CD47, Thr-102 is involved in binding with all the potent antagonists as seen in the crystal structures (**Figure 2.4A**). Likewise, Lys-96 in SIRP α is a conserved contact residue (**Figure 2.4B**). Considering which residues are conserved in terms of binding can assist in rational design of protein, peptide, and small molecule inhibitors that are reminiscent of the binding interface of either CD47 or SIRP α based on the overall fold and positioning of these conserved contact residues.

It remains unclear whether CD47 binding to SIRP α leads to structural changes in the latter that somehow promotes cytoplasmic signaling. SIRP α is mobile and accumulates at the phagocytic synapse.⁶⁵ Interestingly, “forcing” SIRP α into the phagocytic synapse in the absence of CD47 also prevents engulfment of opsonized targets indicating the localization of SIRP α in the synapse is sufficient for signaling “don’t eat me” to the macrophage.¹³³ Accumulation of SIRP α to the synapse is thus driven by the presence of CD47 and appears to be the main mechanism by which phagocytosis is inhibited.

Figure 2.4: Constant contact residues in CD47 and SIRP α bound to different inhibitors



Contact Residue	Occurrence	Contact Residue	Occurrence	Contact Residue	Occurrence	Contact Residue	Occurrence
T102	6/6	Pyro-Q1	4/6	E100	3/6	T34	1/6
E97	5/6	E29	4/6	Y37	2/6	K41	1/6
L101	5/6	E35	4/6	K6	1/6	D46	1/6
R103	5/6	K39	4/6	N27	1/6	T49	1/6
E104	5/6	T99	3/6	Q31	1/6	E106	1/6



Contact Residue	Occurrence	Contact Residue	Occurrence	Contact Residue	Occurrence	Contact Residue	Occurrence
K96	4/4	G97	3/4	T67	2/4	S64	1/4
Q52	3/4	D100(V2) D101(V1)	3/4	S98	1/4	D65	1/4
K53	3/4	L30	2/4	V33	1/4	N70	1/4
E54	3/4	G34	2/4	L48	1/4	P99	1/4
R69	3/4	L66(V1) S66(V2)	2/4	H56	1/4	D100(V1)	1/4

Figure 2.4: Crystal structures of various bound CD47/SIRP α inhibitors show location of constant contact residues

Crystal structures of various **A)** CD47 and **B)** SIRP α bound inhibitors. For all antibody bound structures, only the first 100 residues in each of the heavy and light chains are shown. CD47 and SIRP α contact residues in each complex are highlighted in red. Inset tables list all contact residues in the respective receptors and how many times each contact residue is involved in binding across the various complexes.

A. PDB codes 2JJS (CD47/SIRP α v2), 5IWL (CD47/magrolimab), 5TZ4 (CD47/B6H12), 4KJY (CD47/FD6), 5TZT (CD47/C47B161), and 5TZ2 (CD47/C47B222).

B. PDB codes 2JJS (SIRP α v2/CD47), 4CMM (SIRP α v1/CD47), 6BIT (SIRP α v1/KWAR23), and 6NMR (SIRP α v1/FAB 119).

2.10 Conclusions

A balance of activating and passivating signals in the immune system normally maintains homeostasis but also allows cancer cells to evade clearance and spread. Immune checkpoint blockade of the PD-1/PD-L1 axis on T-cells has achieved some success against some cancers as a monotherapy, but current understanding is that T-cells in these patients are being activated by an abundance of mutations that can stimulate only upon checkpoint blockade. Although monotherapy against CD47-SIRP α seemed promising based on multiple syngeneic mouse models of cancer that used cancer lines that were known to be immunogenic, monotherapy also seemed unlikely based on minimally immunogenic lines such as B16 melanoma in C57 mice.⁷³ In this model, even PD-1 blockade is relatively ineffective unless the B16 cells are made more immunogenic with mutations that are also known to favor clinical responses to PD-1 blockade.^{24,25} Combination therapies of CD47-SIRP α blockade with tumor-opsonizing antibodies that activate macrophages through the FcR pathway are thus sensible and promising. They also have the theoretical potential for antigenic spread within a patient, if engulfment of the cancer cell by a macrophage or dendritic cell leads to patient-specific antibodies against tumor mutations that otherwise remain hidden behind the macrophage checkpoint.

Chapter 3: Multivalent, soluble nano-Self peptides increase phagocytosis of antibody-opsonized targets by suppressing self-signaling

Text in this chapter was previously published in:

ACS Nano, **2020**, 14, 15083-15093

Jalil, A.; Hayes, B.; Andrechak, J.; Xia, Y.; Chenoweth, D.; Discher, D.

I was the main researcher in this project and executed all experiments for the data

presented in this Chapter except for:

- a. **B. Hayes** assisted with confirming reproducibility of the red blood cell phagocytosis data with controls.
- b. The GEO microarray analysis on the various human and mouse cells presented in Figure 3.4 (performed by **B. Hayes**)
- c. The flow cytometry experiment presented in Figure 3.8 (performed by **B. Hayes**)
- d. The data from intravenous injections of nS-FF into mice presented in Section 3.4.7 and Figure 3.18 (performed and written by **J. Andrechak**).
- e. The confocal imaging presented in Figure 3.14B (performed by **Y. Xia**)

3.1 Abstract

Macrophages engulf ‘foreign’ cells and particles, but phagocytosis of both healthy cells and cancer cells is inhibited by expression of the ubiquitous membrane protein CD47 that binds SIRP α on macrophages to signal ‘self’. Based on past studies of CD47-derived polypeptides on particles that inhibit particle phagocytosis, we designed soluble, multivalent, nano-Self peptides to bind and block SIRP α function. Bivalent and tetravalent peptides prove more potent ($K_{eff} \sim 10$ nM) than monovalent 8-mers as agonists for phagocytosis of antibody targeted cells including cancer cells. Multivalent peptides outcompete soluble CD47 binding to human macrophages, consistent with SIRP α binding, and also suppress phosphotyrosine in macrophages, consistent with inhibition of ‘self’ signaling through SIRP α . Peptides exhibit low hairpin content, but functionality suggests an induced fit into SIRP α ’s binding pocket. Pre-clinical studies in mice indicate safety, with no anemia or weight loss. Multivalent nano-Self peptides thus constitute an alternative approach to antibody-based CD47 blockade in promoting phagocytosis of ‘self’ – including cancer cells targeted clinically.

3.2 Introduction

Protein-mediated interactions between two cells can convey inhibitory signals such as with ‘checkpoint’ receptors on immune cells. On macrophages, for example, SIRP α (signal regulatory protein- α) is a checkpoint receptor that binds the ubiquitously expressed protein CD47,^{9,10,36,56} which signals inhibition of macrophage engulfment of CD47-expressing cells or particles coated with macrophage-activating antibody. On T-cells, in comparison, PD-1 checkpoint receptor binds to PD-L1 on the surface of cells,^{1,2} which thereby inhibits T-cell activation. Importantly, antibody antagonists of these interactions enable these immune cells to eliminate target cells – although efficacy is lacking in many patients.^{4-6,143,144} Such limitations motivate additional molecular designs.

Nearly half of CD47’s contact surface with SIRP α localizes to 8 residues in a β -hairpin loop within CD47’s immunoglobulin (Ig) domain (**Figure. 3.1A**).^{9,22} A 21-amino acid peptide derived from CD47 binds SIRP α and mimics function of the Ig domain by inhibiting macrophage-mediated clearance of peptide- or Ig- displaying nanoparticles injected in mice.²² Mechanistically, the interaction between CD47 and macrophage SIRP α stimulates dephosphorylation of multiple macrophage factors to signal against phagocytosis.^{37,62,63,65,66,145} The CD47-SIRP α macrophage checkpoint is already targeted in cancer patients with antagonizing antibodies and antibody-like bivalent fusions of SIRP α .^{69,120,122,126,146} Although blockade is effective in patients when combined with a tumor-opsonizing antibody,¹¹⁴ infusion of anti-CD47 is often seen to clear blood cells including red blood cells (RBCs).^{16,27,147} We hypothesized that a multivalent, 8-amino acid nano-Self (nS) peptide could antagonize SIRP α while preventing clearance of blood cells *in vivo*. Here, multivalent peptides substituted at a single key residue (**Figure. 3.1B**)

function as SIRP α antagonists and lead to increased macrophage phagocytosis of antibody-targeted cells as well as association with and net dephosphorylation within macrophages. Compared to large antibodies, the nS peptides potentially represent an additional class of macrophage checkpoint inhibitors.

Figure 3.1A: Phagocytosis of ‘Self’ cells is inhibited by CD47 binding to SIRPα

Figure 3.1B: nano-Self peptides based on CD47 are made to bind SIRPα as competitive antagonists

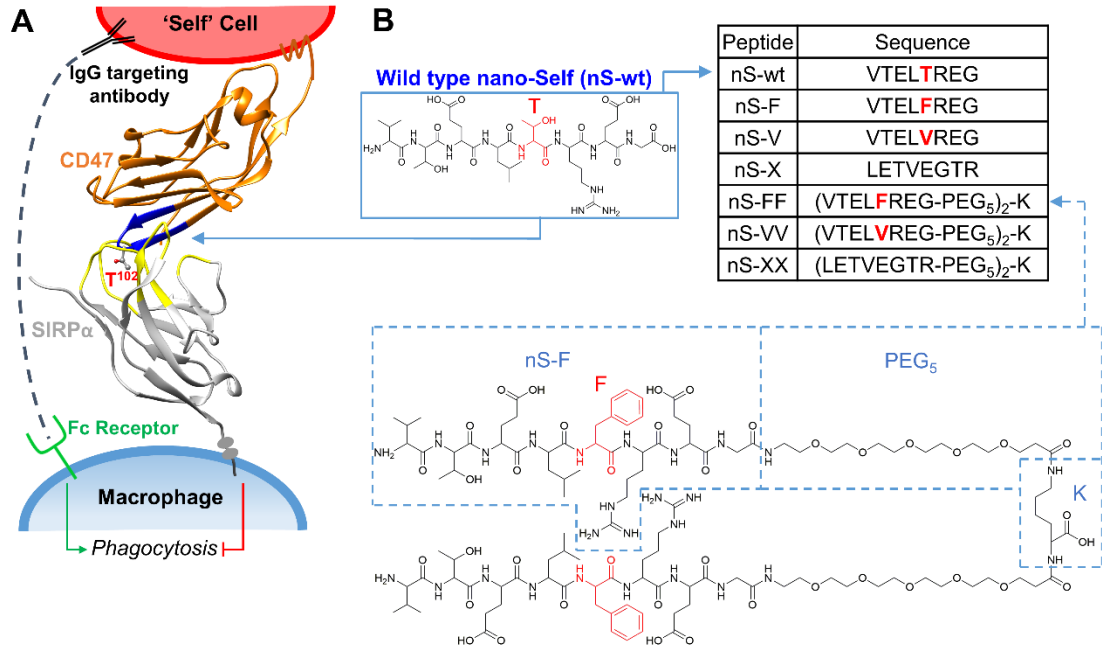


Figure 3.1: nano-Self peptides are designed as competitive inhibitors based on CD47's key binding loop

A. 'Marker of Self' CD47 is expressed on all cells and inhibits phagocytosis of 'Self' cells when it binds its receptor SIRP α on macrophages (Protein Data Base accession number: 2JJS).

B. The nS-wt peptide consists of 8-amino acids (blue) that bind the SIRP α binding pocket (yellow). Substitutions of the Thr residue (red) generate nS peptides as competitive antagonists against SIRP α . nS-X is a scrambled sequence. Bivalent peptides were constructed by linking monomers to (di-PEG)-lysine *via* their C-termini. **Inset table:** Names and sequences of nS peptides.

3.3 Experimental Methods

Solid phase peptide synthesis

a- Standard peptide synthesis

All peptides in this study were synthesized on a Rink Amide MBHA Resin (loading density: 0.33 mmol/g; Novabiochem) on a 100 μ mol scale at room temperature (RT) using 9-fluorenylmethoxycarbonyl (Fmoc) chemistry. The resin was transferred to a solid phase peptide synthesis vessel and swelled in N,N-dimethylformamide (DMF; Sigma) for 30 minutes with stirring. Deprotection of the Fmoc group was achieved by using 1 mL of 1% w/v 1-hydroxybenzotriazole (HoBT; EMD Millipore) and 2% v/v 1,8-diazabicyclo[5.4.0]undec-7-ene (DBU; Acros Organics) in DMF and left to stir for 1 minute (repeated three times). Lastly, resin was then washed thoroughly with DMF. Coupling solutions contained 3 equivalents of Fmoc-amino acids (Chem-Impex or Oakwood Chemicals), 2.8 equivalents of 1-[bis(dimethylamino)methylene]-1H-1,2,3-triazolo[4,5-b]pyridinium 3-oxid hexafluorophosphate (HATU; Oakwood Chemicals), and 6 equivalents of N,N-diisopropylethylamine (DIEA; Sigma) - relative to resin - dissolved in minimal amount of DMF to cover resin (1 – 1.3 mL) and were activated for 5 minutes at RT prior to addition to resin. Coupling reactions were left to proceed for 1 hour. Following each coupling reaction, the resin was drained, washed thoroughly with DMF, deprotected as described above and washed thoroughly with DMF.

b- Bivalent peptide synthesis

Bivalent peptides were prepared by coupling 3 equivalents of Fmoc-Lys(Fmoc)-OH directly on resin and deprotecting the Fmoc groups following the same procedure mentioned above. The coupling solutions of the polyethylene glycol (PEG) acids contained 5 equivalents of Fmoc-NH-PEG₅-CH₂CH₂COOH (PurePEG), 4.5 equivalents of HATU and 10 equivalents of DIEA. The coupling reactions were left to proceed for 3 hours. Every subsequent amino acid coupling was done using 6 equivalents Fmoc-amino acid, 5 equivalents HATU and 10 equivalents DIEA.

c- 5(6)-Carboxyfluorescein (FAM) coupling

All fluorescently labeled peptides were prepared by coupling Boc-Lys(Fmoc)-OH at the N-terminus and deprotection of the Fmoc-protected γ -amine of Lys. FAM (Chem-Impex) was prepared by dissolving 2 equivalents in DMF with 2 equivalents of HATU and added to the resin after activation for 5 minutes at RT. 6 equivalents of DIEA were added dropwise to the stirring solution in order to maintain a homogenous solution.¹⁴⁸ The reaction was left to proceed overnight in the dark.

d- Peptide cleavage

Following the final deprotection of the last Fmoc group (except for fluorescent peptides where the last amino acid contains acid labile Boc protecting group), the resin was washed with DMF twice and then twice more with dichloromethane (DCM; Sigma). A 5 mL cleavage cocktail containing 95% trifluoroacetic acid (TFA; Acros Organics), 2.5% H₂O and 2.5% triisopropylsilane (TIPS; Oakwood) was added to the reaction vessel and left to stir for 4 hours. 45

mL of cold diethyl ether (Sigma) was then added to the cleavage solution precipitating the peptide. To make sure all peptide precipitated, the ether layer was evaporated by air until ~10 mL of solution was left; thereafter, an additional 40 mL of cold ether was added. The peptide was collected by centrifugation, resuspended in cold ether and collected by centrifugation again (repeated three times). Depending on the solubility of the peptide, the ether washed pellet was dissolved in a mixture of 10-40% acetonitrile (ACN; Sigma) in water.

e- Purification and characterization

All peptides were purified using preparative reversed-phase high-performance liquid chromatography (HPLC) on an Agilent 1260 Infinity II system using a Phenomenex Luna Omega 5 μm PS C18 100 Å LC column. Varying gradients of ACN and 0.1% TFA in H₂O were used to separate the respective peptides. Purity of each peptide was checked using an analytical Agilent 1260 Infinity II system using a Phenomenex Luna Omega 5 μm PS C18 100 Å LC column. Mass spectrometry was performed using a Bruker matrix-assisted laser desorption ionization – time of flight (MALDI-TOF) Ultraflex III mass spectrometer and α -Cyano-4-hydroxycinnamic acid (CHCA; Sigma) as the matrix. Peptides were lyophilized using a Labconco FreeZone Plus 12 Liter Cascade Console Freeze Dry system.

f- UV-Vis, circular dichroism (CD) and Fourier Transform infrared (FT-IR) measurements

UV-Vis absorption spectrophotometry was performed using a Jasco V-650 Spectrophotometer and 1 cm path length quartz cells. Lyophilized peptide was

dissolved in 100 μL of phosphate buffered saline pH 7.4 (PBS; Thermo Fischer) and concentration of each peptide was determined by measuring the absorbance at 205 nm and using a calculated extinction coefficient for each peptide due to the lack of aromatic residues in the peptides.^{149,150} For fluorescein labeled peptides, the lyophilized solid was dissolved in 20 μL of dimethyl sulfoxide (DMSO; Sigma) then diluted to 100 μL with PBS. Peptide concentration was determined by measuring the absorbance at 495 nm.

CD experiments were performed using a Jasco J-1500 Circular Dichroism Spectrometer and 1 mm quartz cuvettes. 100 μM samples were prepared for each peptide in sodium phosphate buffer pH 7, and ellipticity was measured from 190 nm to 260 nm at 5 $^{\circ}\text{C}$ and 95 $^{\circ}\text{C}$, respectively.

FT-IR measurements were collected using a Jasco FT/IR-6800 FT-IR spectrometer. Peptide samples were solvent swapped into in deuterated water and deuterated hydrochloric acid. 5 μL droplets of peptide samples were measured at room temperature and absorbance was recorded from 1200-1700 cm^{-1} .

Cell culture

All cells were purchased from American Type Culture Collection (ATCC). Human derived THP-1 monocytes and mouse J774A.1 macrophages were both cultured in RPMI 1640 media (Gibco). Human erythroleukemia K562 cells were cultured in IMDM media (Gibco). All media were supplemented with 10% v/v fetal bovine serum (FBS; Sigma) and 1% v/v penicillin/streptomycin (Sigma). J774A.1 macrophages were grown either as suspension or adherent cultures. To passage adherent J774A.1 macrophages, the cells were gently scraped with a cell scraper (Corning). THP-1 monocytes were cultured in

suspension. Differentiation of THP-1 monocytes to macrophages was achieved by addition of 100 ng/mL phorbol myristate acetate (PMA; Sigma) in media for 2 days (unless stated otherwise) and confirmed by attachment of the macrophages to the bottom of the tissue culture plates.

***In vitro* phagocytosis assay**

Fresh human RBCs were washed twice with 50 mM EDTA (Thermo Fischer) in Dulbecco's phosphate buffered saline (PBS; Gibco) then twice with 5% FBS in PBS. RBCs were opsonized with 20 ug/mL rabbit anti-human RBC antibody (Rockland) in 5% FBS for 1 hour at RT with shaking. For CD47 blocked RBCs, 5 µg/mL of mouse anti-human CD47 (B6H12; BD Biosciences) were added. Thereafter, RBCs were washed with PBS three times and stained with PKH26 dye (1:800 dilution in PBS; Sigma) for 1 hour at RT with shaking in the dark. RBCs were washed and resuspended in PBS.

THP-1 monocytes were PMA differentiated in RPMI for 48 hours. Macrophages were then washed with RPMI media three times. The macrophages were then incubated with 20 nM, 1 µM or 50 µM of the nano-Self peptides for 1 hour at 37 °C, 5% CO₂ and 95% humidity. Those THP-1s were then washed with RPMI three times. J774A.1 macrophages were plated for 24 hours in RPMI. The same peptide blocking procedure as above was used with the addition of a positive control using 5 µg/mL rat anti-mouse SIRPα (P84; BD Biosciences).

Opsonized RBCs were added to macrophages at a ratio of 10:1 for 1 hour at 37 °C, 5% CO₂ and 95% humidity. Macrophages were then washed with RPMI three times. Adherent and uninternalized RBCs were lysed with water for 30 seconds followed by immediate replacement with RPMI media. In order to distinguish the remaining adherent

RBCs from internalized RBCs, opsonized RBCs were stained with AlexaFluor 647 donkey anti-rabbit (binds to rabbit polyclonal opsonin on RBC; Invitrogen) IgG (1:1000) while unopsonized, CD47 blocked RBCs were stained with AlexaFluor 647 donkey anti-mouse (binds to mouse monoclonal anti-CD47 on RBCs; Invitrogen) IgG (1:1000) for 30 minutes. After washing, macrophages were fixed with 4% formaldehyde (Sigma) for 15 minutes at RT, washed with PBS, stained with 1 µg/mL Hoechst 33342 (Invitrogen), and then washed with PBS again.

K562 cells were washed with PBS then stained with 1:10,000 5(6)-carboxyfluorescein diacetate (CFDA; Invitrogen) in PBS for 15 minutes at room temperature in the dark. Cells were washed with PBS to remove excess CFDA dye and then cells were resuspended in IMDM media. K562 cells were opsonized and CD47 blocked using the same antibody concentrations used in the RBC phagocytosis assay (20 µg/mL anti-RBC and 5 µg/mL anti-CD47) for 1 hour on ice in the dark. After washing with IMDM, K562 cells were added to macrophages at a ratio of 5:1 for 2 hours at 37 °C, 5% CO₂ and 95% humidity. THP-1 macrophages were stained with Hoechst 33342 for 15 minutes and then extensively washed prior to the addition of the K562 cells. Afterwards, the macrophages were washed, fixed with 4% formaldehyde, and then washed again.

Fluorescence imaging was performed using an Olympus IX71 with a digital EMCCD camera (Cascade 512B) and a 40x/0.6 NA objective. Confocal imaging was done using a Leica TCS SP8 system with 63x/1.4 NA oil-immersion objective. Quantification was done with ImageJ (NIH). At least 200 cells were analyzed, and experiments were repeated at least three times. Two-tailed student's t-test was used to determine statistical significance.

CD47-Fc inhibition assay

THP-1 monocytes were PMA differentiated in RPMI for 48 hours. The macrophages were washed with RPMI media then incubated with 1 μM or 50 μM of nano-Self peptides for 1 hour at 37 °C, 5% CO₂ and 95% humidity. After washing, the macrophages were incubated with Human TruStain FcX Fc receptor blocking solution (Biolegend) for 10 minutes at room temperature then incubated with 2 $\mu\text{g}/\text{mL}$ CD47-Fc fusion protein (ACRO Biosystems) for 1 hour at 37 °C, 5% CO₂ and 95% humidity. As a negative control, B6H12 was pre-mixed with CD47-Fc at 4 °C on a rotator for one hour. The macrophages were then washed and incubated with 0.5 $\mu\text{g}/\text{mL}$ goat anti-human IgG Fc DyLight 488 (Thermo Fischer) for 1 hour at 37 °C, 5% CO₂ and 95% humidity. Finally, the macrophages were washed, fixed, Hoechst 33342 stained and imaged as described above.

Peptide inhibition assay

THP-1 monocytes were PMA differentiated in RPMI for 48 hours. Macrophages were washed with RPMI three times then incubated with 1 μM or 20 nM nS-FF or nS-VV for 1 hour at 37 °C, 5% CO₂ and 95% humidity. Excess peptide was washed with PBS then 100 μM of either FAM labeled nS-F was added to the bivalent-peptide blocked macrophages for 1 hour as above. As a control, 50 μM of nS-X was used instead of bivalent nS peptides. Excess peptides were washed off with PBS and cells were fixed with 4% formaldehyde for 15 minutes at RT, washed with PBS, stained with 1 $\mu\text{g}/\text{mL}$ Hoechst 33342, and then washed with PBS again. Fluorescence imaging was performed as described above and quantification was done using ImageJ.

SIRP α staining and confocal imaging

THP-1 monocytes were PMA differentiated in RPMI 1640 for 24 hours. J774A.1 cells were plated for 24 hours in media. Cells were washed with RPMI prior to addition of fluorescent peptides. The peptides were left to incubate for 1 hour at 37 °C, 5% CO₂ and 95% humidity. For fixed cell staining, cells were incubated with 4% formaldehyde for 15 minutes prior to the addition of fluorescent peptides whereas for live cell staining, fixation was done after incubation with the FAM-labeled peptides. Nuclei were stained with 1 µg/mL Hoechst 33342. Cells were then washed with PBS three times before analysis. Fluorescence imaging of fixed cells was done as described above. For live cell (without fixation) confocal imaging, cells were washed with respective media three times after nuclei staining instead of PBS. Confocal imaging was done using a Leica TCS SP8 system with 63x/1.4 NA oil-immersion objective. Quantification was done with ImageJ.

Phosphotyrosine staining

THP-1 monocytes were PMA differentiated for 48 hours. Macrophages were washed with RPMI three times then incubated with 50 µM and 20 nM of either nS-F or nS-FF for 1 hour at 37 °C, 5% CO₂ and 95% humidity. The same conditions were replicated with the addition of 5 µg/mL anti-CD47. Excess peptide was washed with PBS and then macrophages were fixed. Permeabilization of the macrophages was achieved with 0.5% Triton-X for 30 minutes. After washing with PBS, the macrophages were incubated with 1:100 mouse anti-pTyr (Santa Cruz Biotechnology) for 1 hour at room temperature with gentle shaking. Macrophages were washed with PBS, then stained with AlexaFluor 488 donkey anti-mouse (1:1000; Invitrogen) and 1 µg/mL Hoechst 33342 for 1 hour with shaking then washed again. Fluorescence imaging and quantification was performed as described above.

Intravenous injections of nS-FF into mice

14-week-old C57BL6/J mice (Jackson Laboratory, Inc.) were anesthetized with 4% isoflurane in air carrier gas, and approximately 140 μ l of blood was drawn retro-orbitally at Days -7, -1, and 4 post-injection of either 100 μ l PBS (vehicle control) or 1 mg/kg ns-FF peptide in 100 μ l PBS. Blood was collected with capillary tubes pre-rinsed with 0.5M EDTA into K₂EDTA microhematocrit tubes to prevent clotting. Injections were given intravenously daily on Days 0, 1, 2, and 3. Mice were weighed at each blood draw and monitored for clinical signs of anemia daily.

GEO microarray analysis

Data from the GEO database was used to obtain gene expression data for key genes associated with macrophage identity. The cell types included in this analysis were human HEK 293T (GEO accession GSE28715), human PMA-differentiated THP-1 macrophages (GEO accession GDS4258), primary mouse macrophages (GEO accession GDS2454) and human K562 erythroleukemia (GEO accession GSE16774 & GSE8832).

Flow cytometry

Fresh human RBCs were washed twice with 50 mM EDTA and then twice with 5% w/v bovine serum albumin (BSA; Sigma) in PBS. K562 cells were collected and washed twice with 5% BSA. RBCs and K562 cells were blocked with 5% BSA for one hour at room temperature on a rotator. Saturating amounts of AlexaFluor 647 mouse anti-human CD47 (B6H12; BD Biosciences) were added to both RBCs and K562 cells and incubated at room temperature on a rotator for one hour. Cells were washed three times with 5% BSA. Flow cytometry was performed on a BD LSRII (Benton Dickinson) at the Penn Cytomics and Cell Sorting Resources Laboratory and analyzed with FCS Express 7 software (De Novo Software).

SIRP α expression and purification

Soluble human SIRP α fused with glutathione s-transferase (SIRP α -GST) was expressed and purified as previously published.⁶⁵

nano-Self peptides binding to soluble SIRP α

a- Peptide biotinylation

NHS-biotin (Thermo Fisher) was mixed with nS-wt and nS-V, respectively, following the manufacturer's protocol. The biotinylated peptides were dialyzed against PBS.

b- Streptavidin-beads binding

Streptavidin-coated polystyrene beads of 2.1 μm radius (Spherotech) were washed and blocked three times in PBS plus 0.4% w/v bovine serum albumin (BSA; Sigma). nS-wt-biotin or nS-V-biotin were incubated with the beads for 1 hour at room temperature with shaking. Beads were washed with PBS, then incubated with recombinant SIRP α for 1 hour on ice. Streptavidin beads were labeled with rabbit anti-streptavidin-FITC (Invitrogen), and SIRP α was stained with mouse anti-SIRP α -allophycocyanin (anti-SIRP α -APC; Invitrogen).

Affinity binding assay

The same binding protocol mentioned above was used. Increasing concentrations (10 nM to 1 mM) of FAM-labeled peptides were incubated with THP-1 macrophages before or after fixation. For J774A.1 macrophages, affinity binding assay was only done on live cells. Fluorescence imaging and analysis were done as described in Methods.

Opsonin Titration

The same phagocytosis protocol as described in Methods was used. Increasing concentrations (from 33 nM to 1.33 μ M) of anti-RBC IgG were incubated with the RBCs. CD47 on RBCs was blocked in all conditions with 5 μ g/mL anti-CD47. Fluorescence imaging and analysis were done as described in Methods.

3.4 Results and Discussion

3.4.1 nano-Self peptide designs, synthesis, and characterization

CD47's 8-amino acid binding loop defines a wildtype nano-Self (nS-wt) and has a central Thr next to a hydrophobic Leu that are buried in SIRP α 's hydrophobic pocket (**Figure. 3.1A**). All co-crystal structures of CD47 and its antagonists show an interaction with this central Thr.¹⁵¹ Furthermore, screening for high affinity mutants of SIRP α 's binding pocket all yielded Phe insertions (with >100-fold higher affinities for CD47 *versus* the sub- μ M affinity of wildtype),¹⁴⁶ which suggests that greater hydrophobicity and/or aromaticity increases affinity. We therefore substituted the Thr with hydrophobic Phe or Val (nS-F and nS-V, respectively, in **Figure. 3.1B: Inset Table**). Phe adds aromaticity and could allow for a pi-stacking interaction with SIRP α 's Phe-74 that points towards CD47's key β -hairpin whereas Val removes the polar hydroxyl group from the similarly sized Thr. Multivalent nS peptide designs are based on the fact that SIRP α is mobile – it accumulates at the phagocytic synapse,⁶⁵ and is likely a homodimer.⁵⁹ A distance of ~2.5 nm between the binding sites of SIRP α homodimers was estimated from simple modeling of crystal structures and led us to design bivalent nS peptides with two flexible PEG₅ nano-linkers of ~1.5 nm length¹⁵² attached to two amines of a central Lys (**Figure. 3.1B**).

All nS peptides were synthesized on a Rink amide resin yielding C-terminal amide functional groups to minimize charge on the peptides. Analytical HPLC followed by MALDI-TOF mass spectrometry characterization showed >98% purity of all synthesized nS peptides (**Figure. 3.2**). Solubility at neutral pH (up to at least 50 μ M) is likely attributable to charge on three of the eight residues.

Figure 3.2: Analytical HPLC traces and MALDI-TOF mass confirmation of all peptides indicate successful and pure synthesis

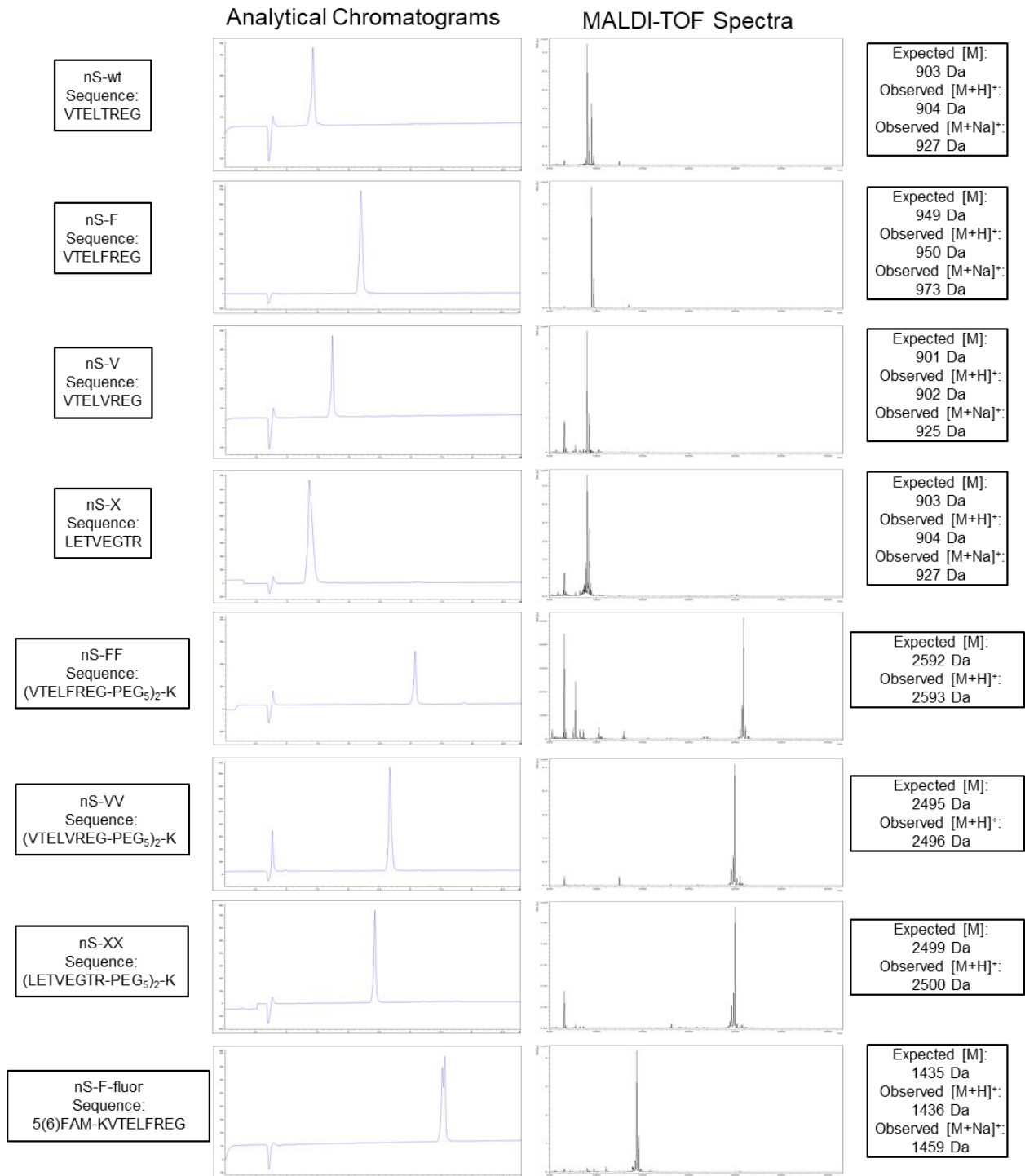


Figure 3.2: Synthesis and purity of nano-self peptides are characterized and confirmed by analytical HPLC and MALDI-TOF mass spectrometry

All peptides used in this assay were run on an analytical HPLC to determine purity of the nS peptides. All analytical traces show one major peak for each peptide. The peptides were all characterized by MALDI-TOF mass spectrometry. Single main peaks appear for the correct mass for all peptides.

3.4.2 nS peptide agonists for human macrophage engulfment of opsonized human cells

Solutions of nS peptides were added to cultures of adherent human THP-1 macrophages (referred to as macrophages; **Figure 3.3A & 3.4**) to study the phagocytosis of two antibody-opsonized human cells: (1) healthy RBCs which serve as a simple ‘self’ cell and are also relevant to the anemia caused by infusion of anti-CD47; and (2) human erythroleukemia K562 cells which serve as a blood cancer cell model relevant to the liquid tumors that show some efficacy when treated with opsonized IgG and anti-CD47.¹¹⁴ After observing and quantifying internalization of RBCs with our bivalent nS-FF peptide by macrophages, we further synthesized a tetravalent peptide to study the effects of multivalency on cancer cells (**Figure 3.3B & 3.5**). Interestingly, all nS peptides, except for scrambled nS-X and nS-XX, enhanced phagocytosis of RBCs opsonized by anti-RBC IgG (**Figures 3.3C & 3.6**). nS-FF was effective even at 20 nM with ~40% of peptide-treated macrophages showing at least one opsonized RBC internalized by the end of the 1 h assay, with an efficacy constant (K_{eff}) of ~ 8 nM indicating >100-fold higher activity than that of nS-wt (**Figure 3.3C**). This key metric of efficacy in promoting phagocytosis follows the trend:

nS-FF > nS-F > nS-VV > nS-V > nS-wt (**Figure 3.3C**)

Furthermore, maximum peptide concentrations of 50 μ M show phagocytosis levels for nS-wt and all nS-F and nS-V variants are well above those for nS-X and nS-XX controls that do not affect baseline engulfment of opsonized RBCs (**Figures 3.3C & D**).

Maximum peptide concentrations reveal an additional effect when compared to anti-CD47 blockade. Combining anti-CD47 with anti-RBC causes ~30% of macrophages

to phagocytose opsonized RBCs, which is higher than the effect of anti-RBC alone (~20% of macrophages contain opsonized RBCs; red open bar in **Figure 3.3D**), consistent with anti-CD47 inhibiting recognition by the macrophage's SIRP α . Likewise, combining nS-wt with anti-RBC also causes ~30% of macrophages to internalize opsonized RBCs. Note that saturating amounts of anti-CD47 on RBCs has minimal effect on baseline engulfment (~5-10% of macrophages) and that anti-RBC is always used at ~133 nM (**Figure 3.7A**). Surprisingly, the highest levels of phagocytosis – with ~40-50% of macrophages containing opsonized RBCs – are seen for all F and V substituted peptides at maximum peptide concentrations (**Figure 3.3D**).

Opsonized erythroleukemia K562 cancer cells were similarly tested for phagocytosis in the presence of our most potent nS-FF and our tetravalent nS-F4 peptides. The anti-RBC successfully opsonized and triggered phagocytosis of K562 cells by macrophages (**Figures 3.3E, F and 3.7B**). Multivalent nS-FF and nS-F4 nearly doubled the percentage of phagocytic macrophages relative to *trans* anti-CD47 blockade whereas macrophages were unaffected by nS-XX control (**Figure 3.3D**). Interaction of the nS peptides with K562 cells is likely minimal due to the relative lack of SIRP α expression (**Figure 3.4**). However, saturation at ~40% of macrophages engulfing opsonized K562 cells is less than the ~50% for opsonized RBCs, perhaps because K562 cells have more CD47 molecules than RBCs, suggesting more “don't eat me” signaling (**Figure 3.8**).

For both opsonized RBCs and opsonized K562s (**Figures 3.3D, F**), the *hyper-phagocytosis* that is achieved with soluble F- and V- nS peptides matches the recently measured increases for disruption of both (i) the *trans* interactions between CD47 on a target and macrophage SIRP α and also, importantly, (ii) the *cis* interactions between CD47

and SIRP α on the same macrophage (**Figure 3.3G-left**).⁷⁴ Expression profiling of macrophages confirms these cells generally express CD47 at roughly similar levels to other cell types (**Figure 3.4**). The recent study showed that macrophage-CD47 knockdown removed a basal level of inhibitory ‘self’ signaling from the *cis* interaction and thereby caused hyper-phagocytosis, with similarly increased phagocytosis when anti-CD47 was added to macrophages separate from adding anti-CD47 to block the target. A preliminary conclusion is that nS-FF and the other substituted peptides, which were designed to bind SIRP α , inhibit both the *cis* and *trans* interactions between SIRP α and CD47 (**Figure 3.3G G-right**).

Consistent with the results with human macrophages, mouse-derived J774A.1 macrophages show all of the same trends for nS-F, nS-V, nS-wt, and nS-X peptides, including 3-fold more phagocytosis with nS-F relative to the minimal internalization of opsonized RBCs in the presence of nS-X control (**Figures. 3.7C**). The ~10-20% increase in phagocytic mouse macrophages with F and V substituted nS peptides relative to anti-CD47 on opsonized RBCs agrees with the *cis* and *trans* inhibition effect, and the nS-wt peptide matches anti-CD47 blockade effects – at least for high concentration (50 μ M). Indeed, the effective activity of nS-wt is ~100-fold weaker in the mouse macrophage assay than in the human assay (**Figure 3.3C**). The difference could reflect a singular difference between the 8-residue sequences of human and mouse CD47’s: the Thr in human-CD47 is replaced by a less bulky and less hydrophobic Ser in mouse-CD47, which again affirms that sequence matters. The various phagocytosis results lead us to further hypotheses on peptide functions (**Figure 3.3G**). First, nS-F peptide should associate directly with

macrophages, and moreso than nS-X but less so than nS-FF. Second, nS-F and nS-FF peptides affect phosphotyrosine levels that are downstream of SIRP α binding to CD47.⁷⁴

Figure 3.3: Soluble nano-Self peptides show nanomolar activity in enhancing phagocytosis of antibody opsonized targets

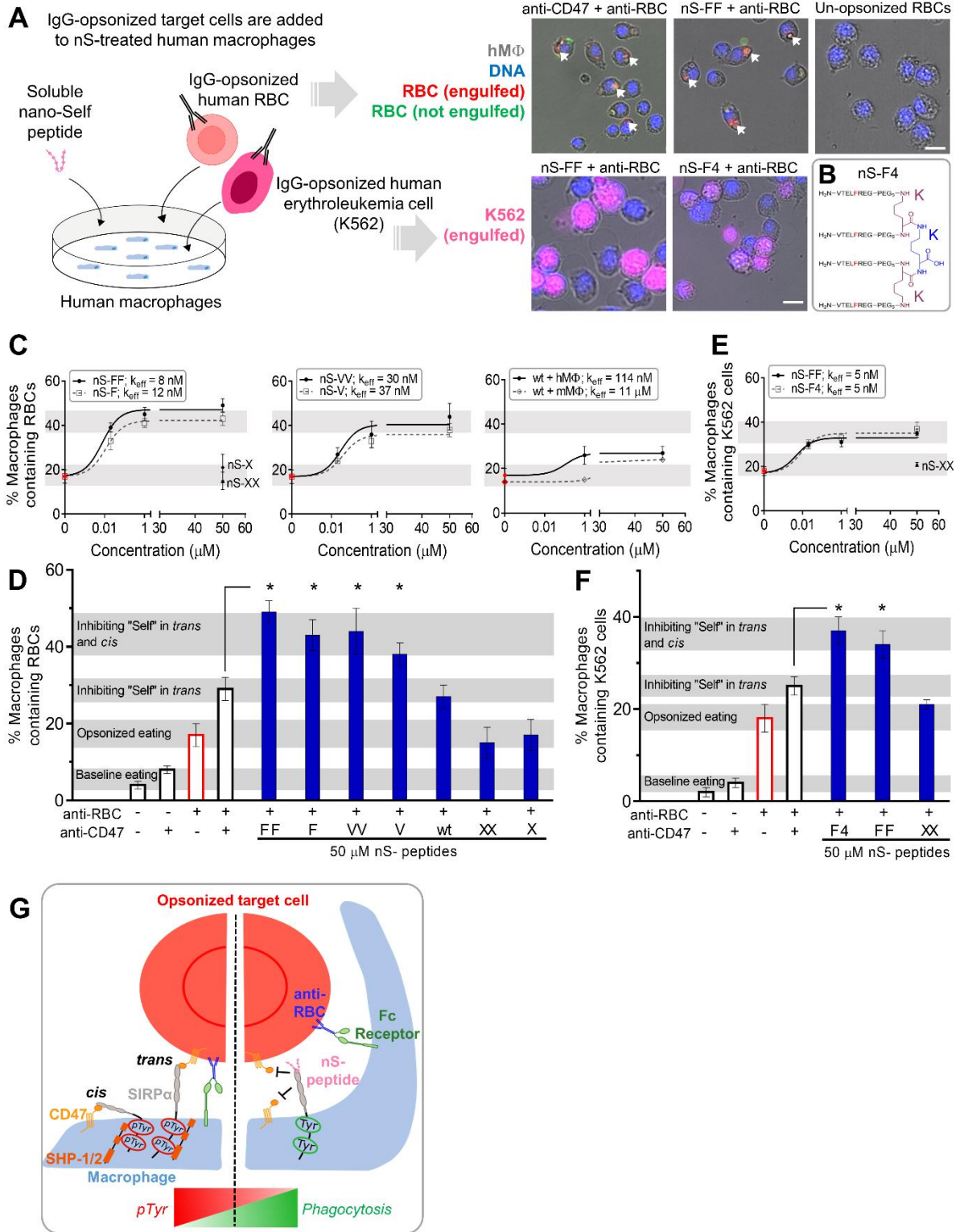


Figure 3.3: Multivalent nano-Self peptides enhance human macrophage phagocytosis of opsonized targets

A. Schematic of the phagocytosis assay. RBC and K562 erythroleukemia cell opsonization and the treatment of the macrophages with the nS peptides are done separately. Afterwards, opsonized cells are added to the macrophages, and then phagocytosis is measured by counting macrophages with internalized target cells. Addition of nS peptides effectively increases phagocytosis of opsonized cells per fluorescence microscopy images (scale bar: 25 μm).

B. Sketch of the tetravalent nS-F4 which consists of a core lysine coupled through both amine functional groups to two lysine residues giving rise to four reactive amine groups. Four simultaneous couplings of the nS-F sequence results with the tetravalent scaffold.

C. Incubating various concentrations of the nS peptides with macrophages results in varying levels of macrophages that internalize at least one opsonized RBC. Relative to nS-wt, substitutions of the key Thr enhanced phagocytosis as did multivalency. Scrambled nS-X or nS-XX peptides do not have effects on phagocytosis. Phagocytosis by mouse macrophages is also affected by nS-wt, albeit not as much as with human macrophages. Baseline phagocytosis of opsonized red blood cells is represented by the red data points. Microscopy fields were selected randomly and at least 200 macrophages were analyzed per condition ($n = 3 \pm \text{SEM}$).

D. Saturating macrophages with nS-FF, nS-F and nS-VV enhances phagocytosis of opsonized RBCs significantly by an additional ~10-20% relative to anti-CD47 treatment of opsonized RBCs. nS-wt is least effective but gives the same result as anti-CD47 and is greater than just opsonized RBCs. Microscopy fields were selected randomly and at least

200 macrophages were analyzed per condition ($n = 3 \pm \text{SEM}$; * denotes $p < 0.05$ relative to CD47-blocked and opsonized RBCs).

E. Effects on phagocytosis of K562 erythroleukemia cells are enhanced by nS-FF and nS-F4. The increase in valency appears to have a slight effect at high concentration of peptide but phagocytosis levels were largely similar between bivalent and tetravalent peptides.

F. Saturating macrophages with nS-FF and nS-F4 significantly increases phagocytosis of opsonized K562 cancer cells by about two-fold relative to opsonized and CD47 blocked cells with only opsonization effect observed with nS-XX addition.

G. Schematic of potential mechanism by which the nS peptides engage and enhance phagocytosis. **Left panel:** CD47-expressing cells signal 'self' to macrophage through engagement of CD47 on the cell surface with SIRP α on the macrophage, increasing pTyr signals, and overriding pro-phagocytic signaling from the opsonizing anti-RBC IgG antibody ultimately inhibiting phagocytosis. **Right panel:** nS peptides engage with SIRP α , inhibiting *trans* binding of CD47 on opsonized cells and inhibiting *cis* binding on the macrophages, leading to increased phagocytosis.

Figure 3.4: PMA differentiated THP-1 macrophages have an identical gene profile as primary mouse macrophages based on microarray gene expression analysis

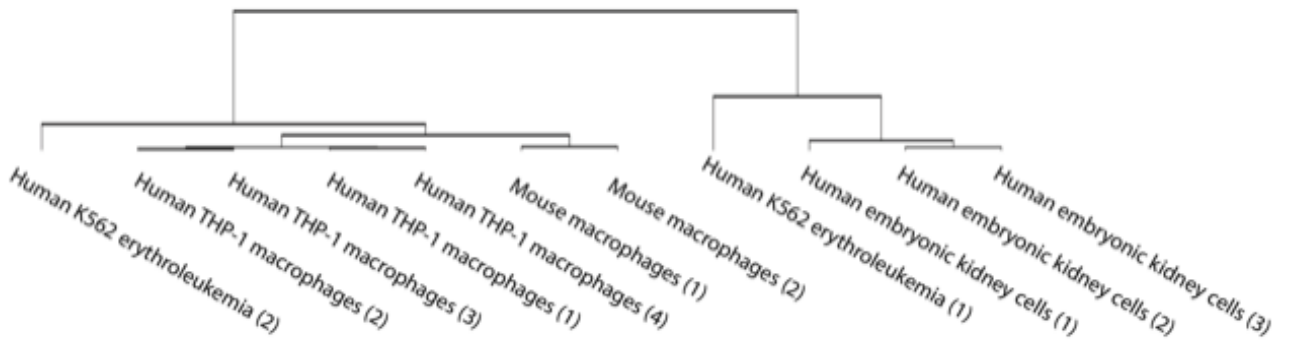
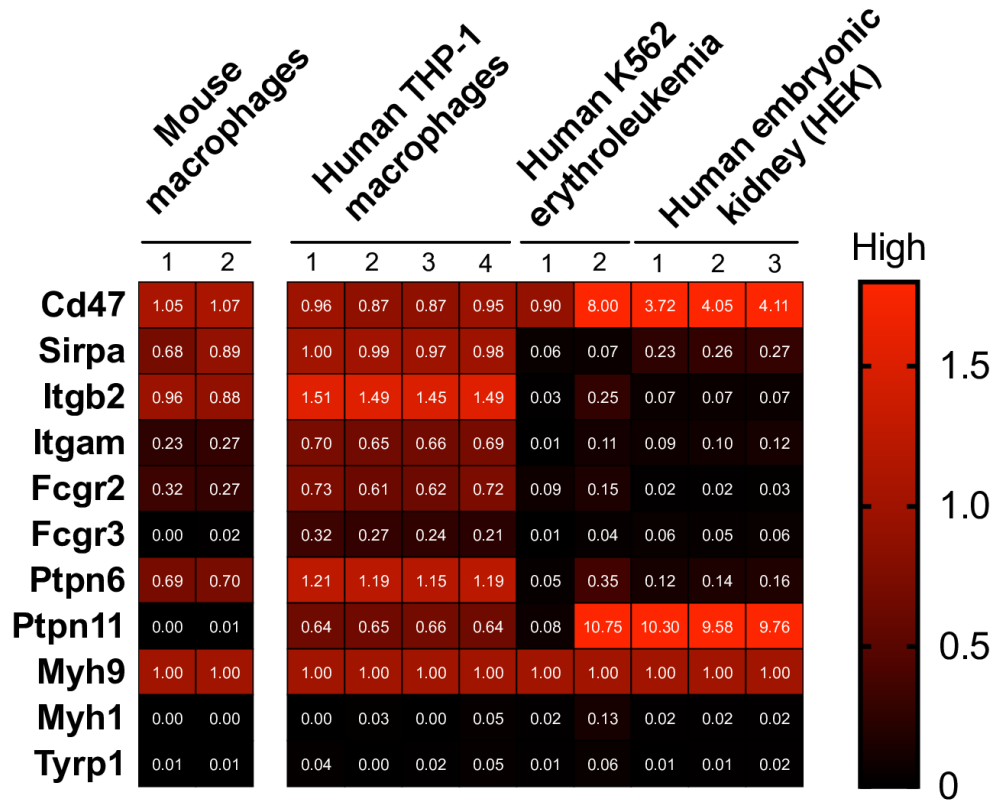


Figure 3.4: PMA differentiated THP-1 cells share identical gene profiles as primary macrophages for key, pathway-relevant factors

(Top) Microarray gene expression analysis⁷⁴ verification that PMA differentiated THP-1 macrophages express several key macrophage factors at similar levels as primary mouse macrophages (*i.e.* Sirpa, the Integrin (Itg) genes, Fcgr genes, and SHP1 gene Ptpn6), while differing from other hematopoietic and non-hematopoietic cells (K562 and HEK, respectively). Positive control genes are the ubiquitous Cd47 and the widely expressed nonmuscle myosin-II gene, Myh9. Negative control genes are skeletal muscle myosin, Myh1, and melanin synthesis gene, Tyrp1.

(Bottom) Dendrogram from hierarchical clustering analysis validating similar profiles between marrow-derived mouse macrophages and PMA-differentiated THP-1 macrophages while clearly distinct from other cell types.

Figure 3.5A: Sequence of tetravalent nano-Self peptide “nS-F4”

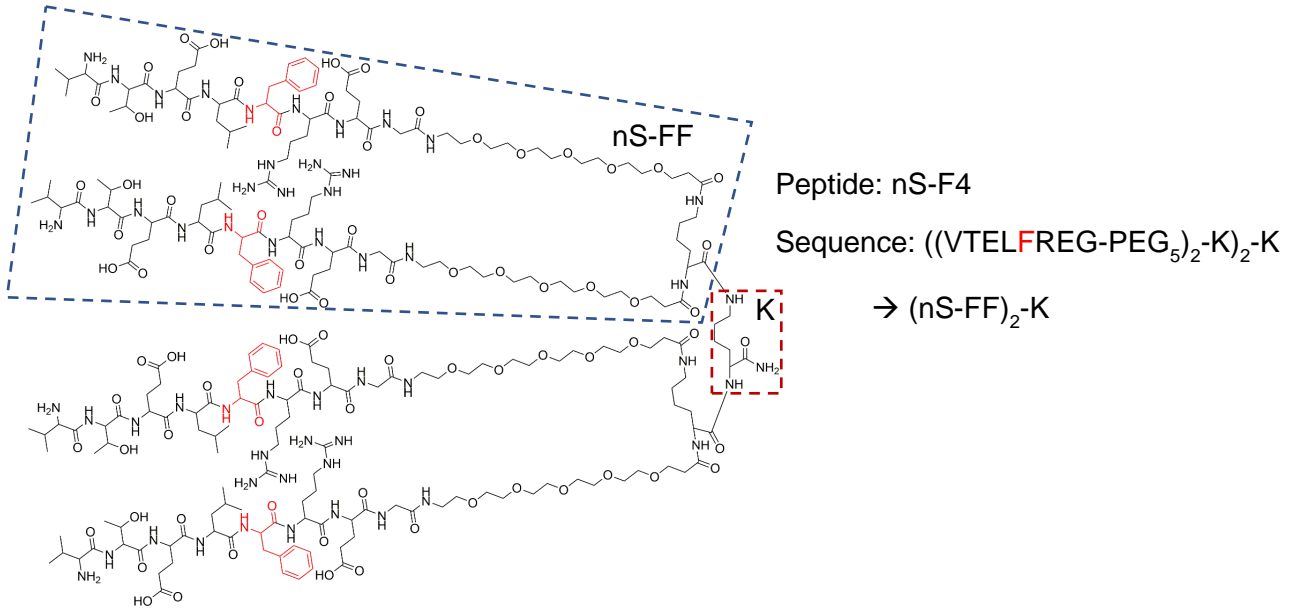
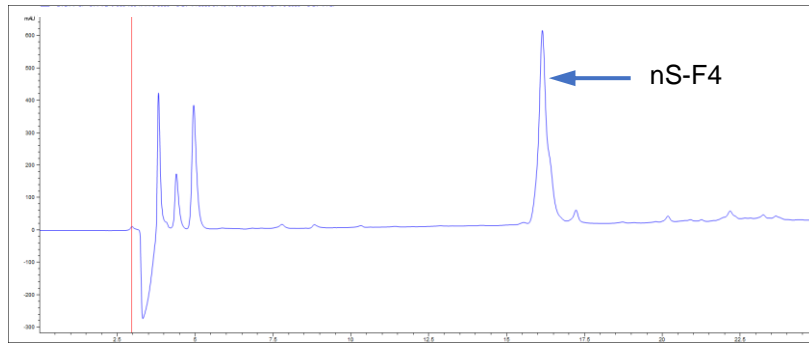


Figure 3.5B: Analytical HPLC chromatogram and MALDI-TOF mass spectrum

indicate successful synthesis of tetravalent nS-F4

HPLC: 5-40% CH₃CN in 0.1% TFA/H₂O over 24 minutes at room temperature



MALDI-TOF: 2 μL CHCA matrix + 2 μL of sample

Expected mass [M]: 5295 Da Observed mass [M]⁺: 5295 Da

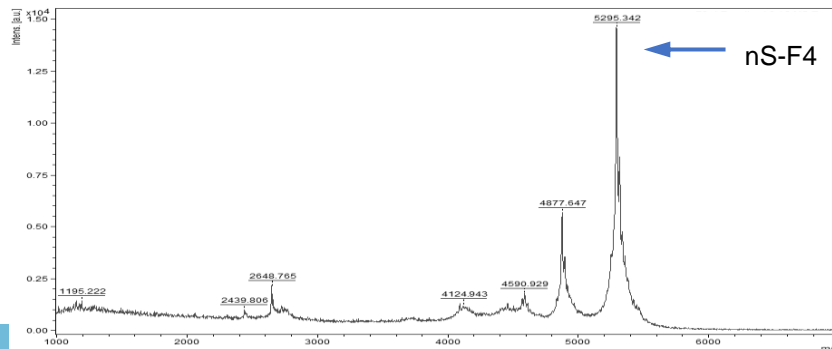


Figure 3.5: Successful synthesis and purification of tetravalent nano-Self-F peptide (nS-F4)

A. Chemical structure sketch of tetravalent nano-Self peptide.

B. One main peak was observed in the analytical trace and MALDI-TOF chromatogram corresponding to the correct mass of nS-F4 indicating successful and pure synthesis of nS-F4.

Figure 3.6: Phagocytosis levels are significantly greater than all control conditions when macrophages are incubated with bivalent nano-Self peptides

	+ 50 μ M X + anti-RBC	+ 50 μ M XX + anti-RBC	+ 50 μ M wt + anti-RBC	+ 50 μ M V + anti-RBC	+ 50 μ M VV + anti-RBC	+ 50 μ M F + anti-RBC	+ 50 μ M FF + anti-RBC	+ anti-CD47 + anti-RBC	+ anti-RBC	+ anti-CD47
RBCs alone	*	*	*	*	*	*	*	*	*	*
+ anti-CD47	*		*	*	*	*	*	*	*	
+ anti-RBC			*	*	*	*	*	*		
+ anti-CD47 + anti-RBC		*		*	*	*	*			
+ 50 μ M FF + anti-RBC	*	*	*							
+ 50 μ M F + anti-RBC	*	*	*							
+ 50 μ M VV + anti-RBC	*	*	*							
+ 50 μ M V + anti-RBC	*	*								
+ 50 μ M wt + anti-RBC		*								
+ 50 μ M XX + anti-RBC										

Figure 3.6: Treatment of human macrophages with multivalent nano-Self peptides enhances phagocytosis levels significantly relative to peptide and antibody controls

All conditions were compared with each other to determine which conditions were significantly different (* denotes $p < 0.05$ for statistical significance between conditions). Both multivalent peptides enhanced macrophage phagocytosis significantly compared to all control conditions.

Figure 3.7A & B: Anti-RBC titration curves to determine amount of opsonin needed for optimal and comparable engulfment of target cells by macrophages

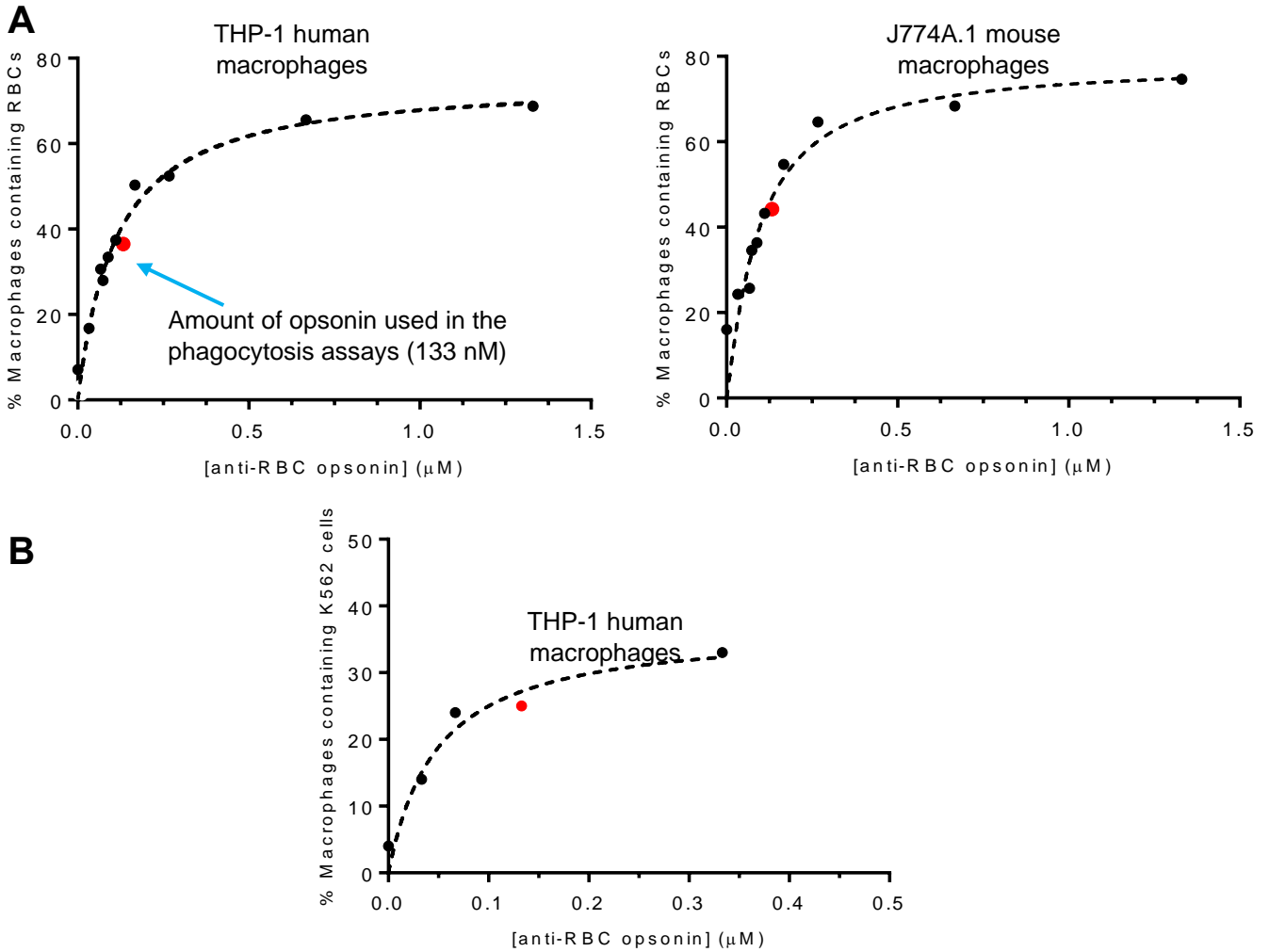


Figure 3.7C: Soluble nano-Self peptides enhance phagocytosis of opsonized red blood cells in J774A.1 mouse macrophages

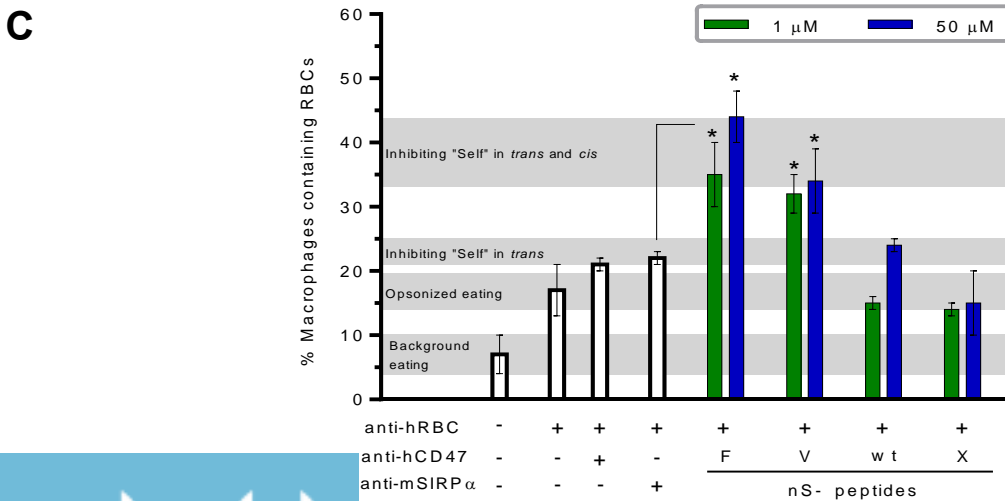


Figure 3.7: Using optimal concentration of opsonin allows for comparison of macrophage phagocytosis

Varying concentrations of anti-RBC opsonin incubated with CD47-blocked RBCs (**A**) and K562 cells (**B**) to determine the optimal amount of opsonization necessary for optimal phagocytosis. Human and mouse macrophages responded differently to RBC opsonization, which may be a result of the polyclonal antibody and how it engages with FcRs on the respective macrophages. The optimal concentration for phagocytosis assays was selected to be 133 nM (red point) because it gave a reasonable phagocytosis response far from baseline and saturation.

C. Treating mouse macrophages with nS peptides results in enhanced engulfment of opsonized RBCs.

Figure 3.8: Greater number of CD47 molecules are on the surface of human erythroleukemia K562 cells when compared to healthy red blood cells

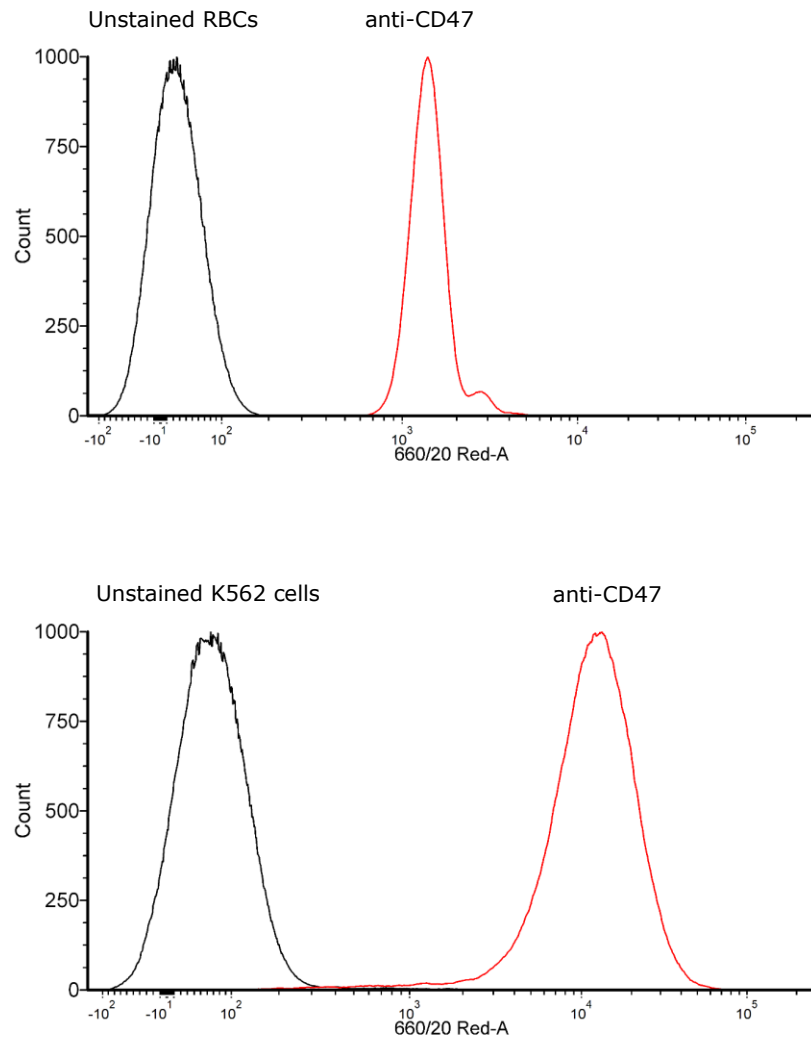


Figure 3.8: CD47 expression on RBCs and K562 cancer cells

Flow cytometry quantitation of primary fluorescent anti-CD47 antibody. Samples were analyzed the same day using the same voltage settings on the flow cytometer. Higher numbers of CD47 molecules are present on the surface of K562 cells when compared to RBCs.

3.4.3 Multivalent nS peptides inhibit CD47-Fc binding to human macrophages

To determine whether the nS peptides bind to SIRP α , we used nS-FF and nS-F4 as soluble competitive inhibitors of saturable CD47-Fc fusion protein binding to macrophages (**Figure 3.9**). Addition of multivalent nS peptides was followed by Fc-receptor blockade to minimize Fc-driven binding of construct. Afterwards, CD47-Fc was added and then finally anti-Fc fluorescence imaging was performed (**Figure 3.10**). Quantitation of fluorescence shows the expected trend for the levels of inhibition:

$$\text{nS-F4} \sim \text{nS-FF} > \text{nS-wt} > \text{nS-XX} (= 0)$$

Anti-CD47 was pre-incubated with CD47 as a positive control for inhibition of binding to SIRP α .¹⁵¹ This showed that both nS-F4 and nS-FF are as inhibitory as anti-CD47.

Figure 3.9: CD47-Fc binding assay to determine apparent binding constant for THP-1

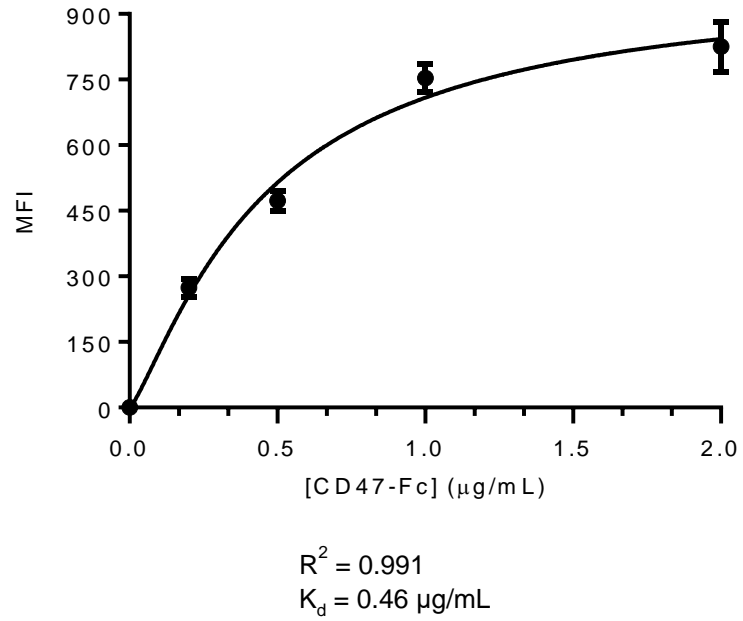


Figure 3.9: CD47-Fc binding curve

Varying concentrations of CD47-Fc incubated with human THP-1 macrophages and measured by anti-Fc fluorescence. Apparent K_d was determined to be 0.46 $\mu\text{g}/\text{mL}$.

Figure 3.10: Multivalent nano-Self peptides inhibit high affinity CD47-Fc binding to THP-1, which suggests peptide binding to SIRP α

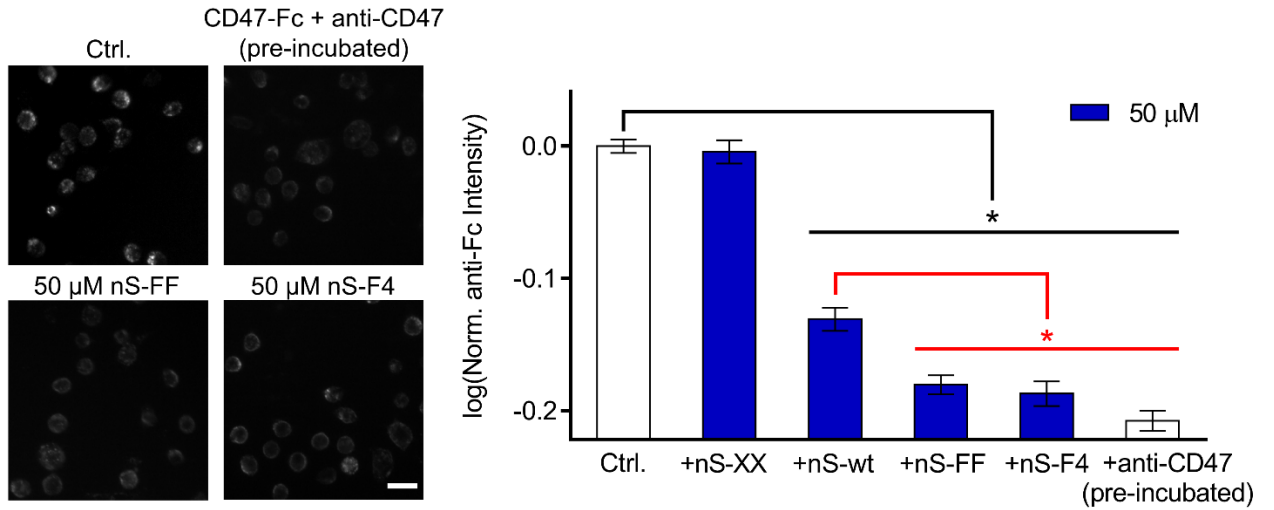


Figure 3.10: Binding of nano-Self peptides is consistent with SIRP α inhibition

Representative fluorescence microscopy images of CD47-Fc inhibition by multivalent nS-F4 and nS-F4 peptides. Anti-CD47 and CD47-Fc were incubated together prior to their addition to macrophages. All conditions were compared to saturating concentration of CD47-Fc. Quantitation was done by measuring anti-Fc fluorescence ($n = 2 \pm \text{SEM}$; * denotes $p < 0.05$; scale bar: 50 μm).

3.4.4 Tyrosine phosphorylation in macrophages is suppressed by nS peptides

Given that the interaction of CD47 with SIRP α initiates a de-phosphorylation cascade regardless of whether the interaction occurs in *trans* or in *cis*,^{65,74} two key nS peptides were again added to the macrophages for quantitative fluorescence microscopy. Basal levels of phosphotyrosine (pTyr) in wildtype macrophages are indeed suppressed by nS-FF and by anti-CD47 (**Figure 3.11A**). Importantly, nS-FF suppressed pTyr signal at the low peptide concentration (20 nM; **Figure 3.11A**) that maximizes phagocytosis by blocking both *trans* and *cis* interactions (**Figure 3.3C**). Monovalent nS-F at the high concentration (50 μ M) – that likewise maximized phagocytosis – also suppressed pTyr, whereas 20 nM nS-F did not significantly affect pTyr, consistent with blocking only *trans* interactions at the low concentration (**Figures 3.3C & D**). The negative control peptide nS-X (50 μ M) had no effect on pTyr, which is consistent with the lack of effect in phagocytosis. Note that anti-CD47 in the phagocytosis studies was added to the opsonized RBCs and K562 cells blocking only the *trans* interactions, whereas in these pTyr experiments (**Figure 3.11A**), anti-CD47 was added to the macrophages to determine the effect on basal signaling in the absence of phagocytosis. The pTyr results are not only consistent with peptide disruption of *cis* interactions between CD47 on the surface of the macrophage and SIRP α (**Figure 3.11B**), but further underscore the functional potency of multivalent nS peptides.

Figure 3.11: Bivalent nano-Self peptides at nanomolar concentration suppress macrophage phosphotyrosine

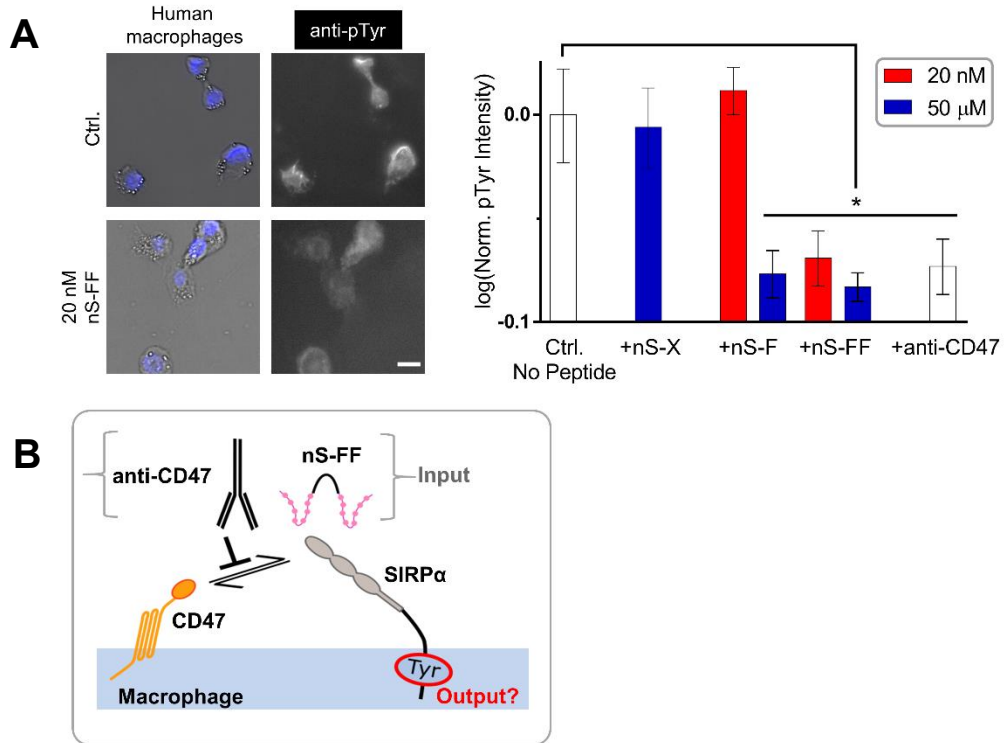


Figure 3.11: Bivalent nano-Self peptides suppress macrophage phosphotyrosine levels consistent with disruption of ‘Self’ signaling in *cis*

A. Basal levels of pTyr signal are observed in isolated macrophages. pTyr signal is suppressed upon the addition of nS-FF. pTyr levels decrease in isolated macrophages when either CD47 is blocked or nS peptides are added. This inhibition of phosphorylation is not observed when macrophages are treated with nS-X, supporting that the loss of phosphorylation signal is due to inhibition of CD47-SIRP α binding. Multivalent nS-FF suppressed pTyr at nanomolar concentrations, whereas no effect was observed with monovalent nS-F, consistent with higher affinity of multivalent nS peptides ($n = 3 \pm \text{SEM}$; * denotes $p < 0.05$ relative to control; scale bar: 25 μm).

C. Schematic representing potential mechanism of nS peptides antagonizing the macrophage checkpoint. Anti-CD47 binds CD47 on the surface of macrophages, inhibiting its binding to SIRP α binding thus suppressing pTyr. Addition of nS peptides replicates the same effect of suppressing pTyr to similar levels as anti-CD47 blockade, consistent with - and providing an explanation for - the phagocytosis results. This suggests disruption of the CD47-SIRP α axis.

3.4.5 Competitive binding of nS peptides to macrophages

To assess peptide association, nS-F was fluorescently labeled (denoted nS-F-fluor) and added to macrophages. Fluorescence microscopy shows nS-F-fluor associates with all cells (**Figure 3.12A**, Ctrl), consistent with SIRP α expression on all macrophages. Some evidence of internalized fluorescent peptide signal is consistent with SIRP α internalization as part of the recycling of such cell surface receptors.¹⁵³⁻¹⁵⁵ To demonstrate the increased affinity of bivalent nS peptides relative to monovalent nS-F, unlabeled nS-FF and nS-VV were added as inhibitors to cultures with 100 μ M nS-F-fluor. Bivalent peptides at just 20 nM significantly decreased association of nS-F-fluor with macrophages whereas nS-X showed no effect up to 50 μ M (**Figure 3.12B**).

Biotinylated-nS peptides were also used to confirm association with SIRP α by incubating streptavidin-coated polystyrene micro-beads first with a biotinylated-nS and then with purified recombinant human SIRP α extracellular domain⁶⁵ plus fluorescent (non-blocking) anti-SIRP α (**Figure 3.13**). Given the effect on phagocytosis after the addition of nS peptides to both human and mouse macrophages, association of nS-fluor peptides with both species of macrophages was investigated. From imaging analysis, there was indication of some internalization similar to anti-mouse SIRP α (P84-FITC) (**Figures 3.14A & B**), especially at high peptide concentrations ($\gg 1$ μ M). For nS-X, which showed no effect on phagocytosis, total fluorescence intensity of nS-X-fluor associating with the macrophages proved significantly lower and >5 -fold weaker than the other functional peptides (**Figure 3.14C**).

Figure 3.12: Bivalent nano-Self peptides outcompete monovalent nano-Self in interacting with macrophages

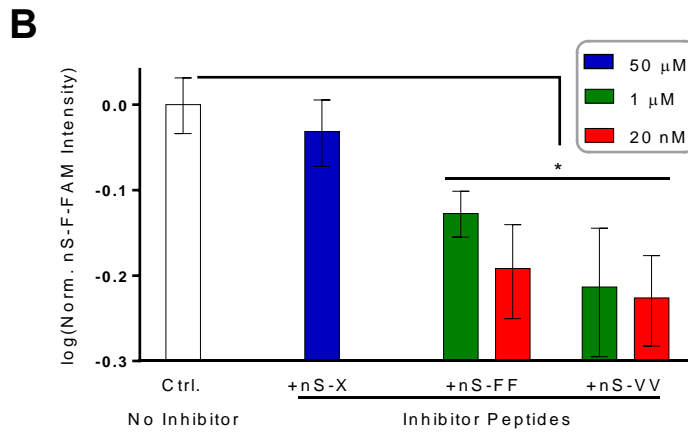
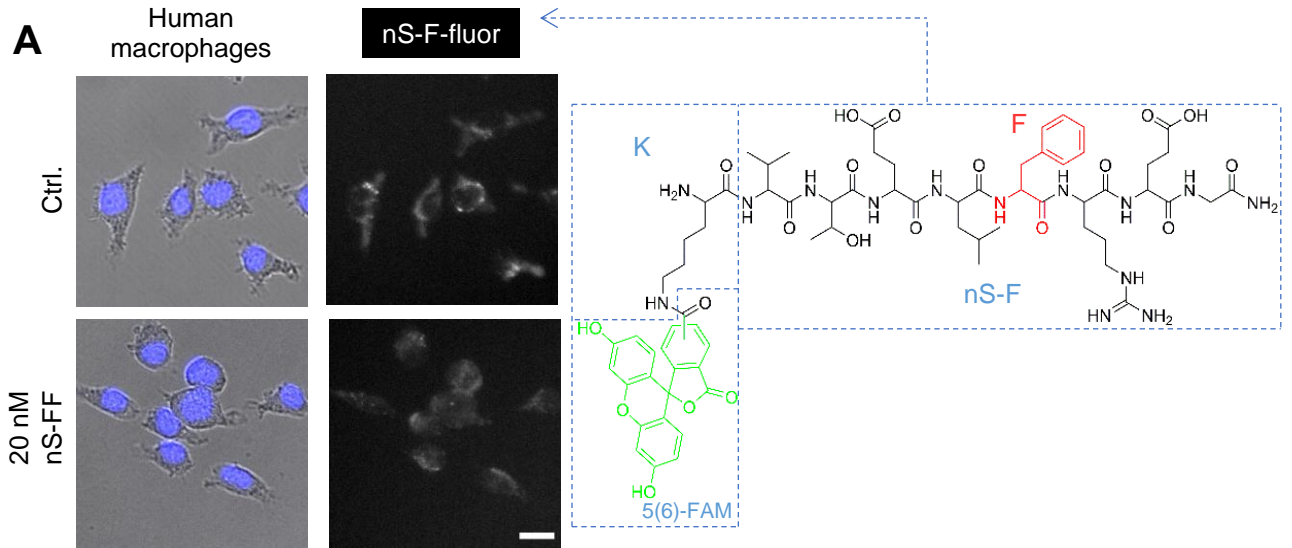


Figure 3.12: Bivalent nano-Self outcompete monovalent association with macrophages

A. Representative fluorescence microscopy images of nS-F-fluor fluorescence inhibition on macrophages after addition of multivalent nS peptide inhibitors (scale bar: 25 μm).

B. Bivalent peptides show higher affinity towards macrophages by outcompeting the binding of monovalent nS-F-fluor ($n = 2 \pm \text{SEM}$; * denotes $p < 0.05$ relative to control).

Figure 3.13: Immobilized nano-Self peptides bind to recombinant SIRP α

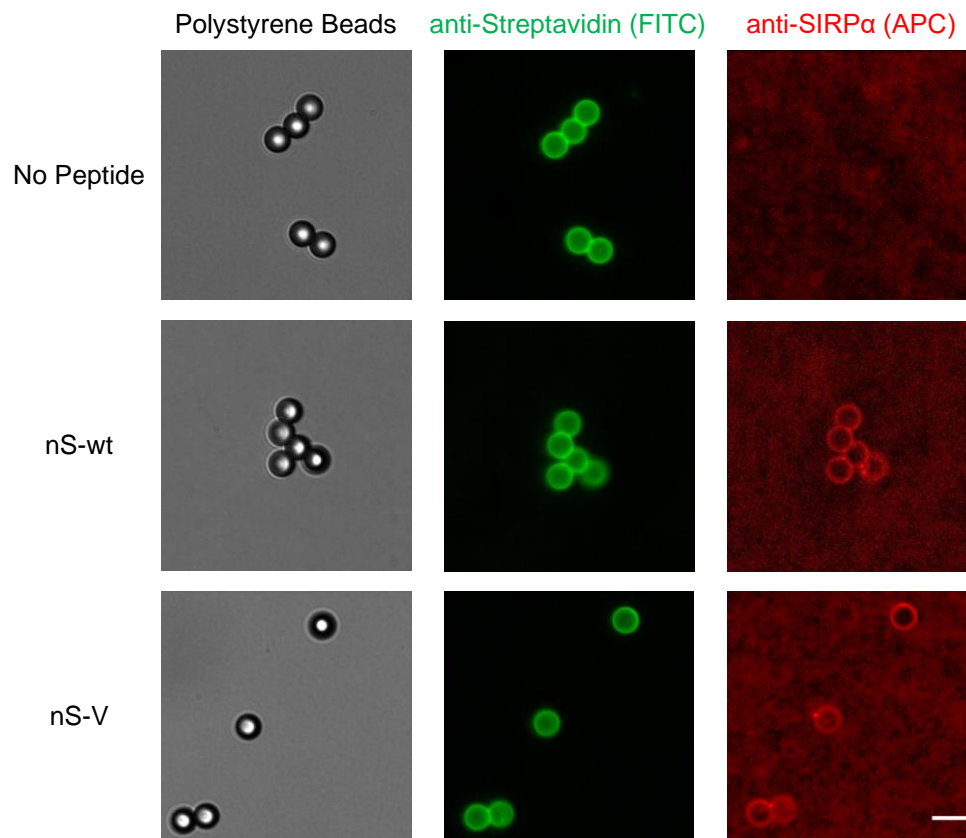


Figure 3.13: Immobilized nano-Self peptides bind to soluble SIRP α

Polystyrene beads coated with streptavidin incubated with or without biotinylated nS-wt or nS-V. After immobilizing the nS peptides, recombinant CD47-binding domain of SIRP α was added. SIRP α was then stained with nonblocking APC-labeled primary antibody. Fluorescence is only observed in the presence of biotinylated peptide (scale bar: 5 μ m).

Figure 3.14: nano-Self peptides bind SIRP α on macrophages

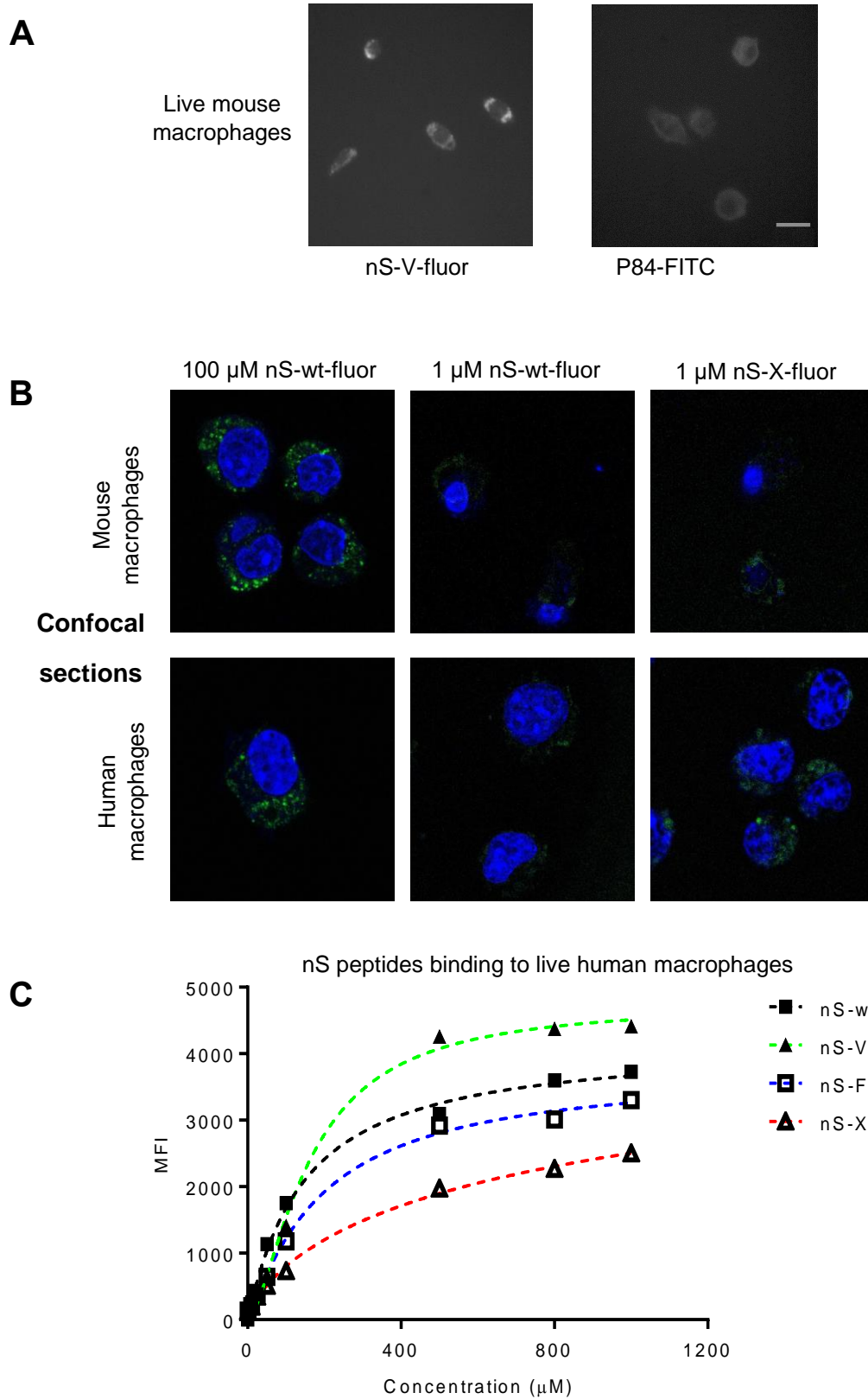


Figure 3.14: nano-Self peptides bind to membrane bound SIRP α and are also internalized by human and mouse macrophages

A. Fluorescence images of nS-V-fluor and P84-FITC bound to the surface of live mouse macrophages (scale bar 25 μ m).

B. Confocal z-stack images of mouse and human macrophages incubated with FAM-labelled peptides. In addition to membrane binding, internalization of nS-wt occurs more readily at higher concentrations leading to higher fluorescence intensity. At low concentrations (1 μ M), the peptide is mainly internalized with minimal membrane staining hence the decrease in fluorescence.

C. Fluorescent nS peptides binding to the surface of live human macrophages.

3.4.6 nS peptides are mainly disordered, with binding likely to enhance β -hairpin structure

Because of the snug fit of the key CD47 β -hairpin within SIRP α (**Figure 3.1A**), we investigated the secondary structures of the 8-amino acid peptides in solution using circular dichroism (CD) (**Figures 3.15 & 3.16**). At low temperature (5 °C), the peptides are largely random coils with a minor fraction of β -turn structure when compared to other short peptides.¹⁵⁶⁻¹⁵⁸ This is evident for the most functional peptide nS-FF as a slight positive ellipticity peak at 215-220 nm and deep negative ellipticity peak around 195 nm — signals that are somewhat clear for the slightly less functional nS-VV peptide but much attenuated for nS-XX or nS-X. Thermal unfolding at 90 °C is evident in suppression of the ellipticity peaks. Difference spectra (**Figure 3.15B**) are the same for the bivalent nS-FF and nS-VV, whereas nS-XX is attenuated – showing a trend similar to the phagocytosis results (**Figures 3.3C-F**).

The nS peptides here are mainly random coils (**Figures 3.15 & 3.16**), which suggests an induced fit association with SIRP α on macrophages. Phagocytosis levels of nS peptide treated macrophages were compared to anti-CD47 blockade of the target, with bivalent nS-FF and tetravalent nS-F4 proving to be more potent in enhancing phagocytosis at pharmacologically relevant concentrations (20 nM) (**Figures 3.3C-F**). The slight increase of phagocytic macrophages when cultured with nS-F4 *versus* nS-FF (**Figure 3.3F**) seems consistent with increased avidity as a soluble inhibitor (**Figure 3.17**), which supports an advantage of multivalency, even though the effects plateau. The increased levels of target phagocytosis are consistent with *cis* and *trans* inhibition,⁷⁴ and nS-FF's suppression

of phosphorylation in isolated macrophages is consistent with blocking of *cis* binding of SIRP α to CD47 (**Figures 3.11A & B**).

Figure 3.15: Disordered structure with *some* hairpin content suggests induced fit into SIRP α binding pocket

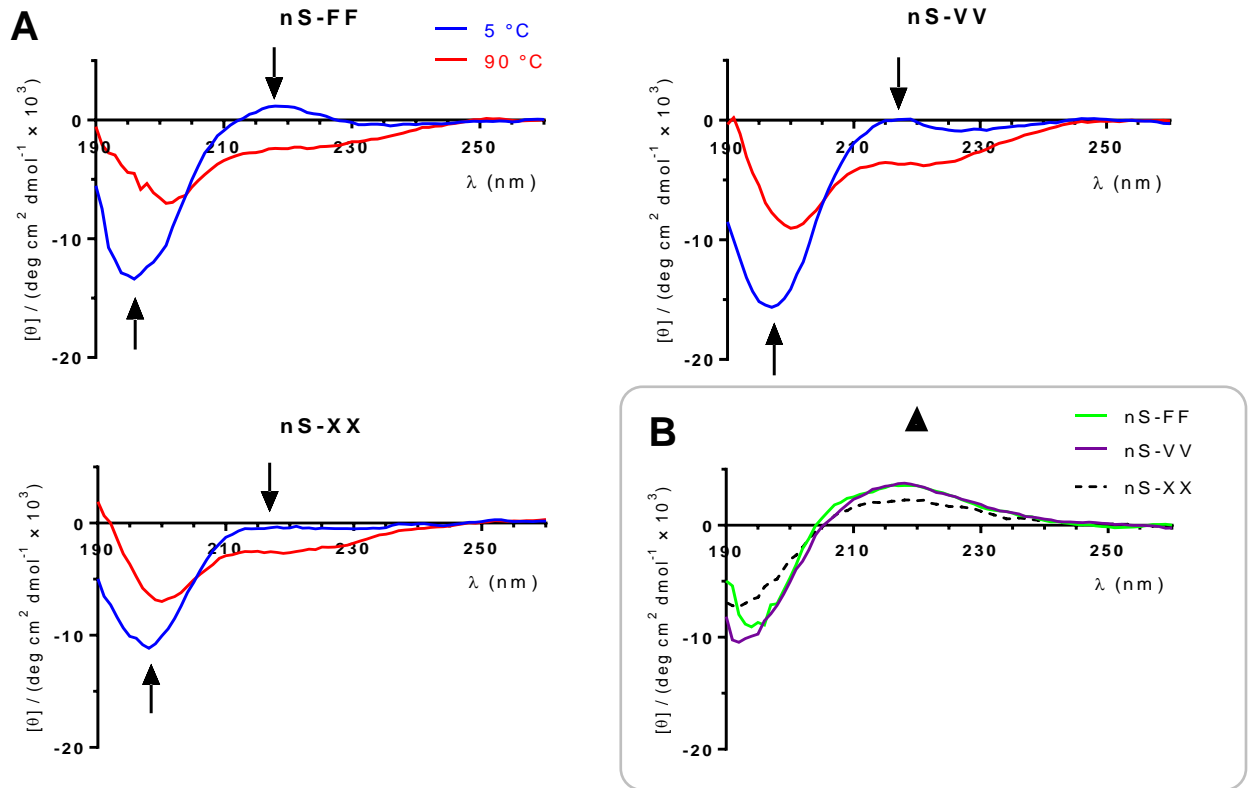


Figure 3.15: Random coil structure with some hairpin folding suggests induced fit mechanism into SIRP α binding pocket

A. CD spectra of nS-FF, nS-VV, nS-XX at 5 and 90 °C. Arrows indicate the molar ellipticity at 215-220 nm and 195 nm, respectively, suggestive of some β -hairpin turn which is lost in nS-XX.

B. Difference plots show nS-FF and nS-VV are in agreement in terms of structure, consistent with phagocytosis results.

Figure 3.16: Hairpin structure of monovalent nano-Self peptides is consistent with fitting into SIRP α binding pocket

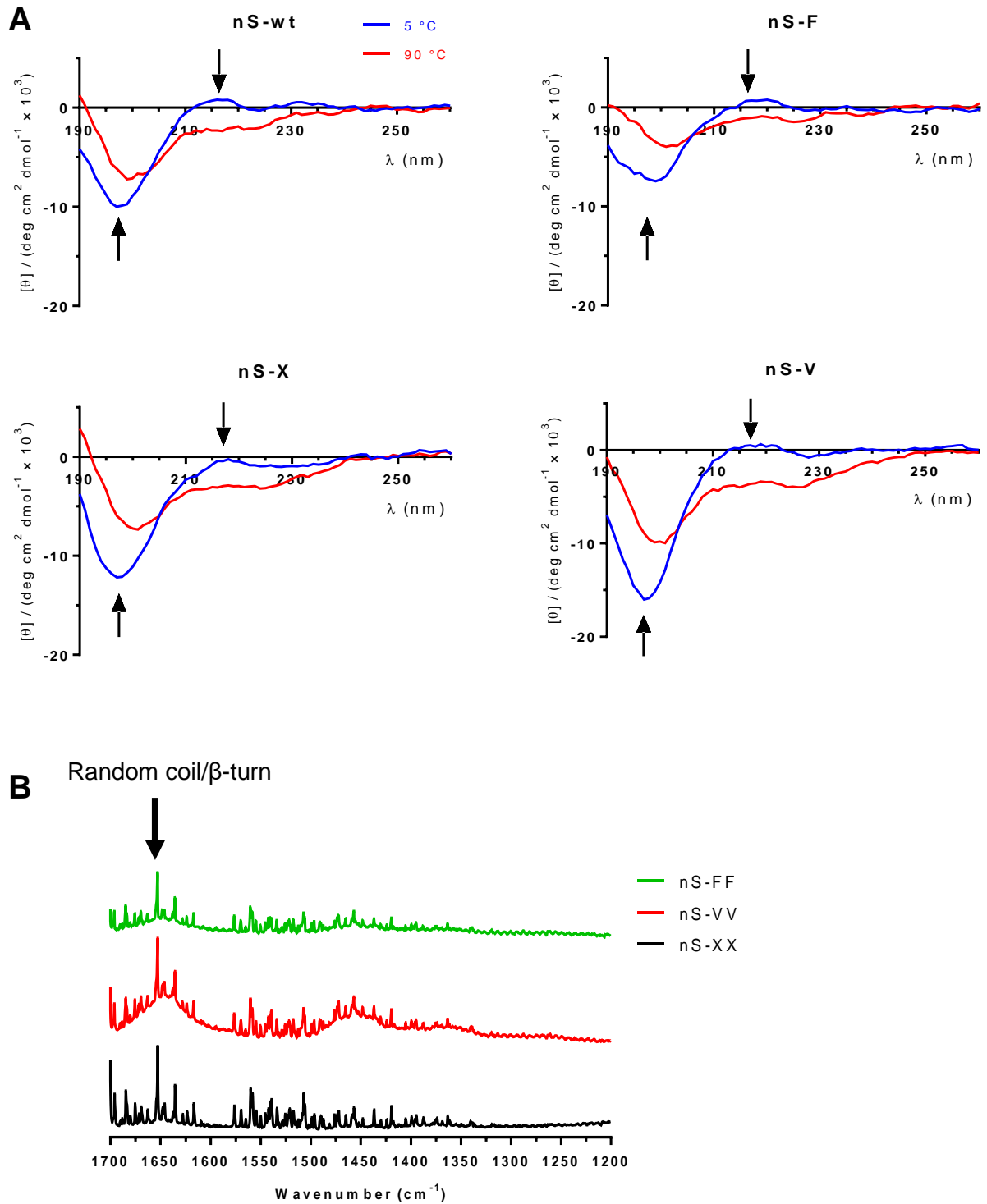


Figure 3.16: nano-Self peptides conform to some β -hairpin structure but mainly random coil

A. CD spectra of monovalent nS peptides.

B. FT-IR spectra of bivalent nS peptides. Main peak appears near 1650 cm^{-1} , which is a characteristic peak shared by both random coil and β -turn peptides.

Figure 3.17: Tetraivalent nS-F4 inhibits bivalent association with macrophages and apparently has stronger avidity for SIRP α than bivalent

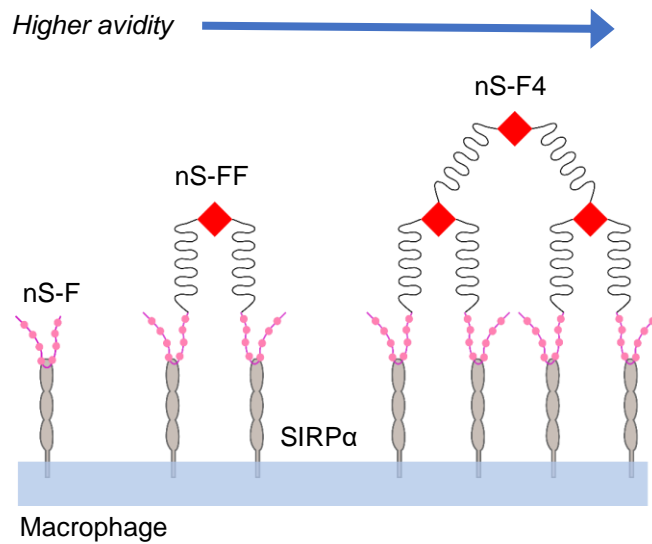
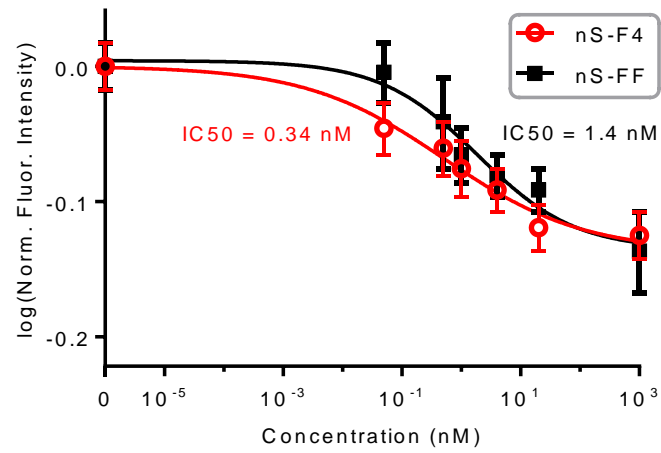


Figure 3.17: Avidity of SIRP α appears to scale with the increase of nano-Self multivalency

Tetravalent nS-F4 was more potent in inhibiting monovalent nS-F-fluor association with macrophages than bivalent nS-FF suggesting multivalency increases avidity of the nS-peptides to SIRP α .

3.4.7 Safety of ns-FF injections in a pre-clinical trial

Phase 1 clinical trials for safety of anti-CD47 in patients have shown that infusion into the bloodstream decreases RBC numbers (*i.e.* hematocrit) and increases reticulocytes (*i.e.* new RBCs),^{16,69} and related blood safety concerns apply to a bivalent CD47-binding protein made with SIRP α domains fused to a macrophage-binding domain (Fc domain).⁸⁴ Given that our nS-F peptide increases phagocytosis of opsonized RBCs and also associates with mouse macrophages (**Figures 3.7 & 3.14**), we assessed safety of the more potent nS-FF peptide by intravenous injection into mice. Overall, nS-FF in PBS showed no differences *versus* PBS vehicle control in its effects on mouse hematology and body weight after four daily tail-vein injections of 1 mg/kg peptide (**Figure 3.18**). This corresponds to about 8 μ M in the blood, assuming rapid mixing and no dilution within the ~1.5 mL blood volume of the mouse. Withdrawal of ~140 μ L from this blood volume was necessary to obtain a complete hematology profile, and such a volume is expected to cause slight decreases in hematocrit and platelets as shown (**Figure 3.18-i,ii**). Consistent with this loss, more RBCs should be produced in each mouse to compensate for the RBC loss, and the ~30% increase in reticulocytes after the first two blood draws over 11 days (**Figure 3.18-iii**) is similar to the prior amount of blood removed (~300 μ l/1500 μ l). The mice (~14 weeks) also continued to gain weight at the same rates (~5% over 11 days) regardless of peptide injections. These changes are thus expected but, importantly, unaffected by the nS-FF peptide, which establishes some safety.

Figure 3.18: Preliminary hematological data showing nS-FF is safe *in vivo*

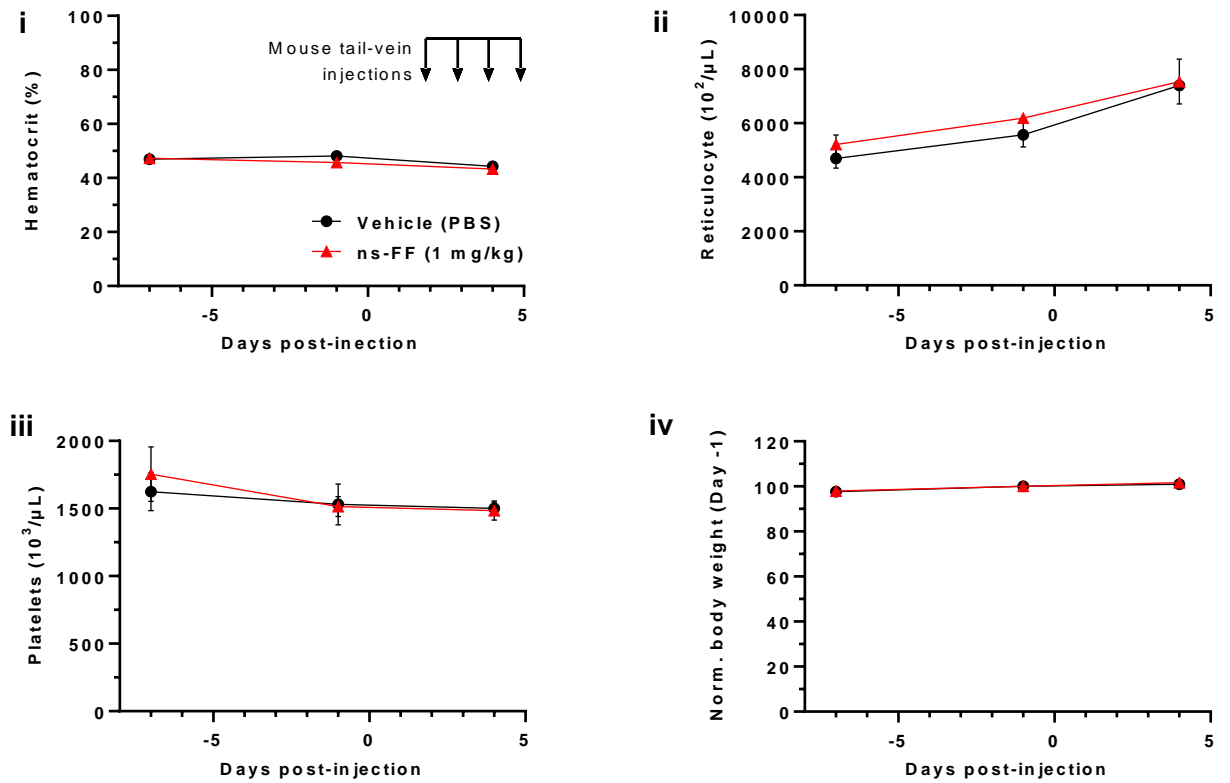


Figure 3.18: Pre-clinical assessments indicate nS-FF is safe *in vivo*

Phase 1 pre-clinical trial: Intravenous injections of nS-FF were done for four consecutive days followed by blood withdrawal 24 hours after last injection. Blood parameters show that nS-FF at 1 mg/kg is safe, with no anemia or weight loss.

3.5 Conclusions

Peptide-based therapies are numerous,¹⁵⁹ and for cancer, they include approved analogs of naturally occurring molecules (*e.g.* bortezomib, carfilzomib, and goserelin). In cell adhesion signaling for example, the tripeptide RGD derived from extracellular matrix¹⁶⁰ led to a synthetic analog with increased affinity for matrix receptors¹⁶¹ and with utility as a soluble competitive inhibitor of adhesion in clinical trials against cancer.¹⁶² Peptides are usually synthesized at low cost (~\$1/mg here) and can be stored at high concentration relative to therapeutic IgG's.¹³⁴ To be clear, lab-grade anti-CD47, anti-SIRP α , and anti-PD1 are ~\$100/mg, and clinical grade antibodies such as anti-PD1 cost >\$100K/patient/year.^{135,136} Moreover, very few residues in a ~150 kDa antibody physically contact a target antigen.

The 21-amino acid 'Self' peptide was the first peptide shown to bind SIRP α and recapitulate the anti-phagocytic signaling of full length CD47. Although a similar 21-amino acid peptide was reported to not bind soluble SIRP α ,⁵⁵ our 8-amino acid nano-Self peptides (1) enhanced phagocytosis of antibody-opsonized human cells (normal and cancer) by human macrophages and (2) were as effective as anti-CD47 in inhibiting a CD47-Fc construct in binding to human macrophages. The underlying concept of our nS peptides is to bind and inhibit SIRP α rather than target CD47. Anti-CD47 infusions in the clinic show some efficacy against opsonized liquid tumors but also cause anemia,¹¹⁴ which is not evident in initial studies here and could in part reflect the Fc function of anti-CD47.

When displayed on particles, the 21-amino acid 'Self' peptide inhibited phagocytosis of opsonized particles,²² whereas the soluble peptides here function as antagonists consistent with prior use of large, soluble CD47 ectodomain as inhibitors of

SIRP α to enhance phagocytosis of tumor cells.^{60,140} The smaller peptides here are more likely to penetrate a tumor from the circulation, or they might be delivered to tumors (which are typically rich in macrophages) by various methods that range from nanoparticle-mediated ‘nano-gene’ therapy to packaging them into either peptide-secreting bacteria¹⁶³ or backpacks that attach to tumor-injected macrophages.¹⁶⁴ Furthermore, anti-CD47 can directly opsonize cells and cause engulfment by macrophages, because the antibody’s Fc-domain activates the Fc receptor (FcR) on the macrophages^{70,71} – although our data with the B6H12 clone of anti-CD47 does not greatly stimulate phagocytosis.⁶⁵ A bivalent anti-CD47 nanobody that lacks an Fc-domain caused modest anemia and mild thrombocytopenia in mice (following a similar injection and bleeding protocol as used here) but addition of an Fc domain increased the adverse effects.⁷³ Importantly, the nS peptides lack an activating Fc domain and should solely antagonize SIRP α , eliminating opsonization, and thereby minimizing clearance of healthy cells.

In sum, synthesis and functional tests of multivalent, CD47-inspired nano-Self peptides with hydrophobic substitutions at a central Thr demonstrate potential as a nanomolar agonist for phagocytosis of targeted diseased cells such as cancer cells. Sequence analyses of various species beyond human and mouse¹⁵¹ suggest the nS peptides will function with macrophages in monkey and dog, which are important species for evaluation of safety and efficacy. Lastly, the increased phagocytosis of soluble nano-Self relative to anti-CD47 on the cell that is targeted for phagocytosis certainly motivates further investigation of CD47-SIRP α ’s molecular mechanisms.

Chapter 4: Future directions

I performed the experiments for the data presented in this Chapter except for:

- a. Generating the plasmids for the mutant variants of CD47 and expressing them in HEK293 cells as shown in Figure 4.4 (performed by **M. Tewari** and **B. Hayes**)

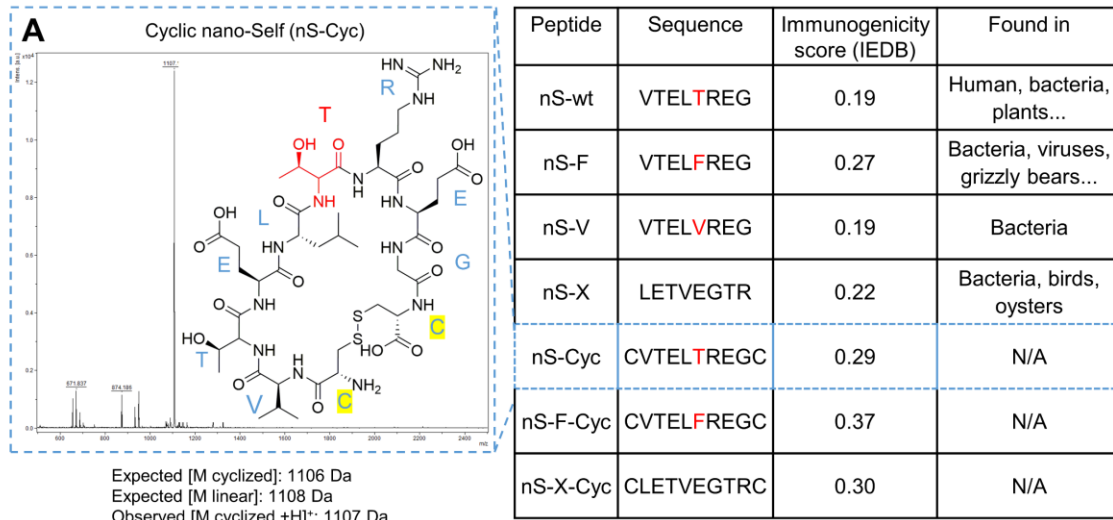
The immune checkpoint interaction between CD47 on the membrane of healthy and cancer cells and the macrophage receptor SIRP α inhibits macrophage-mediated phagocytosis. The dominant class of inhibitors against this checkpoint interaction is monoclonal antibodies, often used as monotherapies, but more often in combination with a pro-phagocytic IgG therapeutic to promote clearance of cancer cells. Recombinant fusion proteins (i.e. CD47 IgV domain or SIRP α IgV-like domain(s) fused to human IgG) serve as a second class of CD47-SIRP α inhibitors. Most antagonists from these two groups of inhibitors target CD47, with success in many clinical trials in treating hematological and solid tumors but at the expense of unwanted side effects (i.e. anemia). Development of therapeutics to block this key immunological interaction while minimizing toxic side effects and maintaining efficacy is needed. Peptide inhibitors serve as non-immunogenic alternatives to antibodies with many advantages such as tissue penetration, low inherent toxicity, facile production and low costs.

Peptide inhibitors against the CD47-SIRP α axis exist and continue to emerge.^{22,58,165-169} We have designed multivalent linear peptides that inhibit SIRP α which motivates the development of more peptide agonists, in particular cyclic peptides. These types of peptides have advantages such as higher affinity and selectivity for protein receptors when compared to linear peptides due to their limited conformational flexibility and higher surface area. Cyclic peptides are also more resistant to enzyme degradation due to the lack of free termini and more stable cores, a result of increased intramolecular interactions.¹⁷⁰

We designed a cyclic nano-Self peptide (nS-Cyc) based on our wild type nano-Self (nS-wt) peptide by bridging the ends with a disulfide bond and verified its synthesis by

MALDI-TOF mass spectrometry (**Figure 4.1A**). While some of our linear nS peptide sequences are found in proteins expressed mostly in bacteria, no organism was found to express a ribosomal protein that contains the nS-Cyc sequence (**Figure 4.1A Inset Table**). A kinase protein expressed in rosary peas contains the closest sequence to nS-Cyc (**Figure 4.1B**), and while this plant is toxic, toxicity seems unrelated to the aligned protein suggesting low immunogenicity (**Figure 4.1A Inset Table**).¹⁷¹

Figure 4.1: Linear nano-Self peptides are found in many bacteria, but no natural organism expresses a protein which contains cyclic nano-Self peptide sequences.



B

```

nS-Cyc                               1 CVTELTREGC   10
Receptor-like protein kinase 201 CVPELTREGC 210
Plant (Rosary pea)
Accession number: XP_027364751.1

nS-F-Cyc                               1 CVTELFREGC   10
Ribosomal protein L17              75 CVTELFREVS   84
Bacteria (Bacteroidetes strain F0058)
Accession number: EFI17015.1

nS-X-Cyc                               1 CLETVEGTRC   10
Adenylate kinase                   47 CLETVDGTRS  56
Bacteria (Rubrobacter sp.)
Accession number: MBA2374999.1
    
```

Figure 4.1: The sequence of the cyclic nano-Self peptide is not found in nature suggesting low immunogenicity

A. The chemical structure of nS-Cyc consists of the 8-amino acid sequence of nS-wt bridged through a disulfide bond at the termini. Synthesis of the construct was verified by MALDI-TOF mass spectrometry indicating the oxidation of the cysteine thiols forming a disulfide bond. **Inset table:** The sequences of the linear and cyclic nS-peptides are shown. Although the linear peptides are found primarily in bacteria, the nS-peptides are not likely to elicit immune responses. Immunogenicity scores were generated using the IEDB Analysis Resource (<http://tools.iedb.org/immunogenicity>).

B. Sequence search analysis reveals that there are no proteins expressed by any organism that contain the exact sequence of the cyclic nS peptides. The closest sequence to nS-Cyc is found in a toxic plant; however, the aligned protein seems unrelated to the toxicity of the plant. The residues that do not match the nS-Cyc sequences the subject protein sequence are highlighted in red.

The phagocytosis of IgG-opsonized human red blood cells (RBCs) was tested by incubating solutions of nS-Cyc with adherent human and mouse macrophages (**Figure 4.2A: Left Panel**). Internalization of opsonized RBCs after treatment of both human and mouse macrophages with nS-Cyc was observed (**Figure 4.2A: Images**) at slightly higher levels than opsonized and anti-CD47 blocked RBCs (**Figure 4.2B**). nS-Cyc phagocytic activity in mouse macrophages at saturating concentrations is weaker than in human, consistent with nS-wt activity (**Figure 4.2C**). However, nS-Cyc enhanced human and mouse macrophage internalization more than the linear nS-wt, supporting an advantage of using cyclic peptides. nS-F potency on both human and mouse macrophages is significantly greater than any other peptide tested, indicating that sequence is an important determining factor of efficacy. Based on these preliminary data with nS-Cyc, in addition to data obtained from our linear nano-Self peptide library, cyclic nS-F (nS-F-Cyc) and cyclic bivalent nS-F (nS-FF-Cyc) will be synthesized and tested for effects on phagocytosis (**Figure 4.3**). We predict that the point mutation of the critical Thr residue will enhance effects of phagocytosis with additional effects by adding valency to the peptide. Moreover, nS-Cyc will be engineered to include orthogonal reactive handles (i.e. lysine) to allow for on-resin fluorescent labeling or addition of large PEG groups for enhanced solubility and prolonged circulation *in vivo*.

Our main interest is to develop potent and stable peptide antagonists to replace anti-SIRP α antibodies for treating solid tumors.¹⁹ In addition to K562 erythroleukemia cells, which we have shown to be efficiently phagocytosed by human macrophages in the presence of our linear nS-peptides, we will study the efficacy of nS-Cyc and the proposed

cyclic peptides in promoting phagocytosis of tumor cells such as B16 mouse melanoma and A549 human lung carcinoma cells.

Figure 4.2: nS-Cyc enhances phagocytosis of opsonized RBCs by macrophages, suggesting an increased effect of cyclization

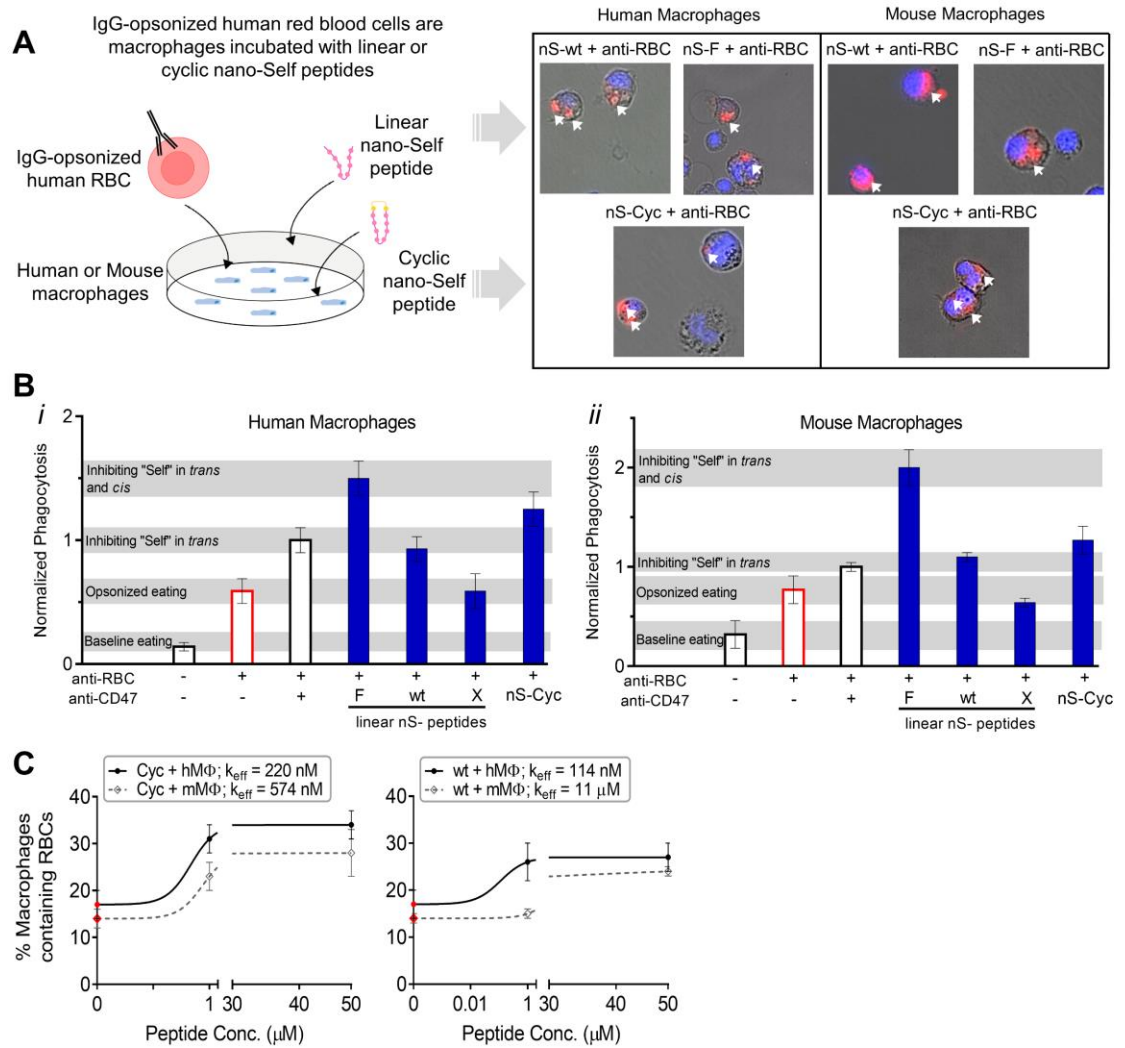


Figure 4.2: RBC phagocytosis by human and mouse macrophages increases with the addition of nS-Cyc

A. A cartoon representation of the phagocytosis assay performed. Briefly, adherent human or mouse macrophages are incubated with either linear or cyclic nS-peptides and then fed opsonized human RBCs. Internalization of RBCs is analyzed by fluorescence microscopy.

B. Phagocytosis levels in human (*i*) and mouse (*ii*) macrophages are enhanced with the addition of linear and cyclic nS-peptides. nS-Cyc appears to have a greater effect in perturbing the CD47-SIRP α interaction compared to linear nS-wt in human macrophages, but is not as potent as nS-F. This suggests that cyclization increases potency, but the sequence is also an important component of activity. Values are all normalized relative to anti-CD47 blockade and anti-RBC opsonization (+,+).

C. Addition of low concentration of nS-Cyc results with macrophages internalizing at least one opsonized RBC, with levels of phagocytic macrophages slightly greater than linear nS-wt. Although efficacy of nS-Cyc is less in mouse macrophages than in human, it is still roughly 20-fold more active than the linear counterpart.

Figure 4.3: Proposed nS-F-Cyc peptide in addition to bivalent variant

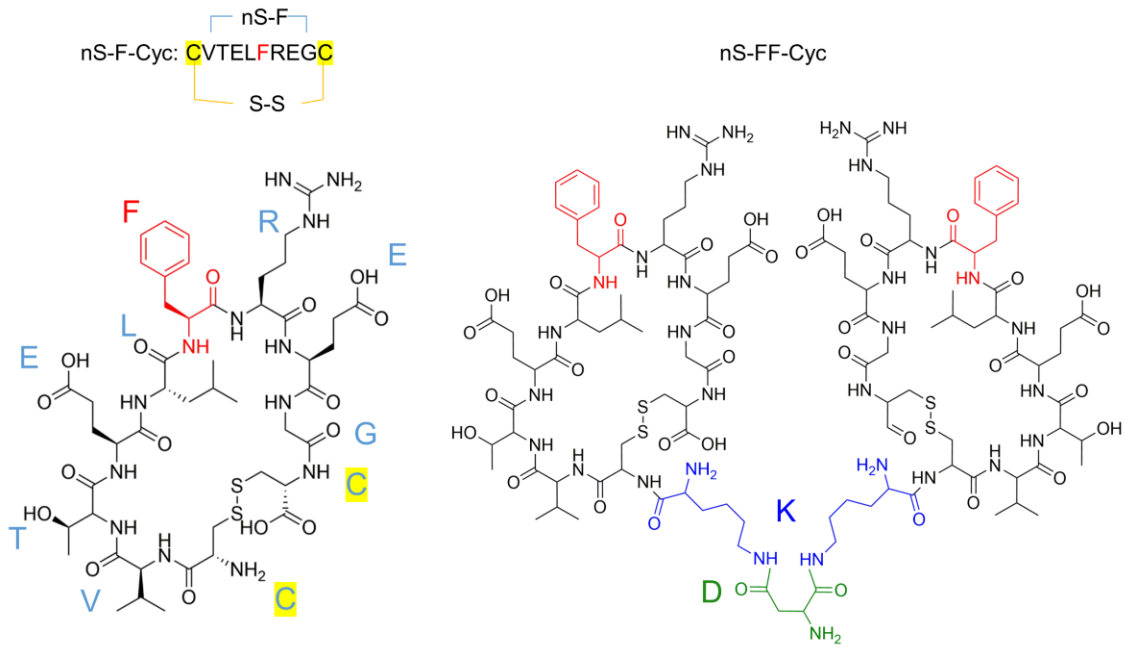


Figure 4.3: Investigating mutated and bivalent nS-Cyc peptides seems promising

The chemical structures of the proposed nS-F-Cyc and nS-FF-Cyc peptides to be synthesized and tested for phagocytosis activity and binding efficiency.

In mouse, the critical Thr-102 residue in the CD47 β -hairpin which binds SIRP α is replaced with a less bulky, but polar Ser residue, along with other non-conserved mutations to contact residues which disrupt SIRP α binding.¹⁵¹ Mutating this same critical Thr residue to hydrophobic Phe and Val in the nS-peptides enhanced phagocytosis suggesting tighter binding to SIRP α . To investigate the effects of these mutations on SIRP α binding, we transduced HEK293 cells with wild type CD47-GFP as well as mutant versions; namely, T102S, T102F and T102V (**Figure 4.4A**). SIRP α -Fc fusion protein binding will be evaluated to determine changes in SIRP α affinity towards these mutated variants. Additionally, inhibition assays using linear and cyclic nano-Self peptides will be explored to determine efficacy of these peptides to inhibit SIRP α -Fc binding (**Figure 4.4B**).

Figure 4.4: Various CD47-GFP mutants expressed on HEK-293 cells for SIRP α -Fc binding assays

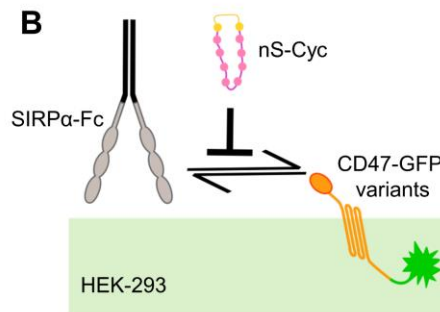
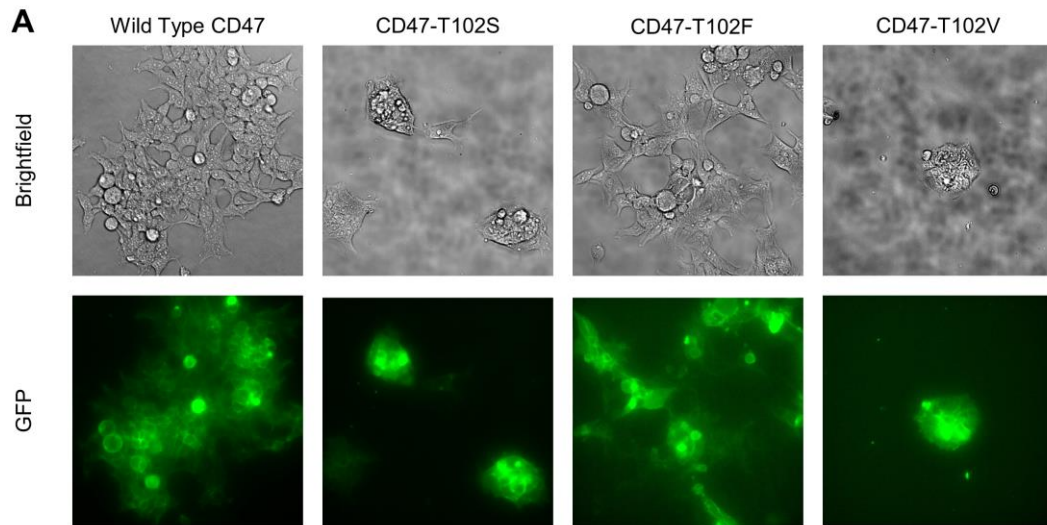


Figure 4.4: Successful transduction of CD47-GFP variants will be used for binding assays

A. Viral transduction and expression of wild type CD47-GFP and various mutants on HEK-293 cells was confirmed with fluorescence microscopy. The T102S mutation is based on the single point mutation found in the mouse CD47 β -hairpin that interacts with SIRP α . T102F and T102V are based the nS-peptides that showed the most potent activity in prior phagocytosis and inhibition studies.

B. Binding of SIRP α -Fc fusion protein to the mutated CD47 variants will be evaluated as well as efficacy of the nS-Cyc peptides to inhibit SIRP α binding to CD47.

Lastly, we plan to conduct more mouse studies and understand how these peptides function *in vivo*. Preliminary data indicated safe administration of nS-FF at low doses. However, a possible alternative can be immediate clearance of the peptide by mouse kidneys which also will result with no net change in blood parameters. Further studies with escalated nS-FF doses will be conducted to delineate any possible side effects. We will also investigate the novel tetravalent construct (nS-F4) and compare it to data obtained from the bivalent counterpart *in vivo*. The extra PEG linker groups in nS-F4 may potentiate an enhancement in blood circulation. Moreover, fluorescently labeling the peptides to visualize them *in vivo* will be done to decipher how long the peptides remain in circulation and to determine what types of blood cells they interact with.

Immunotherapies such as the development of genetically modified chimeric antigen receptor T-cells (CAR-T cells) utilize immune cells from the same patient enhancing the clearance of tumor cells.¹⁷² While results with such therapy has been dramatic against cancer and received FDA approval for use as a treatment, serious side effects remain.¹⁷³ Adapting SIRP α -blocked macrophages harvested from patients poses a potentially safer alternative where targeting antibodies or peptides are cleared after time leaving the unmodified macrophages in circulation. Macrophage immunotherapy also has an advantage over T-cells in clearing solid tumors. Furthermore, our nano-Self peptides add more advantages over antibodies as they are much smaller but are similar in terms of potency. Rationally designing CD47-inspired peptides introduces a new direction in developing macrophage checkpoint inhibitors.

WORKS CITED

1. Sharma, P.; Allison, J. P. Immune Checkpoint Targeting in Cancer Therapy: Toward Combination Strategies with Curative Potential. *Cell* **2015**, *161*, 205-214.
2. Sharma, P.; Allison, J. P. The Future of Immune Checkpoint Therapy. *Science* **2015**, *348*, 56-61.
3. Marin-Acevedo, J. A.; Dholaria, B.; Soyano, A. E.; Knutson, K. L.; Chumsri, S.; Lou, Y. Next generation of immune checkpoint therapy in cancer: new developments and challenges. *Journal of Hematology & Oncology* **2018**, *11*, 39.
4. Brahmer, J. R.; Tykodi, S. S.; Chow, L. Q. M.; Hwu, W.; Topalian, S. L.; Hwu, P.; Drake, C. G.; Camacho, L. H.; Kauh, J.; Odunsi, K.; Pitot, H. C.; Hamid, O.; Bhatia, S.; Martins, R.; Eaton, K.; Chen, S.; Salay, T. M.; Alaparthi, S.; Grosso, J. F.; Korman, A. J.; Parker, S. M.; Agrawal, S.; Goldberg, S. M.; Pardoll, D. M.; Gupta, A.; Wigginton, J. M. Safety and Activity of Anti-PD-L1 Antibody in Patients with Advanced Cancer. *N. Engl. J. Med.* **2012**, *366*, 2455-2465.
5. Ansell, S. M.; Lesokhin, A. M.; Borrello, I.; Halwani, A.; Scott, E. C.; Gutierrez, M.; Schuster, S. J.; Millenson, M. M.; Cattray, D.; Freeman, G. J.; Rodig, S. J.; Chapuy, B.; Ligon, A. H.; Zhu, L.; Grosso, J. F.; Kim, S. Y.; Timmerman, J. M.; Shipp, M. A.; Armand, P. PD-1 Blockade with Nivolumab in Relapsed or Refractory Hodgkin's Lymphoma. *N. Engl. J. Med.* **2015**, *372*, 311-319.
6. Yang, J. C.; Hughes, M.; Kammula, U.; Royal, R.; Sherry, R. M.; Topalian, S. L.; Suri, K. B.; Levy, C.; Allen, T.; Mavroukakis, S.; Lowy, I.; White, D. E.; Rosenberg, S. A. Ipilimumab (Anti-CTLA4 Antibody) Causes Regression of Metastatic Renal Cell Cancer Associated with Enteritis and Hypophysitis. *Journal of Immunotherapy* **2007**, *30*.
7. Pulido, A. d. M.; Gardner, A.; Hiebler, S.; Soliman, H.; Rugo, H. S.; Krummel, M. F.; Coussens, L. M.; Ruffell, B. TIM-3 Regulates CD103(+) Dendritic Cell Function and Response to Chemotherapy in Breast Cancer. *Cancer Cell* **2018**, *33*, 60-+.
8. Broz, M. L.; Binnewies, M.; Boldajipour, B.; Nelson, A. E.; Pollack, J. L.; Erle, D. J.; Barczak, A.; Rosenblum, M. D.; Daud, A.; Barber, D. L.; Amigorena, S.; van't Veer, L. J.; Sperling, A. I.; Wolf, D. M.; Krummel, M. F. Dissecting the Tumor Myeloid Compartment Reveals Rare Activating Antigen-Presenting Cells Critical for T Cell Immunity. *Cancer Cell* **2014**, *26*, 638-652.
9. Hatherley, D.; Graham, S. C.; Turner, J.; Harlos, K.; Stuart, D. I.; Barclay, A. N. Paired Receptor Specificity Explained by Structures of Signal Regulatory Proteins Alone and Complexed With CD47. *Mol. Cell* **2008**, *31*, 266-277.

10. Barclay, A. N. Signal Regulatory Protein Alpha (SIRP α)/Cd47 Interaction and Function. *Curr. Opin. Immunol.* **2009**, *21*, 47-52.
11. Willingham, S. B.; Volkmer, J.; Gentles, A. J.; Sahoo, D.; Dalerba, P.; Mitra, S. S.; Wang, J.; Contreras-Trujillo, H.; Martin, R.; Cohen, J. D.; Lovelace, P.; Scheeren, F. A.; Chao, M. P.; Weiskopf, K.; Tang, C.; Volkmer, A. K.; Naik, T. J.; Storm, T. A.; Mosley, A. R.; Edris, B.; Schmid, S. M.; Sun, C. K.; Chua, M.; Murillo, O.; Rajendran, P.; Cha, A. C.; Chin, R. K.; Kim, D.; Adorno, M.; Raveh, T.; Tseng, D.; Jaiswal, S.; Enger, P. O.; Steinberg, G. K.; Li, G.; So, S. K.; Majeti, R.; Harsh, G. R.; van de Rijn, M.; Teng, N. N. H.; Sunwoo, J. B.; Alizadeh, A. A.; Clarke, M. F.; Weissman, I. L. The CD47-signal regulatory protein alpha (SIRP α) interaction is a therapeutic target for human solid tumors. *Proc. Natl. Acad. Sci. U. S. A.* **2012**, *109*, 6662-6667.
12. Jaiswal, S.; Jamieson, C. H. M.; Pang, W. W.; Park, C. Y.; Chao, M. P.; Majeti, R.; Traver, D.; van Rooijen, N.; Weissman, I. L. CD47 Is Upregulated on Circulating Hematopoietic Stem Cells and Leukemia Cells to Avoid Phagocytosis. *Cell* **2009**, *138*, 271-285.
13. Majeti, R.; Chao, M. P.; Alizadeh, A. A.; Pang, W. W.; Jaiswal, S.; Gibbs, K. D., Jr.; van Rooijen, N.; Weissman, I. L. CD47 Is an Adverse Prognostic Factor and Therapeutic Antibody Target on Human Acute Myeloid Leukemia Stem Cells. *Cell* **2009**, *138*, 286-299.
14. Massuger, L.; Claessens, R.; Kenemans, P.; Hanselaar, T.; Corstens, F. Nonantigen-Specific Tissue Localization of Monoclonal-Antibodies. *Journal of Nuclear Medicine* **1990**, *31*, 1438-1438.
15. Gholamin, S.; Mitra, S. S.; Feroze, A. H.; Liu, J.; Kahn, S. A.; Zhang, M.; Esparza, R.; Richard, C.; Ramaswamy, V.; Remke, M.; Volkmer, A. K.; Willingham, S.; Ponnuswami, A.; McCarty, A.; Lovelace, P.; Storm, T. A.; Schubert, S.; Hutter, G.; Narayanan, C.; Chu, P.; Raabe, E. H.; Harsh, G.; Taylor, M. D.; Monje, M.; Cho, Y.; Majeti, R.; Volkmer, J. P.; Fisher, P. G.; Grant, G.; Steinberg, G. K.; Vogel, H.; Edwards, M.; Weissman, I. L.; Cheshier, S. H. Disrupting the CD47-SIRP alpha anti-phagocytic axis by a humanized anti-CD47 antibody is an efficacious treatment for malignant pediatric brain tumors. *Science Translational Medicine* **2017**, *9*, eaaf2968.
16. Andrechak, J. C.; Dooling, L. J.; Discher, D. E. The Macrophage Checkpoint CD47: SIRP Alpha for Recognition of 'Self' Cells: From Clinical Trials of Blocking Antibodies to Mechanobiological Fundamentals. *Philosophical Transactions of the Royal Society B-Biological Sciences* **2019**, *374*, 20180217.
17. Murata, Y.; Tanaka, D.; Hazama, D.; Yanagita, T.; Saito, Y.; Kotani, T.; Oldenborg, P.; Matozaki, T. Anti-human SIRP antibody is a new tool for cancer immunotherapy. *Cancer Science* **2018**, *109*, 1300-1308.

18. Ring, N. G.; Herndler-Brandstetter, D.; Weiskopf, K.; Shan, L.; Volkmer, J.; George, B. M.; Lietzenmayer, M.; McKenna, K. M.; Naik, T. J.; McCarty, A.; Zheng, Y.; Ring, A. M.; Flavell, R. A.; Weissman, I. L. Anti-SIRP alpha antibody immunotherapy enhances neutrophil and macrophage antitumor activity. *Proc. Natl. Acad. Sci. U. S. A.* **2017**, *114*, E10578-E10585.
19. Alvey, C. M.; Spinler, K. R.; Irianto, J.; Pfeifer, C. R.; Hayes, B.; Xia, Y.; Cho, S.; Dingal, P. C. P. D.; Hsu, J.; Smith, L.; Tewari, M.; Discher, D. E. SIRP α -Inhibited, Marrow-Derived Macrophages Engorge, Accumulate, and Differentiate in Antibody-Targeted Regression of Solid Tumors. *Current Biology* **2017**, *27*, 2065-2077.
20. Piccione, E. C.; Juarez, S.; Tseng, S.; Liu, J.; Stafford, M.; Narayanan, C.; Wang, L.; Weiskopf, K.; Majeti, R. SIRP alpha-Antibody Fusion Proteins Selectively Bind and Eliminate Dual Antigen-Expressing Tumor Cells. *Clinical Cancer Research* **2016**, *22*, 5109-5119.
21. Irandoust, M.; Zarate, J. A.; Hubeek, I.; van Beek, E. M.; Schornagel, K.; Broekhuizen, A. J. F.; Akyuz, M.; van de Loosdrecht, A. A.; Delwel, R.; Valk, P. J.; Sonneveld, E.; Kearns, P.; Creutzig, U.; Reinhardt, D.; de Bont, E. S. J. M.; Coenen, E. A.; van den Heuvel-Eibrink, M. M.; Zwaan, C. M.; Kaspers, G. J. L.; Cloos, J.; van den Berg, T. K. Engagement of SIRP alpha Inhibits Growth and Induces Programmed Cell Death in Acute Myeloid Leukemia Cells. *Plos One* **2013**, *8*, e52143.
22. Rodriguez, P. L.; Harada, T.; Christian, D. A.; Pantano, D. A.; Tsai, R. K.; Discher, D. E. Minimal "Self" Peptides That Inhibit Phagocytic Clearance and Enhance Delivery of Nanoparticles. *Science* **2013**, *339*, 971-975.
23. Matlung, H. L.; Szilagy, K.; Barclay, N. A.; van den Berg, T. K. The CD47-SIRP alpha signaling axis as an innate immune checkpoint in cancer. *Immunol. Rev.* **2017**, *276*, 145-164.
24. Mandal, R.; Samstein, R. M.; Lee, K.; Havel, J. J.; Wang, H.; Krishna, C.; Sabio, E. Y.; Makarov, V.; Kuo, F.; Blecula, P.; Ramaswamy, A. T.; Durham, J. N.; Bartlett, B.; Ma, X.; Srivastava, R.; Middha, S.; Zehir, A.; Hechtman, J. F.; Morris, L. G. T.; Weinhold, N.; Riaz, N.; Le, D. T.; Diaz, L. A., Jr.; Chan, T. A. Genetic diversity of tumors with mismatch repair deficiency influences anti-PD-1 immunotherapy response. *Science* **2019**, *364*, 485-+.
25. Perumal, D.; Imai, N.; Lagana, A.; Finnigan, J.; Melnekoff, D.; Leshchenko, V. V.; Solovyov, A.; Madduri, D.; Chari, A.; Cho, H. J.; Dudley, J. T.; Brody, J. D.; Jagannath, S.; Greenbaum, B.; Gnjatic, S.; Bhardwaj, N.; Parekh, S. Mutation-derived Neoantigen-specific T-cell Responses in Multiple Myeloma. *Clinical Cancer Research* **2020**, *26*, 450-464.

26. Mantovani, A.; Marchesi, F.; Malesci, A.; Laghi, L.; Allavena, P. Tumour-associated macrophages as treatment targets in oncology. *Nature Reviews Clinical Oncology* **2017**, *14*, 399-416.
27. Alvey, C.; Discher, D. E. Engineering Macrophages to Eat Cancer: From “Marker of Self” CD47 and Phagocytosis to Differentiation. *J. Leukoc. Biol.* **2017**, *102*, 31-40.
28. Brooke, G.; Holbrook, J.; Brown, M.; Barclay, A. Human lymphocytes interact directly with CD47 through a novel member of the signal regulatory protein (SIRP) family. *Journal of Immunology* **2004**, *173*, 2562-2570.
29. Campbell, I.; Freemonth, P.; Foulkes, W.; Trowsdale, J. An Ovarian Tumor-Marker with Homology to Vaccinia Virus Contains an Igv-Like Region and Multiple Transmembrane Domains. *Cancer Res.* **1992**, *52*, 5416-5420.
30. Brown, E.; Hooper, L.; Ho, T.; Gresham, H. Integrin-Associated Protein - a 50-Kd Plasma-Membrane Antigen Physically and Functionally Associated with Integrins. *J. Cell Biol.* **1990**, *111*, 2785-2794.
31. Lindberg, F.; Lublin, D.; Telen, M.; Veile, R.; Miller, Y.; Doniskeller, H.; Brown, E. Rh-Related Antigen Cd47 is the Signal-Transducer Integrin-Associated Protein. *J. Biol. Chem.* **1994**, *269*, 1567-1570.
32. Reinhold, M.; Lindberg, F.; Plas, D.; Reynolds, S.; Peters, M.; Brown, E. In-Vivo Expression of Alternatively Spliced Forms of Integrin-Associated Protein (Cd47). *J. Cell. Sci.* **1995**, *108*, 3419-3425.
33. Rebres, R.; Vaz, L.; Green, J.; Brown, E. Normal ligand binding and signaling by CD47 (integrin-associated protein) requires a long range disulfide bond between the extracellular and membrane-spanning domains. *J. Biol. Chem.* **2001**, *276*, 34607-34616.
34. Soto-Pantoja, D. R.; Kaur, S.; Roberts, D. D. CD47 signaling pathways controlling cellular differentiation and responses to stress. *Crit. Rev. Biochem. Mol. Biol.* **2015**, *50*, 212-230.
35. Oldenborg, P.; Zheleznyak, A.; Fang, Y.; Lagenaur, C.; Gresham, H.; Lindberg, F. Role of CD47 as a marker of self on red blood cells. *Science* **2000**, *288*, 2051-2054.
36. Veillette, A.; Thibaudeau, E.; Latour, S. High Expression of Inhibitory Receptor SHPS-1 and Its Association with Protein-Tyrosine Phosphatase SHP-1 in Macrophages. *J. Biol. Chem.* **1998**, *273*, 22719-22728.
37. Fujioka, Y.; Matozaki, T.; Noguchi, T.; Iwamatsu, A.; Yamao, T.; Takahashi, N.; Tsuda, M.; Takada, T.; Kasuga, M. A Novel Membrane Glycoprotein, SHPS-1, That

- Binds the SH2-Domain-Containing Protein Tyrosine Phosphatase SHP-2 in Response to Mitogens and Cell Adhesion. *Mol. Cell. Biol.* **1996**, *16*, 6887-6899.
38. Seiffert, M.; Cant, C.; Chen, Z.; Rappold, I.; Brugger, W.; Kanz, L.; Brown, E. J.; Ullrich, A.; Bühring, H. Human Signal-Regulatory Protein Is Expressed on Normal, But Not on Subsets of Leukemic Myeloid Cells and Mediates Cellular Adhesion Involving Its Counterreceptor CD47. *Blood* **1999**, *94*, 3633-3643.
39. van Beek, E.; Cochrane, F.; Barclay, A.; van den Berg, T. Signal regulatory proteins in the immune system. *Journal of Immunology* **2005**, *175*, 7781-7787.
40. Barclay, A.; Brown, M. The SIRP family of receptors and immune regulation. *Nature Reviews Immunology* **2006**, *6*, 457-464.
41. Dietrich, J.; Cella, M.; Seiffert, M.; Bühring, H.; Colonna, M. Cutting edge: Signal-regulatory protein beta 1 is a DAP12-associated activating receptor expressed in myeloid cells. *Journal of Immunology* **2000**, *164*, 9-12.
42. Takenaka, K.; Prasolava, T. K.; Wang, J. C. Y.; Mortin-Toth, S. M.; Khalouei, S.; Gan, O. I.; Dick, J. E.; Danska, J. S. Polymorphism in Sirpa modulates engraftment of human hematopoietic stem cells. *Nat. Immunol.* **2007**, *8*, 1313-1323.
43. Janssen, W. J.; McPhillips, K. A.; Dickinson, M. G.; Linderman, D. J.; Morimoto, K.; Xiao, Y. Q.; Oldham, K. M.; Vandivier, R. W.; Henson, P. M.; Gardai, S. J. Surfactant proteins A and D suppress alveolar macrophage phagocytosis via interaction with SIRP alpha. *American Journal of Respiratory and Critical Care Medicine* **2008**, *178*, 158-167.
44. Fournier, B.; Andargachew, R.; Robin, A. Z.; Laur, O.; Voelker, D. R.; Lee, W. Y.; Weber, D.; Parkos, C. A. Surfactant Protein D (Sp-D) Binds to Membrane-proximal Domain (D3) of Signal Regulatory Protein alpha (SIRP alpha), a Site Distant from Binding Domain of CD47, while Also Binding to Analogous Region on Signal Regulatory Protein beta (SIRP beta). *J. Biol. Chem.* **2012**, *287*, 19386-19398.
45. Matozaki, T.; Murata, Y.; Okazawa, H.; Ohnishi, H. Functions and molecular mechanisms of the CD47-SIRP alpha signalling pathway. *Trends Cell Biol.* **2009**, *19*, 72-80.
46. Barclay, A. N.; van den Berg, T. K. The Interaction Between Signal Regulatory Protein Alpha (SIRP alpha) and CD47: Structure, Function, and Therapeutic Target. *Annual Review of Immunology, Vol 32* **2014**, *32*, 25-50.
47. Subramanian, S.; Parthasarathy, R.; Sen, S.; Boder, E.; Discher, D. Species- and cell type-specific interactions between CD47 and human SIRP alpha. *Blood* **2006**, *107*, 2548-2556.

48. Kwong, L. S.; Brown, M. H.; Barclay, A. N.; Hatherley, D. Signal-regulatory protein alpha from the NOD mouse binds human CD47 with an exceptionally high affinity - implications for engraftment of human cells. *Immunology* **2014**, *143*, 61-67.
49. Boettcher, A. N.; Cunnick, J. E.; Powell, E. J.; Egner, T. K.; Charley, S. E.; Loving, C. L.; Tuggle, C. K. Porcine signal regulatory protein alpha binds to human CD47 to inhibit phagocytosis: Implications for human hematopoietic stem cell transplantation into severe combined immunodeficient pigs. *Xenotransplantation* **2019**, *26*, e12466.
50. Chung, J.; Gao, A.; Frazier, W. Thrombospondin acts via integrin-associated protein to activate the platelet integrin alpha(IIb)beta(3). *J. Biol. Chem.* **1997**, *272*, 14740-14746.
51. Fujimoto, T.; Katsutani, S.; Shimomura, T.; Fujimura, K. Thrombospondin-bound integrin-associated protein (CD47) physically and functionally modifies integrin alpha(IIb)beta(3) by its extracellular domain. *J. Biol. Chem.* **2003**, *278*, 26655-26665.
52. Barazi, H.; Li, Z.; Cashel, J.; Krutzsch, H.; Annis, D.; Mosher, D.; Roberts, D. Regulation of integrin function by CD47 ligands - Differential effects on alpha(v)beta(3) and alpha(4)beta(1) integrin-mediated adhesion. *J. Biol. Chem.* **2002**, *277*, 42859-42866.
53. Isenberg, J. S.; Annis, D. S.; Pendrak, M. L.; Ptaszynska, M.; Frazier, W. A.; Mosher, D. F.; Roberts, D. D. Differential Interactions of Thrombospondin-1,-2, and-4 with CD47 and Effects on cGMP Signaling and Ischemic Injury Responses. *J. Biol. Chem.* **2009**, *284*, 1116-1125.
54. Kaur, S.; Kuznetsova, S. A.; Pendrak, M. L.; Sipes, J. M.; Romeo, M. J.; Li, Z.; Zhang, L.; Roberts, D. D. Heparan Sulfate Modification of the Transmembrane Receptor CD47 Is Necessary for Inhibition of T Cell Receptor Signaling by Thrombospondin-1. *J. Biol. Chem.* **2011**, *286*, 14991-15002.
55. Hatherley, D.; Lea, S. M.; Johnson, S.; Barclay, A. N. Polymorphisms in the Human Inhibitory Signal-Regulatory Protein Alpha Do Not Affect Binding to Its Ligand CD47. *The Journal of biological chemistry* **2014**, *289*, 10024-10028.
56. Hatherley, D.; Harlos, K.; Dunlop, D. C.; Stuart, D. I.; Barclay, A. N. The Structure of the Macrophage Signal Regulatory Protein Alpha (SIRP α) Inhibitory Receptor Reveals a Binding Face Reminiscent of That Used by T Cell Receptors. *J. Biol. Chem.* **2007**, *282*, 14567-14575.
57. Weiskopf, K.; Ring, A. M.; Ho, C. C. M.; Volkmer, J.; Levin, A. M.; Volkmer, A. K.; Oezkan, E.; Fernhoff, N. B.; van de Rijn, M.; Weissman, I. L.; Garcia, K. C. Engineered SIRP Alpha Variants as Immunotherapeutic Adjuvants to Anticancer Antibodies. *Science* **2013**, *341*, 88-91.

58. Martinez-Torres, A.; Quiney, C.; Attout, T.; Bouillet, H.; Herbi, L.; Vela, L.; Barbier, S.; Chateau, D.; Chapiro, E.; Florence Nguyen-Khac; Davi, F.; Le Garff-Tavernier, M.; Moumne, R.; Sarfati, M.; Karoyan, P.; Merle-Beral, H.; Launay, P.; Susin, S. A. CD47 Agonist Peptides Induce Programmed Cell Death in Refractory Chronic Lymphocytic Leukemia B Cells via PLC gamma 1 Activation: Evidence from Mice and Humans. *Plos Medicine* **2015**, *12*, e1001796.
59. Lee, W. Y.; Weber, D. A.; Laur, O.; Stowell, S. R.; Mccall, I.; Andargachew, R.; Cummings, R. D.; Parkos, C. A. The Role of Cis Dimerization of Signal Regulatory Protein Alpha (SIRP Alpha) in Binding to CD47. *J. Biol. Chem.* **2010**, *285*, 37953-37963.
60. Ho, C. C. M.; Guo, N.; Sockolosky, J. T.; Ring, A. M.; Weiskopf, K.; Oezkan, E.; Mori, Y.; Weissman, I. L.; Garcia, K. C. "Velcro" Engineering of High Affinity CD47 Ectodomain as Signal Regulatory Protein Alpha (SIRP Alpha) Antagonists that Enhance Antibody-Dependent Cellular Phagocytosis. *J. Biol. Chem.* **2015**, *290*, 12650-12663.
61. Gozlan, Y. M.; Hilgendorf, S.; Aronin, A.; Sagiv, Y.; Ben-gigi-Tamir, L.; Amsili, S.; Tamir, A.; Pecker, I.; Greenwald, S.; Chajut, A.; Foley-Comer, A.; Pereg, Y.; Peled, A.; Dranitzki-Elhalel, M.; Bremer, E. DSP107-a novel SIRP α -4-1BBL dual signaling protein (DSP) for cancer immunotherapy. *Cancer Immunol Res* **2019**, *7*, A076.
62. Kant, A.; De, P.; Peng, X.; Yi, T.; Rawlings, D.; Kim, J.; Durden, D. SHP-1 Regulates Fc Gamma Receptor-Mediated Phagocytosis and the Activation of RAC. *Blood* **2002**, *100*, 1852-1859.
63. Ishikawa-Sekigami, T.; Kaneko, Y.; Okazawa, H.; Tomizawa, T.; Okajo, J.; Saito, Y.; Okuzawa, C.; Sugawara-Yokoo, M.; Nishiyama, L.; Ohnishi, H.; Matozaki, T.; Nojima, Y. SHPS-1 Promotes the Survival of Circulating Erythrocytes through Inhibition of Phagocytosis by Splenic Macrophages. *Blood* **2006**, *107*, 341-348.
64. Oldenborg, P. A.; Gresham, H. D.; Lindberg, F. P. CD47-Signal Regulatory Protein Alpha (SIRP α) Regulates Fc Gamma and Complement Receptor-Mediated Phagocytosis. *J. Exp. Med.* **2001**, *193*, 855-861.
65. Tsai, R. K.; Discher, D. E. Inhibition of "Self" Engulfment Through Deactivation of Myosin-II at the Phagocytic Synapse Between Human Cells. *J. Cell Biol.* **2008**, *180*, 989-1003.
66. Johansen, M. L.; Brown, E. J. Dual Regulation of SIRP Alpha Phosphorylation by Integrins and CD47. *J. Biol. Chem.* **2007**, *282*, 24219-24230.
67. Richards, D. M.; Endres, R. G. The Mechanism of Phagocytosis: Two Stages of Engulfment. *Biophys. J.* **2014**, *107*, 1542-1553.

68. Chao, M. P.; Jaiswal, S.; Weissman-Tsukamoto, R.; Alizadeh, A. A.; Gentles, A. J.; Volkmer, J.; Weiskopf, K.; Willingham, S. B.; Raveh, T.; Park, C. Y.; Majeti, R.; Weissman, I. L. Calreticulin Is the Dominant Pro-Phagocytic Signal on Multiple Human Cancers and Is Counterbalanced by CD47. *Science Translational Medicine* **2010**, *2*, 63ra94.
69. Sikic, B. I.; Lakhani, N.; Patnaik, A.; Shah, S. A.; Chandana, S. R.; Rasco, D.; Colevas, A. D.; O'Rourke, T.; Narayanan, S.; Papadopoulos, K.; Fisher, G. A.; Villalobos, V.; Prohaska, S. S.; Howard, M.; Beeram, M.; Chao, M. P.; Agoram, B.; Chen, J. Y.; Huang, J.; Axt, M.; Liu, J.; Volkmer, J.; Majeti, R.; Weissman, I. L.; Takimoto, C. H.; Supan, D.; Wakelee, H. A.; Aoki, R.; Pegram, M. D.; Padda, S. K. First-in-Human, First-in-Class Phase I Trial of the Anti-CD47 Antibody Hu5F9-G4 in Patients with Advanced Cancers. *JCO* **2019**, *37*, 946-953.
70. Cox, D.; Greenberg, S. Phagocytic Signaling Strategies: Fc(γ) Receptor-Mediated Phagocytosis as a Model System. *Semin. Immunol.* **2001**, *13*, 339-345.
71. Bakalar, M. H.; Joffe, A. M.; Schmid, E. M.; Son, S.; Podolski, M.; Fletcher, D. A. Size-Dependent Segregation Controls Macrophage Phagocytosis of Antibody-Opsonized Targets. *Cell* **2018**, *174*, 131-+.
72. Veillette, A.; Chen, J. SIRP α -CD47 Immune Checkpoint Blockade in Anticancer Therapy. *Trends Immunol.* **2018**, *39*, 173-184.
73. Sockolosky, J. T.; Dougan, M.; Ingram, J. R.; Ho, C. C. M.; Kauke, M. J.; Almo, S. C.; Ploegh, H. L.; Garcia, K. C. Durable Antitumor Responses to CD47 Blockade Require Adaptive Immune Stimulation. *Proc. Natl. Acad. Sci. U. S. A.* **2016**, *113*, E2646-E2654.
74. Hayes, B. H.; Tsai, R. K.; Dooling, L. J.; Kadu, S.; Lee, J. Y.; Pantano, D.; Rodriguez, P. L.; Subramanian, S.; Shin, J.; Discher, D. E. Macrophages Eat More After Disruption of Cis Interactions between CD47 and the Checkpoint Receptor SIRP α . *J. Cell. Sci.* **2020**, jcs.237800.
75. Chao, M. P.; Alizadeh, A. A.; Tang, C.; Jan, M.; Weissman-Tsukamoto, R.; Zhao, F.; Park, C. Y.; Weissman, I. L.; Majeti, R. Therapeutic Antibody Targeting of CD47 Eliminates Human Acute Lymphoblastic Leukemia. *Cancer Res.* **2011**, *71*, 1374-1384.
76. Lin, G. H. Y.; Viller, N. N.; Chabonneau, M.; Brinen, L.; Mutukura, T.; Dodge, K.; Helke, S.; Chai, V.; House, V.; Lee, V.; Chen, H.; O'Connor, A.; Jin, D.; Figueredo, R.; Vareki, S. M.; Wong, M.; Linderth, E.; Johnson, L. D.; Pang, X.; Koropatnick, J.; Winston, J.; Petrova, P. S.; Uger, R. A. TTI-622 (SIRP α -IgG4 Fc), a CD47-blocking innate immune checkpoint inhibitor, suppresses tumor growth and demonstrates enhanced efficacy in combination with antitumor antibodies in both hematologic and solid tumor models. *Cancer Res.* **2018**, *78*, 2709.

77. Zeng, D.; Sun, Q.; Chen, A.; Fan, J.; Yang, X.; Xu, L.; Du, P.; Qiu, W.; Zhang, W.; Wang, S.; Sun, Z. A fully human anti-CD47 blocking antibody with therapeutic potential for cancer. *Oncotarget* **2016**, *7*, 83040-83050.
78. Wang, Y.; Yin, C.; Feng, L.; Wang, C.; Sheng, G. Ara-C and anti-CD47 antibody combination therapy eliminates acute monocytic leukemia THP-1 cells in vivo and in vitro. *Genetics and Molecular Research* **2015**, *14*, 5630-5641.
79. Pietsch, E. C.; Dong, J.; Cardoso, R.; Zhang, X.; Chin, D.; Hawkins, R.; Dinh, T.; Zhou, M.; Strake, B.; Feng, P.; Rocca, M.; Dos Santos, C.; Shan, X.; Danet-Desnoyers, G.; Shi, F.; Kaiser, E.; Millar, H. J.; Fenton, S.; Swanson, R.; Nemeth, J. A.; Attar, R. M. Anti-leukemic activity and tolerability of anti-human CD47 monoclonal antibodies. *Blood Cancer Journal* **2017**, *7*, e536.
80. Liu, J.; Wang, L.; Zhao, F.; Tseng, S.; Narayanan, C.; Shura, L.; Willingham, S.; Howard, M.; Prohaska, S.; Volkmer, J.; Chao, M.; Weissman, I. L.; Majeti, R. Pre-Clinical Development of a Humanized Anti-CD47 Antibody with Anti-Cancer Therapeutic Potential. *Plos One* **2015**, *10*, e0137345.
81. Buatois, V.; Johnson, Z.; Salgado-Pires, S.; Papaioannou, A.; Hatterer, E.; Chauchet, X.; Richard, F.; Barba, L.; Daubeuf, B.; Cons, L.; Broyer, L.; D'Asaro, M.; Matthes, T.; LeGallou, S.; Fest, T.; Tarte, K.; Hinojosa, R. K. C.; Ferrer, E. G.; Ribera, J. M.; Dey, A.; Bailey, K.; Fielding, A. K.; Eissenberg, L.; Ritchey, J.; Rettig, M.; DiPersio, J. F.; Kosco-Vilbois, M. H.; Masternak, K.; Fischer, N.; Shang, L.; Ferlin, W. G. Preclinical Development of a Bispecific Antibody that Safely and Effectively Targets CD19 and CD47 for the Treatment of B-Cell Lymphoma and Leukemia. *Molecular Cancer Therapeutics* **2018**, *17*, 1739-1751.
82. Theocharides, A. P. A.; Jin, L.; Cheng, P.; Prasolava, T. K.; Malko, A. V.; Ho, J. M.; Poeppel, A. G.; van Rooijen, N.; Minden, M. D.; Danska, J. S.; Dick, J. E.; Wang, J. C. Y. Disruption of SIRP alpha signaling in macrophages eliminates human acute myeloid leukemia stem cells in xenografts. *J. Exp. Med.* **2012**, *209*, 1883-1899.
83. Holland, P. M.; Normant, E.; Adam, A.; Armet, C. M.; O'Connor, R. W.; Lake, A. C.; Hill, J. A.; Biniskiewicz, D. M.; Chappel, S. C.; Palombella, V. J.; Paterson, A. M. CD47 Monoclonal Antibody SRF231 Is a Potent Inducer of Macrophage-Mediated Tumor Cell Phagocytosis and Reduces Tumor Burden in Murine Models of Hematologic Malignancies. *Blood* **2016**, *128*, 1843.
84. Petrova, P. S.; Viller, N. N.; Wong, M.; Pang, X.; Lin, G. H. Y.; Dodge, K.; Chai, V.; Chen, H.; Lee, V.; House, V.; Vigo, N. T.; Jin, D.; Mutukura, T.; Charbonneau, M.; Tran Truong; Viau, S.; Johnson, L. D.; Linderth, E.; Sievers, E. L.; Vareki, S. M.; Figueredo, R.; Pampillo, M.; Koropatnick, J.; Trudel, S.; Mbong, N.; Jin, L.; Wang, J. C. Y.; Uger, R. A. TTI-621 (SIRP alpha Fc): A CD47-Blocking Innate Immune Checkpoint Inhibitor with Broad Antitumor Activity and Minimal Erythrocyte Binding. *Clinical Cancer Research* **2017**, *23*, 1068-1079.

85. Kauder, S. E.; Kuo, T. C.; Harrabi, O.; Chen, A.; Sangalang, E.; Doyle, L.; Rocha, S. S.; Bollini, S.; Han, B.; Sim, J.; Pons, J.; Wan, H., I. ALX148 blocks CD47 and enhances innate and adaptive antitumor immunity with a favorable safety profile. *Plos One* **2018**, *13*, e0201832.
86. Goto, H.; Kojima, Y.; Matsuda, K.; Kariya, R.; Taura, M.; Kuwahara, K.; Nagai, H.; Katano, H.; Okada, S. Efficacy of anti-CD47 antibody-mediated phagocytosis with macrophages against primary effusion lymphoma. *Eur. J. Cancer* **2014**, *50*, 1836-1846.
87. Chao, M. P.; Alizadeh, A. A.; Tang, C.; Myklebust, J. H.; Varghese, B.; Gill, S.; Jan, M.; Cha, A. C.; Chan, C. K.; Tan, B. T.; Park, C. Y.; Zhao, F.; Kohrt, H. E.; Malumbres, R.; Briones, J.; Gascoyne, R. D.; Lossos, I. S.; Levy, R.; Weissman, I. L.; Majeti, R. Anti-CD47 Antibody Synergizes with Rituximab to Promote Phagocytosis and Eradicate Non-Hodgkin Lymphoma. *Cell* **2010**, *142*, 699-713.
88. Chen, J.; Zhong, M.; Guo, H.; Davidson, D.; Mishel, S.; Lu, Y.; Rhee, I.; Perez-Quintero, L.; Zhang, S.; Cruz-Munoz, M.; Wu, N.; Vinh, D. C.; Sinha, M.; Calderon, V.; Lowell, C. A.; Danska, J. S.; Veillette, A. SLAMF7 is critical for phagocytosis of haematopoietic tumour cells via Mac-1 integrin. *Nature* **2017**, *544*, 493-+.
89. Piccione, E. C.; Juarez, S.; Liu, J.; Tseng, S.; Ryan, C. E.; Narayanan, C.; Wang, L.; Weiskopf, K.; Majeti, R. A bispecific antibody targeting CD47 and CD20 selectively binds and eliminates dual antigen expressing lymphoma cells. *Mabs* **2015**, *7*, 946-956.
90. He, Y.; Bouwstra, R.; Wiersma, V. R.; de Jong, M.; Lourens, H. J.; Fehrmann, R.; de Bruyn, M.; Ammatuna, E.; Huls, G.; van Meerten, T.; Bremer, E. Cancer cell-expressed SLAMF7 is not required for CD47-mediated phagocytosis. *Nature Communications* **2019**, *10*, 533.
91. Ribeiro, M. L.; Normant, E.; Garau, R. D.; Miskin, H. P.; Sportelli, P.; Weiss, M. S.; Bosch, F.; Roué, G. The Novel Bispecific CD47-CD19 Antibody TG-1801 Potentiates the Activity of Ublituximab-Umbralisib (U2) Drug Combination in Preclinical Models of B-NHL. *HemaSphere* **2019**, *3*, 598.
92. Voets, E.; Paradé, M.; Lutje Hulsik, D.; Spijkers, S.; Janssen, W.; Rens, J.; Reinieren-Beeren, I.; van, d. T.; van Duijnhoven, S.; Driessen, L.; Habraken, M.; van Zandvoort, P.; Kreijtz, J.; Vink, P.; van Elsas, A.; van Eenennaam, H. Functional characterization of the selective pan-allele anti-SIRPa antibody ADU-1805 that blocks the SIRPa-CD47 innate immune checkpoint. *Journal for ImmunoTherapy of Cancer* **2019**, *7*, 340.
93. Chan, K. S.; Espinosa, I.; Chao, M.; Wong, D.; Ailles, L.; Diehn, M.; Gill, H.; Presti, J., Jr.; Chang, H. Y.; van de Rijn, M.; Shortliffe, L.; Weissman, I. L. Identification, molecular characterization, clinical prognosis, and therapeutic targeting of human

- bladder tumor-initiating cells. *Proc. Natl. Acad. Sci. U. S. A.* **2009**, *106*, 14016-14021.
94. Zhang, M.; Hutter, G.; Kahn, S. A.; Azad, T. D.; Gholamin, S.; Xu, C. Y.; Liu, J.; Achrol, A. S.; Richard, C.; Sommerkamp, P.; Schoen, M. K.; McCracken, M. N.; Majeti, R.; Weissman, I.; Mitra, S. S.; Cheshier, S. H. Anti-CD47 Treatment Stimulates Phagocytosis of Glioblastoma by M1 and M2 Polarized Macrophages and Promotes M1 Polarized Macrophages In Vivo. *Plos One* **2016**, *11*, e0153550.
95. Hutter, G.; Theruvath, J.; Graef, C. M.; Zhang, M.; Schoen, M. K.; Manz, E. M.; Bennett, M. L.; Olson, A.; Azad, T. D.; Sinha, R.; Chang, C.; Kahn, S. A.; Gholamin, S.; Wilson, C.; Grant, G.; He, J.; Weissman, I. L.; Mitra, S. S.; Cheshier, S. H. Microglia are effector cells of CD47-SIRP alpha antiphagocytic axis disruption against glioblastoma. *Proc. Natl. Acad. Sci. U. S. A.* **2019**, *116*, 997-1006.
96. Zhao, X. W.; van Beek, E. M.; Schornagel, K.; Van der Maaden, H.; Van Houdt, M.; Otten, M. A.; Finetti, P.; Van Egmond, M.; Matozaki, T.; Kraal, G.; Birnbaum, D.; van Elsas, A.; Kuijpers, T. W.; Bertucci, F.; van den Berg, T. K. CD47-signal regulatory protein-alpha (SIRP alpha) interactions form a barrier for antibody-mediated tumor cell destruction. *Proc. Natl. Acad. Sci. U. S. A.* **2011**, *108*, 18342-18347.
97. Cabrales, P. RRX-001 Acts as a dual small Molecule Checkpoint Inhibitor by Downregulating CD47 on Cancer Cells and SIRP-alpha on Monocytes/Macrophages. *Translational Oncology* **2019**, *12*, 626-632.
98. Tseng, D.; Volkmer, J.; Willingham, S. B.; Contreras-Trujillo, H.; Fathman, J. W.; Fernhoff, N. B.; Seita, J.; Inlay, M. A.; Weiskopf, K.; Miyanishi, M.; Weissman, I. L. Anti-CD47 antibody-mediated phagocytosis of cancer by macrophages primes an effective antitumor T-cell response. *Proc. Natl. Acad. Sci. U. S. A.* **2013**, *110*, 11103-11108.
99. Sim, J.; Sockolosky, J. T.; Sangalang, E.; Izquierdo, S.; Pedersen, D.; Harriman, W.; Wibowo, A. S.; Carter, J.; Madan, A.; Doyle, L.; Harrabi, O.; Kauder, S. E.; Chen, A.; Kuo, T. C.; Wan, H.; Pons, J. Discovery of high affinity, pan-allelic, and pan-mammalian reactive antibodies against the myeloid checkpoint receptor SIRP alpha. *Mabs* **2019**, *11*, 1036-1052.
100. Gu, S.; Ni, T.; Wang, J.; Liu, Y.; Fan, Q.; Wang, Y.; Huang, T.; Chu, Y.; Sun, X.; Wang, Y. CD47 Blockade Inhibits Tumor Progression through Promoting Phagocytosis of Tumor Cells by M2 Polarized Macrophages in Endometrial Cancer. *Journal of Immunology Research* **2018**, 6156757.
101. Yoshida, K.; Tsujimoto, H.; Matsumura, K.; Kinoshita, M.; Takahata, R.; Matsumoto, Y.; Hiraki, S.; Ono, S.; Seki, S.; Yamamoto, J.; Hase, K. CD47 is an

- adverse prognostic factor and a therapeutic target in gastric cancer. *Cancer Medicine* **2015**, *4*, 1322-1333.
102. Xiao, Z.; Chung, H.; Banan, B.; Manning, P. T.; Ott, K. C.; Lin, S.; Capoccia, B. J.; Subramanian, V.; Hiebsch, R. R.; Upadhyaya, G. A.; Mohanakumar, T.; Frazier, W. A.; Lin, Y.; Chapman, W. C. Antibody mediated therapy targeting CD47 inhibits tumor progression of hepatocellular carcinoma. *Cancer Lett.* **2015**, *360*, 302-309.
103. Edris, B.; Weiskopf, K.; Volkmer, A. K.; Volkmer, J.; Willingham, S. B.; Contreras-Trujillo, H.; Liu, J.; Majeti, R.; West, R. B.; Fletcher, J. A.; Beck, A. H.; Weissman, I. L.; van de Rijn, M. Antibody therapy targeting the CD47 protein is effective in a model of aggressive metastatic leiomyosarcoma. *Proc. Natl. Acad. Sci. U. S. A.* **2012**, *109*, 6656-6661.
104. Weiskopf, K.; Jahchan, N. S.; Schnorr, P. J.; Cristea, S.; Ring, A. M.; Maute, R. L.; Volkmer, A. K.; Volkmer, J.; Liu, J.; Lim, J. S.; Yang, D.; Seitz, G.; Thuyen Nguyen; Wu, D.; Jude, K.; Guerston, H.; Barkal, A.; Trapani, F.; George, J.; Poirier, J. T.; Gardner, E. E.; Miles, L. A.; de Stanchina, E.; Lofgren, S. M.; Vogel, H.; Winslow, M. M.; Dive, C.; Thomas, R. K.; Rudin, C. M.; van de Rijn, M.; Majeti, R.; Garcia, K. C.; Weissman, I. L.; Sage, J. CD47-blocking immunotherapies stimulate macrophage-mediated destruction of small-cell lung cancer. *J. Clin. Invest.* **2016**, *126*, 2610-2620.
105. Zhang, X.; Fan, J.; Wang, S.; Li, Y.; Wang, Y.; Li, S.; Luan, J.; Wang, Z.; Song, P.; Chen, Q.; Tian, W.; Ju, D. Targeting CD47 and Autophagy Elicited Enhanced Antitumor Effects in Non-Small Cell Lung Cancer. *Cancer Immunology Research* **2017**, *5*, 363-375.
106. Yanagita, T.; Murata, Y.; Tanaka, D.; Motegi, S.; Arai, E.; Daniwijaya, E. W.; Hazama, D.; Washio, K.; Saito, Y.; Kotani, T.; Ohnishi, H.; Oldenburg, P.; Garcia, N. V.; Miyasaka, M.; Ishikawa, O.; Kanai, Y.; Komori, T.; Matozaki, T. Anti-SIRP α antibodies as a potential new tool for cancer immunotherapy. *JCI Insight* **2016**, *2*, e89140.
107. Kim, D.; Wang, J.; Willingham, S. B.; Martin, R.; Wernig, G.; Weissman, I. L. Anti-CD47 antibodies promote phagocytosis and inhibit the growth of human myeloma cells. *Leukemia* **2012**, *26*, 2538-2545.
108. Xu, J.; Pan, X.; Zhang, S.; Zhao, C.; Qiu, B.; Gu, H.; Hong, J.; Cao, L.; Chen, Y.; Xia, B.; Bi, Q.; Wang, Y. CD47 blockade inhibits tumor progression human osteosarcoma in xenograft models. *Oncotarget* **2015**, *6*, 23662-23670.
109. Krampitz, G. W.; George, B. M.; Willingham, S. B.; Volkmer, J.; Weiskopf, K.; Jahchan, N.; Newman, A. M.; Sahoo, D.; Zemek, A. J.; Yanovsky, R. L.; Nguyen, J. K.; Schnorr, P. J.; Mazur, P. K.; Sage, J.; Longacre, T. A.; Visser, B. C.; Poultsides, G. A.; Norton, J. A.; Weissman, I. L. Identification of tumorigenic cells and

- therapeutic targets in pancreatic neuroendocrine tumors. *Proc. Natl. Acad. Sci. U. S. A.* **2016**, *113*, 4464-4469.
110. Cioffi, M.; Trabulo, S.; Hidalgo, M.; Costello, E.; Greenhalf, W.; Erkan, M.; Kleeff, J.; Sainz, B., Jr.; Heeschen, C. Inhibition of CD47 Effectively Targets Pancreatic Cancer Stem Cells via Dual Mechanisms. *Clinical Cancer Research* **2015**, *21*, 2325-2337.
111. Jain, S.; Van Scoyk, A.; Morgan, E. A.; Matthews, A.; Stevenson, K.; Newton, G.; Powers, F.; Autio, A.; Louissaint, A., Jr.; Pontini, G.; Aster, J. C.; Luscinskas, F. W.; Weinstock, D. M. Targeted inhibition of CD47-SIRP α requires Fc-Fc γ R interactions to maximize activity in T-cell lymphomas. *Blood* **2019**, *134*, 1430-1440.
112. Liu, X.; Kwon, H.; Li, Z.; Fu, Y. x. Is CD47 an innate immune checkpoint for tumor evasion? *Journal of Hematology and Oncology* **2017**, *10*, 1-7.
113. Zhang, X.; Fan, J.; Ju, D. Insights into CD47/SIRP α axis-targeting tumor immunotherapy. *Antibody Therapeutics* **2018**, *1*, 27-32.
114. Advani, R.; Flinn, I.; Popplewell, L.; Forero, A.; Bartlett, N. L.; Ghosh, N.; Kline, J.; Roschewski, M.; LaCasce, A.; Collins, G. P.; Tran, T.; Lynn, J.; Chen, J. Y.; Volkmer, J.; Agoram, B.; Huang, J.; Majeti, R.; Weissman, I. L.; Takimoto, C. H.; Chao, M. P.; Smith, S. M. CD47 Blockade by Hu5F9-G4 and Rituximab in Non-Hodgkin's Lymphoma. *N. Engl. J. Med.* **2018**, *379*, 1711-1721.
115. Barkal, A. A.; Brewer, R. E.; Markovic, M.; Kowarsky, M.; Barkal, S. A.; Zaro, B. W.; Krishnan, V.; Hatakeyama, J.; Dorigo, O.; Barkal, L. J.; Weissman, I. L. CD24 signalling through macrophage Siglec-10 is a target for cancer immunotherapy. *Nature* **2019**, *572*, 392-396.
116. Maute, R. L.; Chen, J. Y.; Marjon, K. D.; Duan, J.; Choi, T.; Chao, M.; Takimoto, C. H.; Agoram, B.; Volkmer, J. Translational Study of Cell Surface Proteins in Non-Hodgkin Lymphoma Patients Treated with the First-in-Class Anti-CD47 Antibody Magrolimab (5F9) in Combination with Rituximab. *Blood* **2019**, *134*, 5229-5229.
117. Sallman, D.; Asch, A.; Al Malki, M.; Lee, D.; Donnellan, W.; Marcucci, G.; Kambhampati, S.; Daver, N.; Garcia-Manero, G.; Komrokji, R.; Van Elk, J.; Li, M. The First-in-Class Anti-CD47 Antibody Magrolimab (5F9) in Combination with Azacitidine Is Effective in MDS and AML Patients: Ongoing Phase 1b Results. *Blood* **2019**, *134*, 569-569.
118. AnonymousForty Seven, Inc. Announces Updated Data from Ongoing Clinical Trial of Magrolimab Showing Robust, Durable Activity in Patients with Myelodysplastic Syndrome and Acute Myeloid Leukemia. https://www.drugs.com/clinical_trials/forty-seven-inc-announces-updated-data-

[ongoing-clinical-trial-magrolimab-showing-robust-durable-18389.html](#) (accessed 03/27, 2020).

119. Chao, M. P.; Takimoto, C. H.; Feng, D. D.; McKenna, K.; Gip, P.; Liu, J.; Volkmer, J.; Weissman, I. L.; Majeti, R. Therapeutic Targeting of the Macrophage Immune Checkpoint CD47 in Myeloid Malignancies. *Frontiers in Oncology* **2020**, *9*, 1380.
120. Trillium Therapeutics Inc. A Trial of TTI-621 for Patients with Hematologic Malignancies and Selected Solid Tumors.
121. Ansell, S.; Chen, R. W.; Flinn, I. W.; Maris, M. B.; O'Connor, O.,A.; Johnson, L. D. S.; Irwin, M.; Petrova, P. S.; Uger, R. A.; Sievers, E. L. A Phase 1 Study of TTI-621, a Novel Immune Checkpoint Inhibitor Targeting CD47, in Patients with Relapsed or Refractory Hematologic Malignancies. *Blood* **2016**, *128*, 1812 LP-1812.
122. Trillium Therapeutics Inc. A Trial of TTI-622 in Patients with Advanced Relapsed or Refractory Lymphoma or Myeloma (TTI-622-01).
123. Trillium Therapeutics Inc. Trial of Intratumoral Injections of TTI-621 in Subjects with Relapsed and Refractory Solid Tumors and Mycosis Fungoides.
124. Trillium Therapeutics Inc. Trillium Therapeutics Corporate Overview Presentation. https://s22.q4cdn.com/183592819/files/doc_presentations/2020/01/Trillium-Corp-Overview-07Jan2020.pdf (accessed 03/27, 2020).
125. Abrisqueta, P.; Sancho, J.; Cordoba, R.; Persky, D. O.; Andreadis, C.; Huntington, S. F.; Carpio, C.; Morillo Giles, D.; Wei, X.; Li, Y. F.; Zuraek, M.; Burgess, M. R.; Hege, K.; Martan, A. Anti-CD47 Antibody, CC-90002, in Combination with Rituximab in Subjects with Relapsed and/or Refractory Non-Hodgkin Lymphoma (R/R NHL). *Blood* **2019**, *134*, 4089-4089.
126. Kauder, S. E.; Kuo, T. C.; Chen, A.; Harrabi, O.; Rocha, S. S.; Doyle, L.; Bollini, S.; Han, B.; Sangalang, E. R. B.; Sim, J.; Randolph, S.; Pons, J.; Wan, H. I. ALX148 Is a High Affinity Sirpa Fusion Protein That Blocks CD47, Enhances the Activity of Anti-Cancer Antibodies and Checkpoint Inhibitors, and Has a Favorable Safety Profile in Preclinical Models. *Blood* **2017**, *130*, 112 LP-112.
127. Chow, L. Q. M.; Gainor, J. F.; Lakhani, N. J.; Chung, H. C.; Lee, K.; Lee, J.; LoRusso, P.; Bang, Y.; Hodi, F. S.; Fanning, P.; Zhao, Y.; Jin, F.; Wan, H.; Pons, J.; Randolph, S.; Messersmith, W. A. A phase I study of ALX148, a CD47 blocker, in combination with established anticancer antibodies in patients with advanced malignancy. *Journal of Clinical Oncology* **2019**, *37*, 2514-2514.
128. Ltd., Innovent Biologics (Suzhou) Co. A Study Evaluating the Safety, Tolerability, and Initial Efficacy of Recombinant Human Anti-cluster Differentiation Antigen 47

(CD47) Monoclonal Antibody Injection (IBI188) in Patients With Advanced Malignant Tumors and Lymphomas.

129. Ltd., I. B. C. Study of TJ011133 Subjects With Relapsed/Refractory Advanced Solid Tumors and Lymphoma. *NCT0393481* **2019**.
130. Meng, Z.; Wang, Z.; Guo, B.; Cao, W.; Shen, H. TJC4, a Differentiated Anti-CD47 Antibody with Novel Epitope and RBC Sparing Properties. *Blood* **2019**, *134*, 4063-4063.
131. Anonymous 34th Annual Meeting & Pre-Conference Programs of the Society for Immunotherapy of Cancer (SITC 2019): part 1. *Journal for Immunotherapy of Cancer* **2019**, *7*, 282-282.
132. Immunotherapeutics, O. A Trial of BI 765063 Monotherapy and in Combination With BI 754091 in Patients With Advanced Solid Tumours.
133. Morrissey, M. A.; Vale, R. D. CD47 suppresses phagocytosis by repositioning SIRPA and preventing integrin activation. **2019**.
134. Chames, P.; Van Regenmortel, M.; Weiss, E.; Baty, D. Therapeutic Antibodies: Successes, Limitations and Hopes for the Future. *Br. J. Pharmacol.* **2009**, *157*, 220-233.
135. Verma, V.; Sprave, T.; Haque, W.; Simone, C. B.; Chang, J. Y.; Welsh, J. W.; Thomas, C. R. A Systematic Review of the Cost and Cost-Effectiveness Studies of Immune Checkpoint Inhibitors. *Journal for Immunotherapy of Cancer* **2018**, *6*, 1-15.
136. Hernandez, I.; Bott, S. W.; Patel, A. S.; Wolf, C. G.; Hospodar, A. R.; Sampathkumar, S.; Shrank, W. H. Pricing of Monoclonal Antibody Therapies: Higher if Used for Cancer? *Am. J. Manag. Care* **2018**, *24*, 109-112.
137. Dai, H.; Friday, A. J.; Abou-Daya, K. I.; Williams, A. L.; Mortin-Toth, S.; Nicotra, M. L.; Rothstein, D. M.; Shlomchik, W. D.; Matozaki, T.; Isenberg, J. S.; Oberbarnscheidt, M. H.; Danska, J. S.; Lakkis, F. G. Donor SIRP alpha polymorphism modulates the innate immune response to allogeneic grafts. *Science Immunology* **2017**, *2*, eaam6202.
138. Lee, W. Y.; Weber, D. A.; Laur, O.; Severson, E. A.; McCall, I.; Jen, R. P.; Chin, A. C.; Wu, T.; Gernet, K. M.; Parkos, C. A. Novel structural determinants on SIRP alpha that mediate binding to CD47. *Journal of Immunology* **2007**, *179*, 7741-7750.
139. Subramanian, S.; Boder, E. T.; Discher, D. E. Phylogenetic divergence of CD47 interactions with human signal regulatory protein alpha reveals locus of species specificity - Implications for the binding site. *J. Biol. Chem.* **2007**, *282*, 1805-1818.

140. Lin, Y.; Yan, X.; Yang, F.; Yang, X.; Jiang, X.; Zhao, X.; Zhu, B.; Liu, L.; Qin, H.; Liang, Y.; Han, H. Soluble Extracellular Domains of Human SIRP Alpha and CD47 Expressed in Escherichia Coli Enhances the Phagocytosis of Leukemia Cells by Macrophages *in Vitro*. *Protein Expr. Purif.* **2012**, *85*, 109-116.
141. Ogura, T.; Noguchi, T.; Murai-Takebe, R.; Hosooka, T.; Honma, N.; Kasuga, M. Resistance of B16 melanoma cells to CD47-induced negative regulation of motility as a result of aberrant N-glycosylation of SHPS-1. *J. Biol. Chem.* **2004**, *279*, 13711-13720.
142. Logtenberg, M. E. W.; Jansen, J. H. M.; Raaben, M.; Toebes, M.; Franke, K.; Brandsma, A. M.; Matlung, H. L.; Fauser, A.; Gomez-Eerland, R.; Bakker, N. A. M.; van der Schot, S.; Marijt, K. A.; Verdoes, M.; Haanen, J. B. A. G.; van den Berg, J. H.; Neefjes, J.; van den Berg, T. K.; Brummelkamp, T. R.; Leusen, J. H. W.; Scheeren, F. A.; Schumacher, T. N. Glutaminyl cyclase is an enzymatic modifier of the CD47-SIRP alpha axis and a target for cancer immunotherapy. *Nat. Med.* **2019**, *25*, 612-+.
143. van den Eertwegh, A. J. M.; Versluis, J.; van den Berg, H. P.; Santegoets, S. J. A. M.; van Moorselaar, R. J. A.; van der Sluis, T. M.; Gall, H. E.; Harding, T. C.; Jooss, K.; Lowy, I.; Pinedo, H. M.; Scheper, R. J.; Stam, A. G. M.; von Blumberg, B. M. E.; de Gruijl, T. D.; Hege, K.; Sacks, N.; Gerritsen, W. R. Combined Immunotherapy with Granulocyte-Macrophage Colony-Stimulating Factor-Transduced Allogeneic Prostate Cancer Cells and Ipilimumab in Patients with Metastatic Castration-Resistant Prostate Cancer: A Phase 1 Dose-Escalation Trial. *Lancet Oncology* **2012**, *13*, 509-517.
144. Hodi, F. S.; O'Day, S. J.; McDermott, D. F.; Weber, R. W.; Sosman, J. A.; Haanen, J. B.; Gonzalez, R.; Robert, C.; Schadendorf, D.; Hassel, J. C.; Akerley, W.; van den Eertwegh, A. J. M.; Lutzky, J.; Lorigan, P.; Vaubel, J. M.; Linette, G. P.; Hogg, D.; Ottensmeier, C. H.; Lebbe, C.; Peschel, C.; Quirt, I.; Clark, J. I.; Wolchok, J. D.; Weber, J. S.; Tian, J.; Yellin, M. J.; Nichol, G. M.; Hoos, A.; Urban, W. J. Improved Survival with Ipilimumab in Patients with Metastatic Melanoma. *N. Engl. J. Med.* **2010**, *363*, 711-723.
145. Oldenborg, P.; Gresham, H.; Lindberg, F. CD47-Signal Regulatory Protein Alpha (SIRP α) Regulates Fc Gamma and Complement Receptor-Mediated Phagocytosis. *J. Exp. Med.* **2001**, *193*, 855-861.
146. Weiskopf, K.; Ring, A. M.; Ho, C. C. M.; Volkmer, J.; Levin, A. M.; Volkmer, A. K.; Oezkan, E.; Fernhoff, N. B.; van de Rijn, M.; Weissman, I. L.; Garcia, K. C. Engineered SIRP Alpha Variants as Immunotherapeutic Adjuvants to Anticancer Antibodies. *Science* **2013**, *341*, 88-91.

147. Huang, Y.; Ma, Y.; Gao, P.; Yao, Z. Targeting CD47: The Achievements and Concerns of Current Studies on Cancer Immunotherapy. *Journal of Thoracic Disease* **2017**, *9*, E168-E174.
148. Stahl, P. J.; Cruz, J. C.; Li, Y.; Yu, S. M.; Hristova, K. On-the-Resin N-Terminal Modification of Long Synthetic Peptides. *Anal. Biochem.* **2012**, *424*, 137-139.
149. Anthis, N. J.; Clore, G. M. Sequence-Specific Determination of Protein and Peptide Concentrations by Absorbance at 205 nm. *Protein Science* **2013**, *22*, 851-858.
150. Goldfarb, A.; Saidel, L.; Mosovich, E. The Ultraviolet Absorption Spectra of Proteins. *J. Biol. Chem.* **1951**, *193*, 397-404.
151. Jalil, A. R.; Andrechak, J. C.; Discher, D. E. Macrophage Checkpoint Blockade: Results From Initial Clinical Trials, Binding Analyses, and CD47-SIRPa Structure-Function. *Antibody Ther* **2020**, *3*, 80-94.
152. Oesterhelt, F.; Rief, M.; Gaub, H. E. Single Molecule Force Spectroscopy by AFM Indicates Helical Structure of Poly(ethylene-Glycol) in Water. *New Journal of Physics* **1999**, *1*, 6.1.
153. Posner, B.; Khan, M.; Bergeron, J. Endocytosis of Peptide-Hormones and Other Ligands. *Endocr. Rev.* **1982**, *3*, 280-298.
154. Puthenveedu, M. A.; Lauffer, B.; Temkin, P.; Vistein, R.; Carlton, P.; Thorn, K.; Taunton, J.; Weiner, O. D.; Parton, R. G.; von Zastrow, M. Sequence-Dependent Sorting of Recycling Proteins by Actin-Stabilized Endosomal Microdomains. *Cell* **2010**, *143*, 761-773.
155. Gordon, S. Phagocytosis: An Immunobiologic Process. *Immunity* **2016**, *44*, 463-475.
156. Blanco, F.; Rivas, G.; Serrano, L. A Short Linear Peptide that Folds into a Native Stable Beta-Hairpin in Aqueous-Solution. *Nat. Struct. Biol.* **1994**, *1*, 584-590.
157. Viguera, A.; Jimenez, M.; Rico, M.; Serrano, L. Conformational Analysis of Peptides Corresponding to Beta-Hairpins and a Beta-Sheet That Represent the Entire Sequence of the Alpha-Spectrin SH3 Domain. *J. Mol. Biol.* **1996**, *255*, 507-521.
158. Bochicchio, B.; Pepe, A.; Crudele, M.; Belloy, N.; Baud, S.; Dauchez, M. Tuning Self-Assembly in Elastin-Derived Peptides. *Soft Matter* **2015**, *11*, 3385-3395.
159. Sun, L. Peptide-Based Drug Development Advantages and Disadvantages. *Mod Chem Appl* **2013**, *1*, 1-2.

160. Pytela, R.; Pierschbacher, M. D.; Argraves, S.; Suzuki, S.; Ruoslahti, E. [27] Arginine-glycine-aspartic acid adhesion receptors. *Methods in Enzymology* **1987**, *144*, 475-489.
161. Schense, J.; Hubbell, J. Three-Dimensional Migration of Neurites Is Mediated by Adhesion Site Density and Affinity. *J. Biol. Chem.* **2000**, *275*, 6813-6818.
162. Reardon, D. A.; Fink, K. L.; Mikkelsen, T.; Cloughesy, T. F.; O'Neill, A.; Plotkin, S.; Glantz, M.; Ravin, P.; Raizer, J. J.; Rich, K. M.; Schiff, D.; Shapiro, W. R.; Burdette-Radoux, S.; Dropcho, E. J.; Wittmer, S. M.; Nippgen, J.; Picard, M.; Nabors, L. B. Randomized Phase II Study of Cilengitide, an Integrin-Targeting Arginine-Glycine-Aspartic Acid Peptide, in Recurrent Glioblastoma Multiforme. *Journal of Clinical Oncology* **2008**, *26*, 5610-5617.
163. Chowdhury, S.; Castro, S.; Coker, C.; Hinchliffe, T. E.; Arpaia, N.; Danino, T. Programmable Bacteria Induce Durable Tumor Regression and Systemic Antitumor Immunity. *Nat. Med.* **2019**, *25*, 1057-+.
164. Shields, C. W.; Evans, M. A.; Wang, L. L.; Baugh, N.; Iyer, S.; Wu, D.; Zhao, Z.; Pusuluri, A.; Ukidve, A.; Pan, D. C.; Mitragotri, S. Cellular Backpacks for Macrophage Immunotherapy. *Science Advances* **2020**, *6*, eaaz6579.
165. Liu, Y.; O'Connor, M.; Mandell, K.; Zen, K.; Ullrich, A.; Buhring, H.; Parkos, C. Peptide-mediated inhibition of neutrophil transmigration by blocking CD47 interactions with signal regulatory protein alpha. *Journal of Immunology* **2004**, *172*, 2578-2585.
166. Concepcion Uscanga-Palomeque, A.; Misael Calvillo-Rodriguez, K.; Gomez-Morales, L.; Larde, E.; Deneffe, T.; Caballero-Hernandez, D.; Merle-Beral, H.; Susin, S. A.; Karoyan, P.; Carolina Martinez-Torres, A.; Rodriguez-Padilla, C. CD47 agonist peptide PKHB1 induces immunogenic cell death in T-cell acute lymphoblastic leukemia cells. *Cancer Science* **2019**, *110*, 256-268.
167. Carolina Martinez-Torres, A.; Misael Calvillo-Rodriguez, K.; Concepcion Uscanga-Palomeque, A.; Gomez-Morales, L.; Mendoza-Reveles, R.; Caballero-Hernandez, D.; Karoyan, P.; Rodriguez-Padilla, C. PKHB1 Tumor Cell Lysate Induces Antitumor Immune System Stimulation and Tumor Regression in Syngeneic Mice with Tumoral T Lymphoblasts. *Journal of Oncology* **2019**, *2019*, 9852361.
168. Hazama, D.; Yin, Y.; Murata, Y.; Matsuda, M.; Okamoto, T.; Tanaka, D.; Terasaka, N.; Zhao, J.; Sakamoto, M.; Kakuchi, Y.; Saito, Y.; Kotani, T.; Nishimura, Y.; Nakagawa, A.; Suga, H.; Matozaki, T. Macrocyclic Peptide-Mediated Blockade of the CD47-SIRP alpha Interaction as a Potential Cancer Immunotherapy. *Cell Chemical Biology* **2020**, *27*, 1181-+.

169. Wang, H.; Sun, Y.; Zhou, X.; Chen, C.; Jiao, L.; Li, W.; Gou, S.; Li, Y.; Du, J.; Chen, G.; Zhai, W.; Wu, Y.; Qi, Y.; Gao, Y. CD47/SIRP alpha blocking peptide identification and synergistic effect with irradiation for cancer immunotherapy. *Journal for Immunotherapy of Cancer* **2020**, *8*, e000905.
170. Choi, J.; Joo, S. H. Recent Trends in Cyclic Peptides as Therapeutic Agents and Biochemical Tools. *Biomolecules & Therapeutics* **2020**, *28*, 18-24.
171. GILL, D. Bacterial Toxins - a Table of Lethal Amounts. *Microbiol. Rev.* **1982**, *46*, 86-94.
172. Yu, J. X.; Hubbard-Lucey, V. M.; Tang, J. The global pipeline of cell therapies for cancer. *Nature Reviews Drug Discovery* **2019**, *18*, 821-822.
173. Bonifant, C. L.; Jackson, H. J.; Brentjens, R. J.; Curran, K. J. Toxicity and management in CAR T-cell therapy. *Molecular Therapy-Oncolytics* **2016**, *3*, 16011.